AD-A173 311 DYNAMICS OF FULL ANNULAR ROTOR RUB(U) MASSACHUSETTS INST OF TECH CAMBRIDGE DEPT OF OCEAN ENGINEERING S J STACKLEY JUN 86 1/2

UNCLASSIFIED F/G 20/11 NL

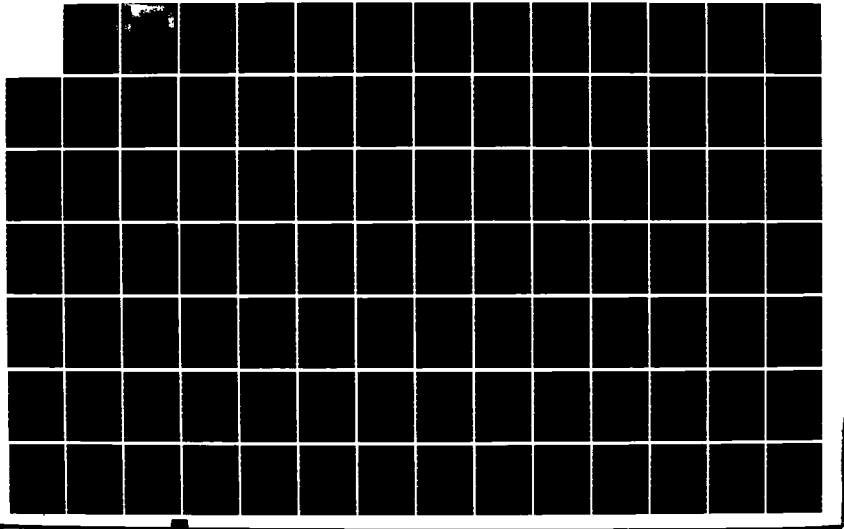

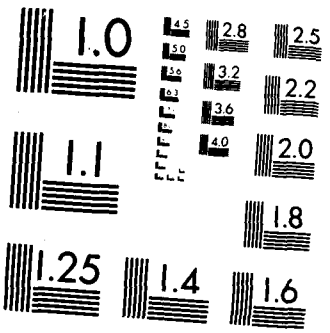

DEPARTMENT OF OCEAN ENGINEERING
MASSACHUSETTS INSTITUTE OF TECHNOLOGY
CAMBRIDGE, MASSACHUSETTS 02139

DYNAMICS OF
[illegible]

by

[illegible]

[illegible]

DYNAMICS OF
FULL ANNULAR ROTOR RUB

by

SEAN JOSEPH STACKLEY
B.S.M.E., United States Naval Academy
(1979)

SUBMITTED IN PARTIAL FULFILLMENT
OF THE REQUIREMENTS FOR THE
DEGREE OF

OCEAN ENGINEER
and
MASTER OF SCIENCE IN MECHANICAL ENGINEERING

at the

MASSACHUSETTS INSTITUTE OF TECHNOLOGY

June 1986

Signature of Author Sean Joseph Stackley
Department of Ocean Engineering
May 1986

Certified by Stephen H. Crandall
Professor Stephen H. Crandall
Thesis Supervisor

Certified by J. Kim Vandiver
Professor J. Kim Vandiver
Thesis Reader

Accepted by A. Douglas Carmichael
Professor A. Douglas Carmichael, Chairman
Ocean Engineering Department Graduate Committee

Accepted by
Professor A.A. Sonin, Chairman
Mechanical Engineering Department Graduate Committee

DYNAMICS OF

FULL ANNULAR ROTOR RUB

by

SEAN JOSEPH STACKLEY

Submitted to the Departments of Ocean Engineering and Mechanical Engineering on May 1986 in partial fulfillment of the requirements for the degree of Ocean Engineer and Master of Science in Mechanical Engineering.

ABSTRACT

Four modes of possible rotor motion are defined: synchronous precession (without rub), partial rub, full annular synchronous rub and reverse whirl. A model is developed to investigate the relationships between a rotational system's characteristic parameters and the conditions of equilibrium for the full annular rub motion. The dynamics of an unconstrained rotor with unbalance are first established. The impact of constraining the rotor's motion by a rigid casing with a finite clearance is then analyzed. For any given system, the speed regimes in which full annular synchronous rub is in equilibrium are defined as a function of the system's unbalance, clearance, rotor stiffness, damping and the coefficient of friction between the rotor and casing. The rigid stator restriction is subsequently alleviated and the equilibrium conditions for full annular synchronous rub are reanalyzed. Additionally, reverse whirl as a possible stable mode of rotor motion is studied. Specific rotational systems are then analyzed according to the model developed to demonstrate tne effect of varying particular parameters.

Thesis Supervisor: Stephen H. Crandall
Title: Professor of Mechanical Engineering

ACKNOWLEDGEMENTS

The author wishes to express his gratitude to Professor Stephen H. Crandall for his guidance and encouragement throughout the development of this thesis. Also, the author must express his most sincere appreciation to his wife and children for their encouragement and patience during the last three years.

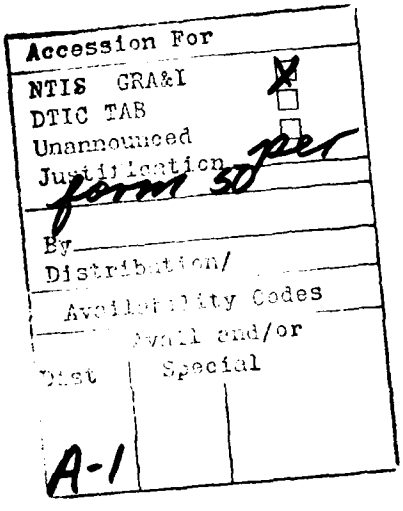

TABLE OF CONTENTS

LIST OF FIGURES

INTRODUCTION

All rotating machinery have some practical degree of unbalance which drives flexural vibrations in the system. These vibrations may be readily calculated in terms of the system's mass, unbalance, rotational speed, radial stiffness and damping imposed by the medium in which the rotating element operates. Should the magnitude of the vibrations exceed the physical constraints of the enclosure which houses the rotating element, the potentially destructive phenomena described here as rotor rub occurs.

Shaft vibrations, misalignment, blade creep and thermal expansion are some of the physical realities which precipitate design of a radial clearance between the high speed rotor and surrounding casing in turbomachinery. Theoretical efficiencies of the turbomachinery are reduced though, by blade tip losses which result from the presence of the radial clearance between the rotor blade tip and the casing. Demand for improved system efficiency thus drives a reduction of the blade tip clearance and so increases the likelihood of rotor rub. Rotor rub in fact may be a design condition and so accounted in the design by the use of abradable materials. [1]

Prior to the occurrence of rub, the rotating element's dynamics may be described as synchronous precession, driven by the system's residual unbalance. If rub develops, it may occur over a fraction of the rotor's precessional orbit (termed partial rub), or may persist over the full orbit (full annular rub). Of these two conditions, full annular rub is potentially more destructive and is the subject of this thesis. For further information regarding partial rub, attention is drawn to reference [2-4]. Examples of full annular rotor rub occur with rotor blade-to-casing or

rotor-seal rub, as well as with a rotating shaft having clearance in a bearing. [5] The rub introduces a reaction force at the rotor's periphery which strongly influences the rotor's dynamics and may additionally excite the casing (further referred to as the stator) into motion. The reaction force may be broken down into its normal and tangential (friction) force components; the two being linearly related by the coefficient of friction. Friction may be moderated by proper lubrication (such as in the case of bearing rub) as well as through suitable selection of materials. Other design considerations or abnormal operating conditions may preclude these preventive measures though, and so friction may take on a particularly destructive nature.

Friction is the resistive force which acts tangentially at the interface between two surfaces in relative motion. By acting tangentially on the rotor's periphery, it essentially establisnes a torque which counters the driving (input) torque for the rotating element. The result is either a lower rotational speed or a higher input torque required to maintain a constant speed. The effect of friction on the mating surfaces is to cause a local heat buildup and, in the very least, some degree of grinding wear and deformation of the rotor and seal or bearing annulus. The more extreme case encompasses catastrophic destruction of the machine. [2] Typically accompanying these mechanisms is the annoying and often unacceptable acoustic phenomenon due to frictional vibration instabilities known as stick slip. Dynamically, the occurrence of rotor rub may destabilize the synchronous precession of the rotor. If friction forces are of large enough magnitude, the counter-torque developed may instigate a reverse whirl condition wherein the precession is in a direction opposite to the direction of rotation of the shaft. The nature of reverse whirl is such that the

rotating element is subjected to high frequency alternating stresses which may lead to rapid fatigue failure of the shaft. [6]

1. DEVELOPMENT OF THE MODEL

The characteristics of rotating machinery designed for the generation or transmission of power vary greatly with their particular application. An exact analysis of the motion is extremely complex, but many meaningful results can be determined through employment of reasonable simplifying assumptions in a single degree of freedom model. Even with these simplifications though, numerous variables are necessary to describe the motion involved.

The model in this thesis is displayed in Figure 1. The rotating element consists of a central disk of mass, M_r, mounted symmetrically on a laterally flexible but torsionally rigid, massless shaft of stiffness K_r. The snaft stiffness is determinable knowing the shaft's material type, cross-sectional properties and length. Tne shaft is then supported at each end by rigid bearings without clearance. The natural frequency of the rotor, ω_{Nr}, the frequency of excitation at which resonance occurs, is given by $\omega_{Nr} = \sqrt{K_r/M_r}$. The rotor disk is enclosed in its casing, separated radially by a symmetric clearance, r_c, existing when the rotor is at rest. (The effects of gravity are neglected in this analysis). The casing, or stator, is characterized by its mass, M_s, and its mounting stiffness, K_s. As in the case of the rotor, the natural frequency of the stator is given by $\omega_{Ns} = \sqrt{K_s/M_s}$. Damping is introduced for motion of the rotor and stator respectively by the damping coefficients, D_r and D_s. It is the presence of damping in both the rotor and stator which limits the magnitude of their responses at their respective resonant frequencies. Damping also causes a phase lag between the system's excitation and response. For ease of analysis, the model has been "compressed" in Figure 2 to a planar diagram

with the element's dynamic characteristics represented as in a simple linear resonator system: a spring-mounted mass with a dashpot in which the energy of the motion is dissipated. Both radial and longitudinal symmetry are implicit in this model.

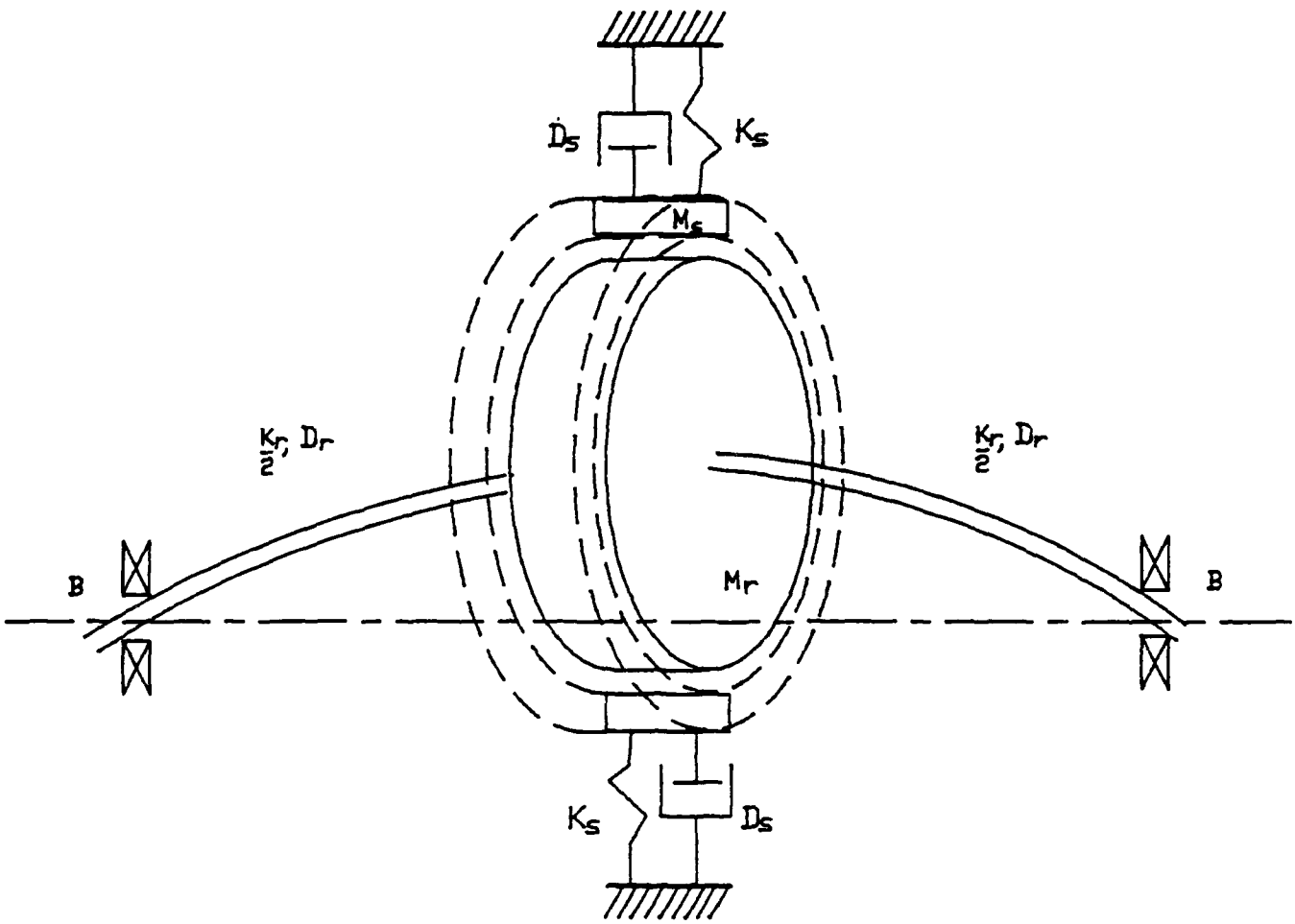

FIGURE 1. ROTOR RUB MODEL

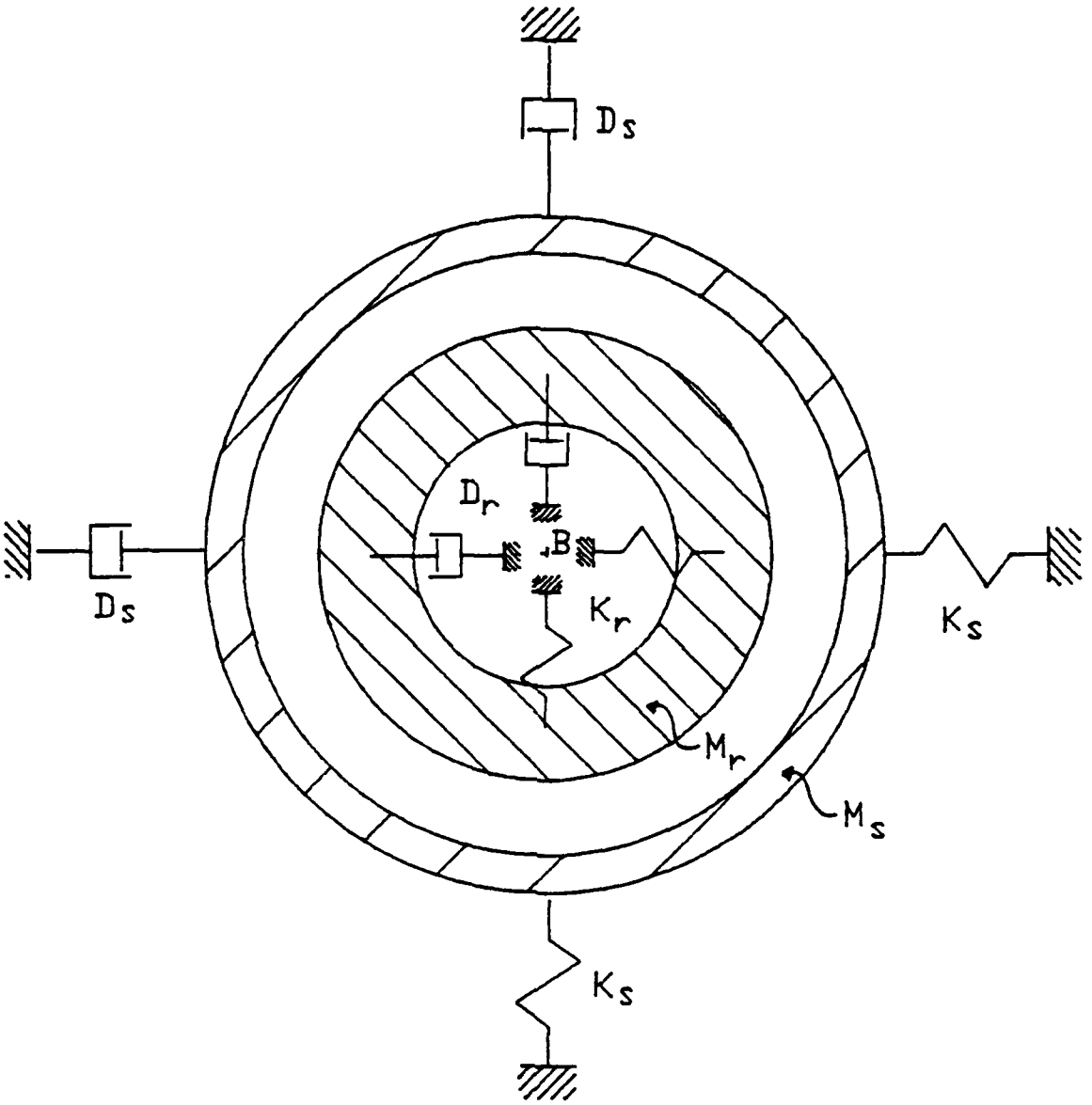

FIGURE 2. ROTOR RUB PLANAR MODEL

2. FREE ROTOR DYNAMICS

It is assumed that under design conditions, the rotor is driven at a constant speed, ω, independent of the external load applied. This assumption essentially neutralizes the effects of fluctuations in the design load due to damping or rub related friction. Under ideal conditions, it is imaginable that the rotor is perfectly balanced. Thus when driven at its design speed, the rotor center remains at the center of rotation; aligned with the axis defined by the supporting bearings' centers. This idealization is not realized in practice though, and to some extent, a residual unbalance exists in the mass distribution of the rotor. This unbalance may be depicted in the planar model by locating the mass center (or center of gravity), g, at a distance δ from the center of the disk. The effect of the unbalance is to establish a centrifugal force acting upon the center of gravity while the rotor is in motion. This centrifugal force, which is proportional to the square of the rotational speed, acts as the driving force for the rotor's dynamical motion.

An analysis of the motion of the free rotor (i.e., without displacement constraints imposed by the stator) provides the baseline condition for which the rub condition may be compared. The equation of motion for the free rotor is derived by applying Newton's 2nd Law to the rotor:
(sum of forces acting on the rotor) =

(mass of the rotor) x (acceleration of the rotor center of gravity).
Referring to the free body diagram for the rotor, Figure 3, the forces which must balance in the steady motion of the rotor are described in the following:

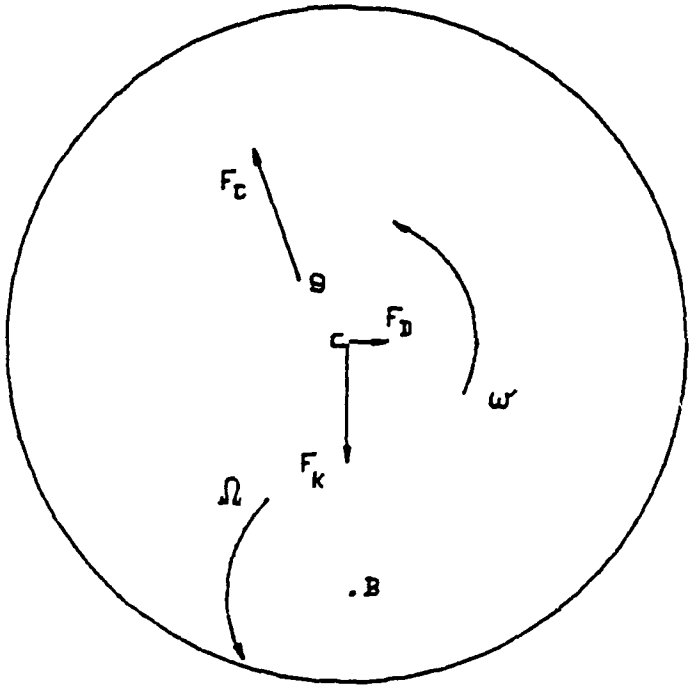

FIGURE 3. FREE-ROTOR FREE BODY DIAGRAM

a. Centrifugal Force - As described above, this force results from the presence of a residual unbalance; i.e., the center of gravity does not coincide with the center of rotation. The centrifugal force acts on the center of gravity and is directed radially outward from the bearing axis (stationary reference position about which the rotor precesses).

b. Spring Force - The spring (or restoring) force acting radially inward on the rotor center results when the rotor center is displaced from the bearing axis. It is assumed in this model that the spring force is a linear function of the shaft stiffness (assumed constant) and magnitude of displacement.

c. Damping Force - The damping force acts on the rotor center such that it resists translational motion by the rotor. The damping force is assumed to be a function of the damping coefficient experienced by the rotor in its particular medium and the linear component of the rotor's velocity.

The nature of the rotor's dynamics readily lend the analysis to description using complex variables. Defining $\vec{z}_c$ as the time dependent position of the rotor's center, referenced such that $\vec{z}_c = 0$ coincides with the rest condition where the rotor center is aligned with the bearing axis, then the equation of motion may be written as:

$$\sum \vec{F} = [-D_r \dot{\vec{z}}_c - K_r \vec{z}_c] = M_r \ddot{\vec{z}}_g \qquad (1)$$

where $\vec{z}_g(t)$ = the vector position of the center of gravity of the rotor. Furthermore, $\vec{z}_g(t)$ may be broken down into the vector sum:

$$\vec{z}_g(t) = \vec{z}_c(t) + \vec{z}_{gc}(t)$$

where $\vec{z}_{gc}(t)$ represents the vector position of the rotor center of gravity relative to the disk center.

The equation of motion then becomes:

$$M_r(\ddot{\vec{z}}_c + \ddot{\vec{z}}_{gc}) = -D_r\dot{\vec{z}}_c - K_r\vec{z}_c$$

or,

$$M_r\ddot{\vec{z}}_c + D_r\dot{\vec{z}}_c + K_r\vec{z}_c = M_r\ddot{\vec{z}}_{gc} \qquad (2)$$

$\vec{z}_{gc}(t)$ is simply a function of the radius of unbalance and rotational speed:

$$\vec{z}_{gc}(t) = \delta e^{j\omega t}$$

Assuming synchronous whirl response, the motion of the rotor may be described by:

$$\vec{z}_c(t) = |\vec{z}_c|e^{j\omega t}$$

Making these substitutions into Equation (2), and simplifying, results in the following:

$$\vec{z}_c(t) = \frac{[M_r\delta]\omega^2 e^{j\omega t}}{[(K_r - \omega^2 M_r) + j(\omega D_r)]}$$

This harmonic motion of the rotor is termed forward synchronous precession since the orbital motion of the rotor is characterized by the forcing function's angular frequency and direction. Breaking down the rotor's mechanical impedance,

$$[(K_r - \omega^2 M_r) + j(\omega D_r)] \quad ,$$

into its magnitude and phase then leads to the harmonic response equation:

$$\vec{z}_c(t) = \frac{[M_r\delta]\omega^2 e^{j(\omega t-\phi)}}{[(K_r - \omega^2 M_r)^2 + (\omega D_r)^2]^{1/2}} \qquad (3)$$

The phase angle ϕ describes the lag between the rotor's response and the forcing function. This phase lag which is due to damping is given by:

$$\phi = \tan^{-1} \frac{(\omega D_r)}{(K_r - \omega^2 M_r)}$$

It is convenient to introduce non-dimensional variables into Equation (3) for ease of future analysis. By defining a non-dimensional rotor speed and damping ratio as given below:

$$\beta = \omega/\omega_{Nr}$$

$$\zeta = \frac{D_r}{2\sqrt{K_r M_r}}$$

then Equation (3) may be rewritten:

$$\vec{z}_c = \frac{\delta\beta^2}{[(1 - \beta^2)^2 + (2\zeta\beta)^2]^{1/2}} e^{j(\omega t - \phi)} \tag{4}$$

Similarly, the phase relationship may be rewritten:

$$\phi = \tan^{-1} \frac{(2\zeta\beta)}{(1 - \beta^2)} \tag{4a}$$

The plots of $\vec{z}_c$ vs. β and ϕ vs. β are typical amplitude and phase plots for a second order system, such as those in Figure 4.

Consider the case of light damping, $\zeta << 1.0$. At low speeds, i.e., $\beta << 1.0$, the magnitude of Equation (4) reduces to $|\vec{z}_c| = \delta\beta^2$. As the speed increases, the displacement increases non-linearly until the maximum displacement occurs at $\beta = (1 - 2\zeta^2)^{1/2}$:

$$|\vec{z}_c|_{max} = \frac{\delta}{2\zeta(1 - \zeta^2)^{1/2}}$$

Here it can be seen that the maximum displacement is solely a function of the radius of unbalance (directly) and the damping ratio (inversely). Further increases in speed bring a reduction in displacement. For very high speeds, i.e., $\beta >> 1.0$, the displacement approaches δ (a constant).

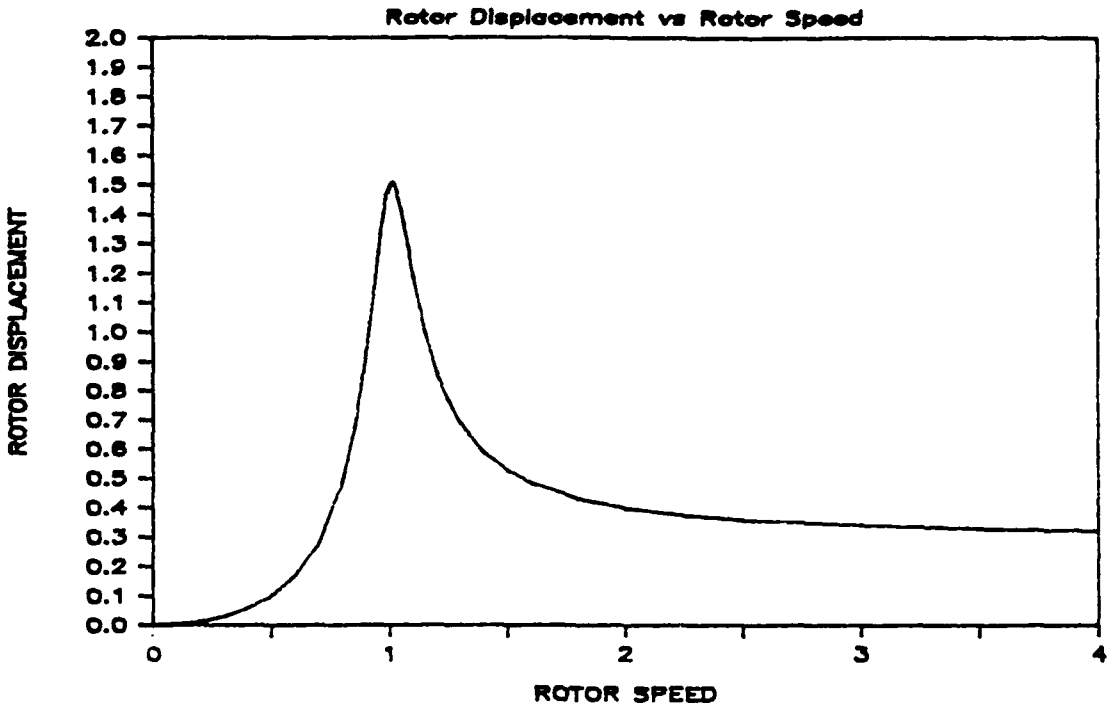

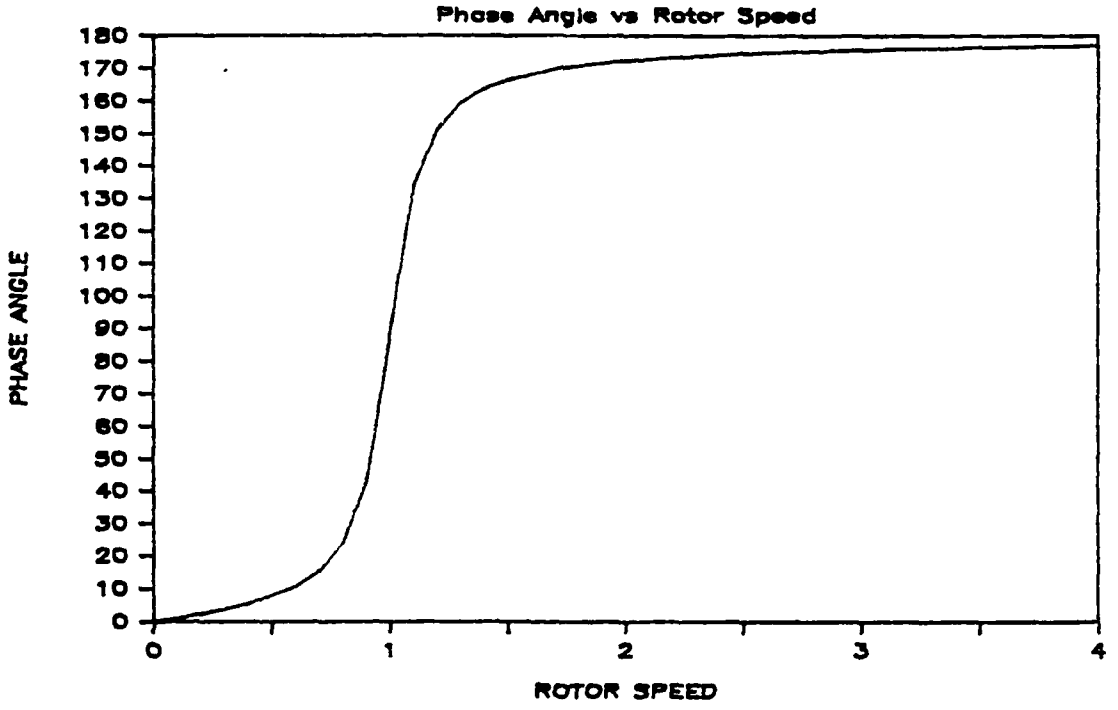

FIGURE 4(a). ROTOR DISPLACEMENT vs ROTOR SPEED (Top)
FIGURE 4(b). PHASE ANGLE vs ROTOR SPEED (Bottom)

The phase relationship for light damping is given by Equation (4a). For low speeds, $\beta << 1.0$, ϕ is approximately zero. Essentially, the forcing function and the response are exactly in phase. As the speed increases though, and approaches the resonant speed, the damping force becomes significant and the response begins to lag the forcing function. Near resonance, a rapid phase shift occurs such that at resonance, $\phi = 90°$. As the speed further increases, ϕ asymptotically approaches π. In the limit, i.e., for $\zeta = 0$; $\phi = 0$ for all values of $\beta < 1.0$ and $\phi = \pi$ for all values of $\beta > 1.0$.

3. CONSTRAINED ROTOR DYNAMICS

As previously described, rotating machinery designed for the generation or transfer of power are typically enclosed within a casing which minimizes the clearance between the rotating element and casing. The dynamics of the constrained rotor motion may simply reduce to those of the free rotor as presented in the preceding section if the rotor and stator never come into contact. This no-rub condition exists if either of two basic criteria are in effect:

(1) The maximum amplitude of free rotor displacement, $|z_c|_{max}$, is less than the constrained rotor clearance, or

(2) The rotor is operated within a speed regime, characterized by a speed ω, such that the amplitude of free rotor displacement, $|\vec{z}_c(\omega)|$, is less than the constrained rotor clearance.

As will become evident through the following analysis, condition (2) above should be further restricted to speed regimes where ω is less than the rotor natural frequency, ω_{Nr}. These two cases are depicted in Figure 5 using the plot of amplitude vs. speed.

If in fact the rotor and stator come into contact, the dynamics may become quite complex. The analysis will be first conducted with the assumption that the stator is perfectly rigid (though this restriction will be alleviated later) and only full annular rub will be considered.

The free body diagram for the rub case is presented in Figure 6. Prior to contact, Equation (4) describes the rotor's motion. It can be seen that upon the initiation of rub, the rigid stator limits the rotor's displacement while introducing a reaction force, $\vec{R}(t)$, at the point of contact. This

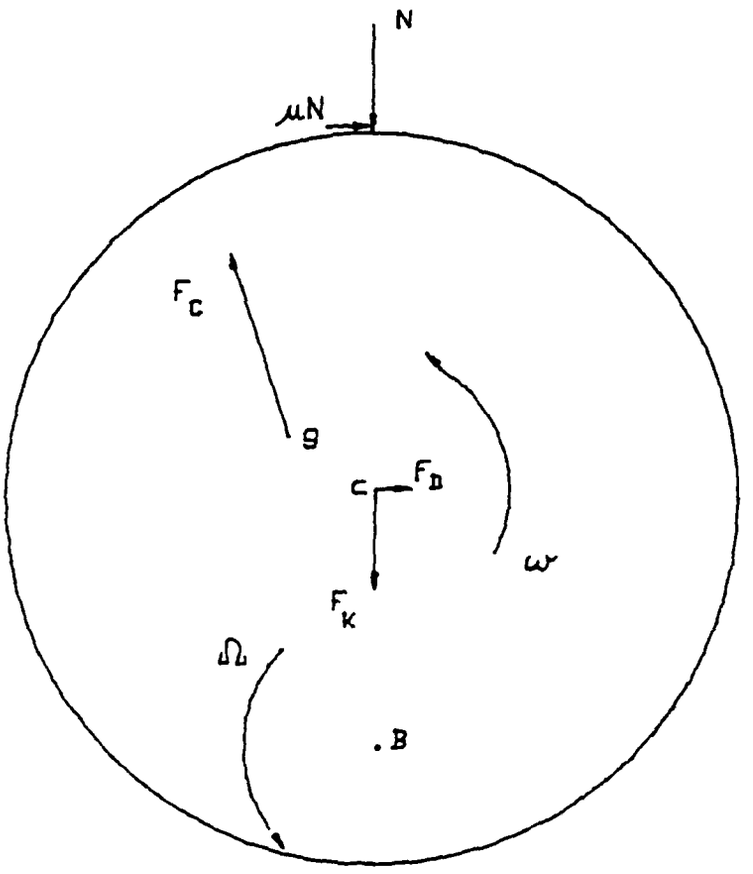

FIGURE 6. ROTOR RUB FREE BODY DIAGRAM

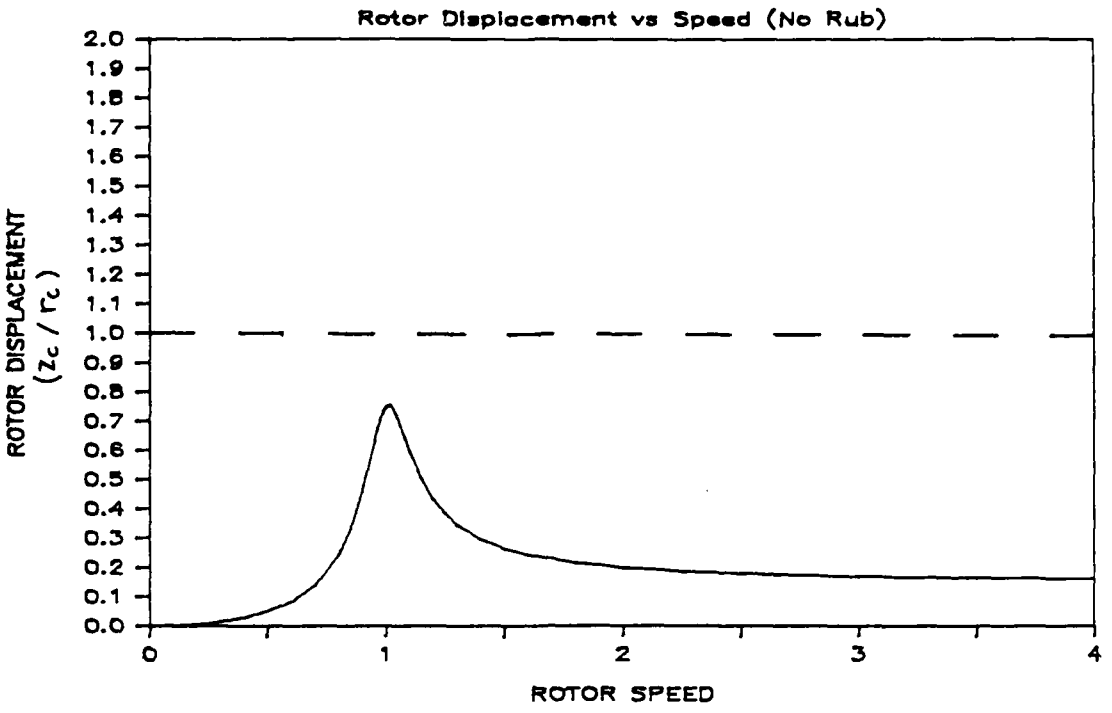

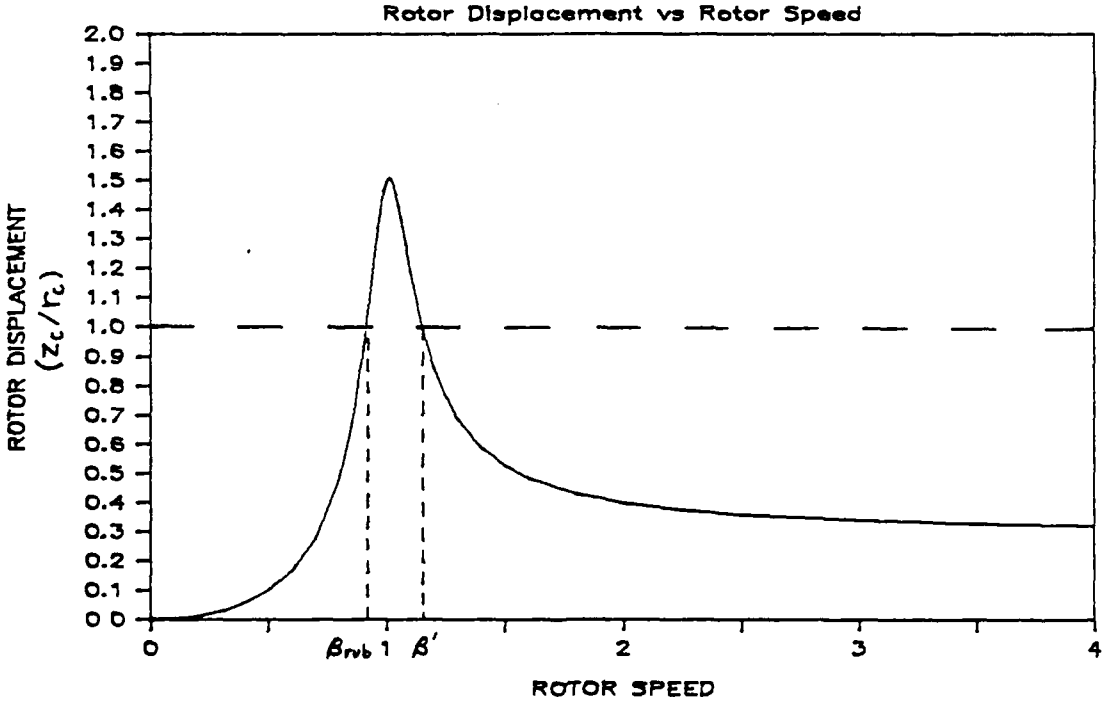

FIGURE 5(a). NORMALIZED ROTOR DISPLACEMENT vs SPEED (No-Rub) (Top)
FIGURE 5(b). NORMALIZED ROTOR DISPLACEMENT vs SPEED (Rub) (Bottom)

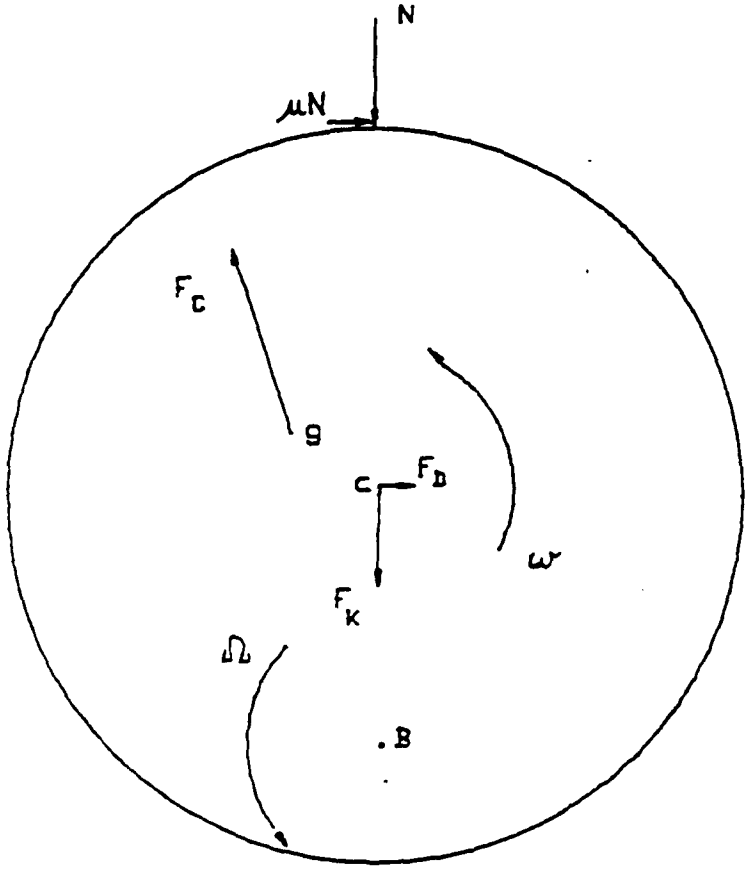

FIGURE 6. ROTOR RUB FREE BODY DIAGRAM

reaction force is comprised of a normal force and a tangential (friction) force. Since the displacement is constant, the restoring force acting on the rotor is also constant (i.e., independent of rotor speed, ω). As in the case of the free rotor, the equation of motion for the rub condition may be developed from Newton's Second Law:

$$M_r\ddot{\vec{z}}_g = -D_r\dot{\vec{z}}_c - K_r\vec{z}_c - \vec{R}(t) \tag{6}$$

Substituting $\vec{z}_g = (\vec{z}_{gc} + \vec{z}_c)$, and $\vec{R}(t) = (N + j\mu N)e^{j\omega t}$, then Equation (6) becomes (after rearranging terms):

$$M_r\ddot{\vec{z}}_c + D_r\dot{\vec{z}}_c + K_r\vec{z}_c = -M_r\ddot{\vec{z}}_{gc} - \vec{R}(t)$$

Since $\vec{z}_{gc} = \delta e^{j\omega t}$, then the above equation may be solved for $\vec{z}_c$ by assuming synchronous precession:

$$\vec{z}_c(t) = \frac{[M_r\delta\omega^2 - (N + j\mu N)]}{[(K_r - \omega^2 M_r) + j(\omega D_r)]} e^{j\omega t} \tag{7}$$

By dividing through Equation (7) with the radial clearance, r_c, and utilizing the previously defined non-dimensional speed and damping ratio variables, Equation (7) is transformed to its non-dimensional form:

$$\frac{\vec{z}_c(t)}{r_c} = \frac{[\varepsilon\beta^2 - (n + j\mu n)]}{[(1 - \beta^2) + j(2\zeta\beta)]} e^{j\omega t} \tag{8}$$

where the new variables are defined:

$$\varepsilon = \delta/r_c$$

$$n = N/kr_c$$

The right hand side of Equation (8) is reduced to a magnitude and a phase in the following rotor rub equation:

$$\frac{\vec{z}_c(t)}{r_c} = \frac{[(\varepsilon\beta^2 - n)^2 + (\mu n)^2]^{1/2}}{[(1 - \beta^2)^2 + (2\zeta\beta)^2]^{1/2}} e^{j(\omega t - \phi - \gamma)} \tag{9}$$

where

$$\gamma = \tan^{-1} \frac{(\mu n)}{(\varepsilon\beta^2 - n)}$$

The following observations may be drawn regarding the physical implications of the rotor rub equation. The parameter δ is a measure of the rotor's unbalance, and as such is not designed into the rotor, but results from manufacturing processes which are unable to meet with ideal design conditions. The value of r_c though is designed into the system, and so tolerances must be placed on δ in order to ultimately control the value of ε, a measure of the rotor's displacement-to-clearance ratio. In the case of the free rotor, any increase in δ leads to a direct increase in the rotor's maximum displacement. Since the maximum displacement is now constrained though, a normal force develops at the interface between the rotor and stator when the rotor's runout equals the clearance. The maximum normal force developed thereafter is directly related to the value of ε. Referring to Figure 5, the normal force developed for rotor speeds less than the rotor resonant speed may be crudely estimated as the magnitude of force necessary to compress a 'spring' of stiffness equivalent to the rotor's impedance a distance equal to the difference between the free rotor's displacement and the radial clearance. For speeds greater than the rotor resonant speed ($\beta > 1.0$) the characteristics of the combined rotor-stator govern the system's behavior and a more detailed analysis is necessary.

Meanwhile, a frictional force, $f = \mu n$, develops at the rotor-stator interface in opposition to the relative motion between the rotor and stator. The coefficient of friction, μ, depends primarily on the material types in contact and the degree of lubrication present. For unlubricated metal-to-metal applications, typical values of μ may range from 0.1 - 0.3. [7] The

frictional force may be replaced by a force and a couple acting upon the rotor's center. The torque thus created acts as an additional load upon the rotor's driving force. Equation (9) emphasizes the phase lag, $(\phi + \gamma)$, between the response of the rotor and the forcing function. ϕ was defined previously as the phase lag caused by the damping force in opposition to the linear component of the rotor's velocity and was given by the expression, $\phi = \tan^{-1} (2\zeta\beta)/(1 - \beta^2)$. γ is the phase lag caused by the frictional force which further opposes the rotor motion as previously given by: $\gamma = \tan^{-1}(\mu n)/(\varepsilon\beta^2 - n)$.

Since rub is presumed, the magnitude of the rotor's displacement is exactly equal to the radial clearance (given a rigid stator). This condition results in the magnitude of Equation (9) being equal to unity. The independent variable in the equation is the rotor speed. The values of μ, ζ and ε are assumed constant, and so the values of the normal force and phase angle may be solved for any value of β. This arises from the condition:

$$\frac{[(\varepsilon\beta^2 - n)^2 + (\mu n)^2]^{1/2}}{[(1 - \beta^2)^2 + (2\zeta\beta)^2]^{1/2}} = 1.0$$

Following a few algebraic steps, the following quadratic equation in n is derived:

$$(1 + \mu^2)n^2 + 2(1 - \beta^2 + 2\zeta\beta\mu)n + [(1 - \beta^2)^2 + (2\zeta\beta)^2 - \varepsilon^2\beta^4] = 0 \qquad (10)$$

which when solved yields the relationship for n as a function of β:

$$n = \frac{-(1-\beta^2+2\zeta\beta\mu) \pm \{(1-\beta^2+2\zeta\beta\mu)^2 - (1+\mu^2)[(1-\beta^2)^2+(2\zeta\beta)^2-\varepsilon^2\beta^4]\}^{1/2}}{(1 + \mu^2)} \qquad (11)$$

Equation (11) indicates two possible solutions for the normal force.

It is the upper, 'positive' root which is of primary interest, yielding a condition of $n = 0$ which is consistent with the rotor speed, β, at which rub initiates. As β varies, so too the values of the normal force and phase angle vary together as necessary to maintain a balance of all forces acting on the rotor.

It is evident from Equation (11) that throughout the regime of possible rotor speeds, depending upon the values of the system parameters μ, ζ and ε; the normal force may be positive, negative or imaginary. A negative value of the normal force here implies tensile stresses existing between the rotor and stator. This is essentially infeasible, and so for all values of $n < 0$, the rotor and stator are deemed not to be in contact. The speed at which rub is actually initiated is determinable by solving Equation (11) for the value of β at which $n = 0$:

$$\beta_{rub} = \frac{(2\zeta^2 - 1) + \sqrt{(2\zeta^2 - 1)^2 + (\varepsilon^2 - 1)}}{(\varepsilon^2 - 1)}$$

This value of β then results in $|\vec{z}_c|$ equal to r_c in both Equations (4) and (9). It should be immediately noted that if $\varepsilon/2\zeta < 1.0$ for a particular system, then rub in fact does not occur at any rotor speed. The inequality above is simply the numerical equivalent to a previously described condition - i.e., the maximum amplitude of the free rotor displacement is less than the radial clearance allowed the rotor. This is indeed the most common designed-for condition. Through service use though, the value of ε for a rotating machine may expectedly change since both the degree of unbalance and the radial clearance are affected by such physical realities as creep caused by high centrifugal loading, thermal and aerodynamic stresses caused by interaction between the rotor and the working fluid, or possible shaft bowing due to uneven heating or cooling or simple static loading.

It is the intent of this analysis to determine the behavior of rotating machinery as the rotor speed is increased beyond the rub speed for systems where $\varepsilon/2\zeta > 1.0$. Figure 5(b) provides a simple plot of the amplitude vs. speed relationship for the rotor. It is known that for $\beta < \beta_{rub}$, Equation (4) describes the rotor's motion. Furthermore, for rotor speeds within the regime $\beta_{rub} < \beta < \beta'$, it is assured that the rotor and stator will be in contact with the normal force given by Equation (11). For rotor speeds greater than β' though, Figure 5(b) can only provide basic insight into the problem. It was alluded earlier that while the rotor is undergoing a full annular synchronous rub, then it is the characteristics of the combined rotor-stator which govern the system's performance. This performance may best be analyzed by investigating the normal force and phase angle experienced by the rotor.

Equation (11) for the normal force may be rearranged algebraically to yield the following expression:

$$n = \frac{-[(1-\beta^2) + \mu(2\zeta\beta)] \pm (1+\mu^2)^{1/2}\sqrt{(\varepsilon\beta^2)^2 - \frac{[\mu(1-\beta^2) + 2\zeta\beta]^2}{(1+\mu)^2}}}{(1+\mu)^2} \qquad (12)$$

The three possible regimes of n (positive, negative or imaginary) may be examined through this equation. It is instrumental to first analyze $\vec{F}$, the sum of the external forces acting on the rotor center, by resolving it into orthogonal components (see Figure 7) - those forces acting parallel to $\vec{z}_c$ (designated the radial or r-direction) and those forces acting normal to $\vec{z}_c$ (designated the tangential or t-direction).

$\vec{F}$ is further resolved into a component due to rotor displacement and a component due to the mass eccentricity itself in Figure 8.

By combining the non-dimensional relationships in Figures (7) and (8),

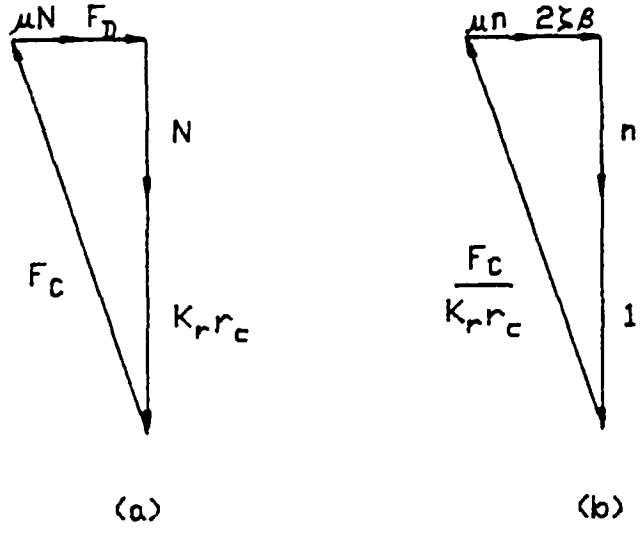

FIGURE 7. RUB FORCES VECTOR DIAGRAM

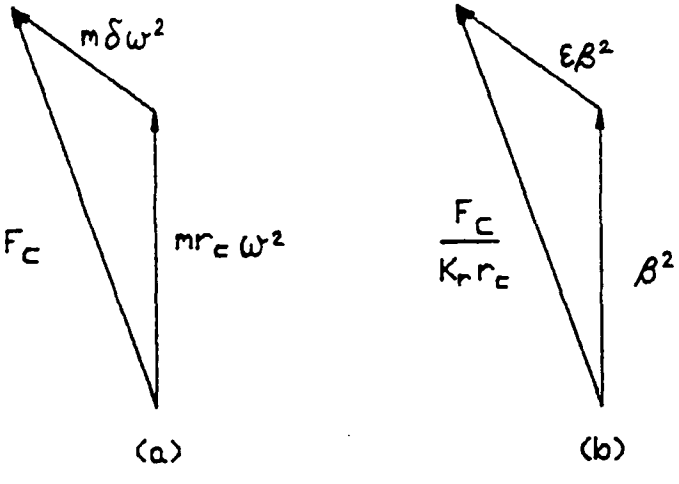

FIGURE 8. CENTRIFUGAL FORCE COMPONENTS

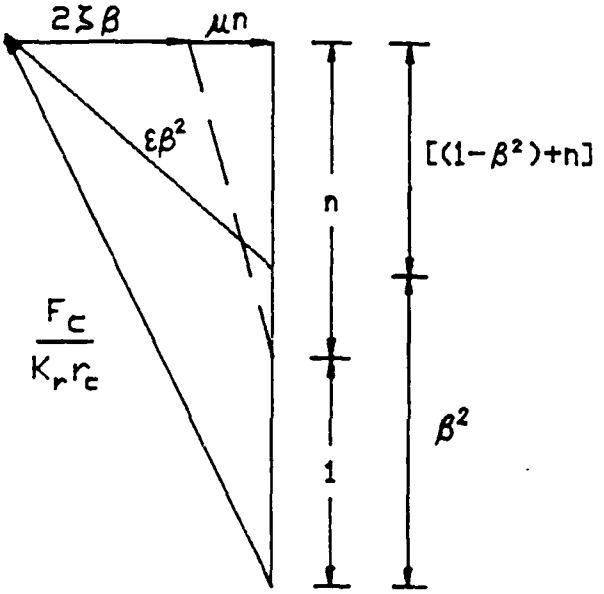

FIGURE 9. COMPOSITE FORCE DIAGRAM

a geometric interpretation for the relationship between forces in Equation (11) is attained in Figure 9.

By applying the Pythagorean Theorem to Figure 9, the variables become related by:

$$(\varepsilon\beta^2)^2 = (2\zeta\beta + \mu n)^2 + [(1 - \beta^2) + n]^2 \qquad (13)$$

Physically, this states that:

[the component of centrifugal force acting on the rotor center due to mass eccentricity], $\varepsilon\beta^2$, is balanced tangentially by [the damping and friction forces], and radially by [the normal and elastic forces lessened by the centrifugal force acting on the rotor center due to rotor displacement]. By solving for the normal force itself, Equation (13) yields:

$$n = -(1 - \beta^2) + \{(\varepsilon\beta^2)^2 - (2\zeta\beta + \mu n)^2\}^{1/2} \qquad (14)$$

The parallel between this equation and Equation (12) is immediately apparent. The following generalizations may now be drawn regarding the nature of the normal force as a function of the remaining system parameters and variables:

(a) As the rotor speed increases:

(i) The normal force, n, first becomes positive when:

$$(\varepsilon\beta^2)^2 = [(1 - \beta^2)^2 + (2\zeta\beta)^2]$$

This simply states what was earlier determined; that rub initiates when the magnitude of the centrifugal force due to mass eccentricity equals the rotor's impedance multiplied by the radial clearance.

(ii) The value of $(\beta^2 - 1)$ increases; which tends to increase the normal force.

(iii) The value of the centrifugal force, $(\varepsilon\beta^2)$ increases; which will increase the normal force if the phase angle, ϕ, is less than 90°; and will decrease the normal force if ϕ exceeds 90°.

(iv) The value of the damping force, $(2\zeta\beta)$ increases; which drives the phase angle towards 90°. For values of ϕ less than 90°, this means a reduction in normal force, and obversely, for values of $\phi > 90°$ this translates to an increase in normal force.

(b) Any increase in the damping ratio, ζ, or friction coefficient, μ, will increase the tangential forces, and in a manner similar to (iv) above will drive the phase angle towards 90°. Again, for values of ϕ less than 90°, this means an increase in normal force, and for values of ϕ greater than 90°, this means a reduction in normal force.

(c) The center of gravity of the rotor will orient itself to that phase angle necessary to balance the forces acting upon the rotor. This assumes that there is in fact some angle ϕ which will satisfy this dynamic requirement.

If for a given rotating system characterized by the parameters μ, ζ and ε operating at a particular speed β; there is no value of the phase angle which will cause the forces acting on the rotor to balance, then the assumption that the rotor is precessing at synchronous speed is no longer valid. When this case arises, i.e., when the radical term in Equation (12) becomes negative and n becomes imaginary, an alternative mechanism for the rotor motion must be determined. The 'equilibrium criterion' for synchronous rub may thus be stated mathematically:

If

$$(\varepsilon\beta^2)^2 - \frac{[\mu(1-\beta^2)+(2\zeta\beta)]^2}{(1+\mu^2)} < 0 \qquad (15)$$

then synchronous rub is not a possible mode of rotor motion.

The multiplicity of rotor speeds (roots) which make the radical term in Equation (15) identically equal to zero lead to three possible sequences of rotor modes of motion occurring within the rub regime:

(i) If all the roots to Equation (15) occur at speeds below the speed at which rub initiates, then a real solution to the rub equation exists for all rotor speeds. This does not preclude the possibility that rub may cease (i.e., $n < 0$), but rather indicates that the rotor dynamics will be governed by the relationships previously developed for synchronous whirl (i.e., Equations (4) and (12)).

(ii) If one of the roots to Equation (15) occurs at a speed greater than the rub speed, then the rub equation has no solution for rotor speeds greater than this limiting speed β_I. It is possible that β_I could occur at a speed for which rub is not in effect (i.e., the normal force is less than zero according to Equation (12)). This condition shall be discussed in greater detail in a later section.

(iii) If two of the roots to Equation (15) occur at a speed greater than the rub speed, then there is a limited regime within which synchronous rub is not in equilibrium. For all rotor speeds less than the first root and greater than the second root, the rotor dynamics may be described by Equations (4) or (12). Otherwise synchronous rub is not a possible mode of rotor motion.

Throughout the speed regime in which synchronous rub is not a solution, three modes of rotor motion are possible - either a forward synchronous whirl without rub, a partial rub or a full annular rub reverse whirl. These cases shall be discussed in greater detail in the following section. In order to provide clarity on the interrelationships of these various modes,

the outline in Figure 10 provides a sequencing of the possible system dynamics as a function of rotor speed. It is informative to demonstrate these various modes by comparing the amplitude of displacement and normal force experienced by the rotor as functions of rotor speed as in Figures 11 through 14.

(i) No rub

The reference case is the simple condition that rub never occurs. This is true for systems where $\varepsilon < 2\zeta$. As can be seen in Figure 11, the radial clearance is greater than the maximum displacement experienced by the rotor and so the normal force is zero for all speeds.

(ii) Limited synchronous rub

As depicted in Figure 12, rotor rub initiates at some speed $\beta_{rub} < 1.0$. Further increases in rotor speed drive the rotor hard against the stator while the normal force steadily increases. The large friction and damping forces which also develop ultimately disrupt the synchronous rub. Further increases in rotor speed do not lead to a restoration of rotor rub but rather follow the course of action for the free rotor.

(iii) Synchronous rub-limited discontinuity

Similar to the limited synchronous rub case, rub initiates at a speed $\beta_{rub} < 1.0$, and ceases at some speed, β_I. At β_I, rotor precession jumps down to the free-rotor synchronous whirl. As shown in Figure 13, at a yet higher speed, dynamic conditions once again become favorable for a stable synchronous rub. At this speed though, some perturbance is required to bring the rotor into contact with the stator and thus initiate the rub. It

must be emphasized that reverse whirl may also be stable at this speed (dependent upon the slip condition), thus making it difficult to predict the exact motion which would ensue.

(iv) Continuous synchronous rub

As in the limited rub case, rotor rub initiates at some rotor speed, $\beta_{rub} < 1.0$. As rotor speed is further increased, the rub reaction force also steadily increases. In this case though, the damping and friction forces are not significant enough to disrupt the equilibrium of the synchronous rub (see Figure 14).

Analytically, regimes where the various modes dictate the behavior of the rotor may be defined and mapped onto a family of curves using variables thus far defined. Figure 15 depicts the impact on rotor motion of varying the coefficient of friction, unbalance (or inversely the radial clearance), or speed ratio for a fixed value of rotor damping. For this particular case of $\zeta = .10$, region (i) of the plot depicts the condition for which no rub occurs (independent of the rotor speed) and is described by the inequality of $\varepsilon < 2\zeta$. For a particular value of $\varepsilon > 2\zeta$, rub first initiates at the speed defined by the previously derived relationship:

$$\beta_{rub} = \frac{(2\zeta^2 - 1) + \sqrt{(2\zeta^2 - 1)^2 + (\varepsilon^2 - 1)}}{(\varepsilon^2 - 1)}$$

This value provides the lower bound to region (ii) in Figure 15. Region (ii) depicts the speed regime wherein synchronous rub is in equilibrium. If we consider the specific case where the coefficient of friction, $\mu = 0.25$, then region (iii) depicts the speed regime where synchronous rub has fallen

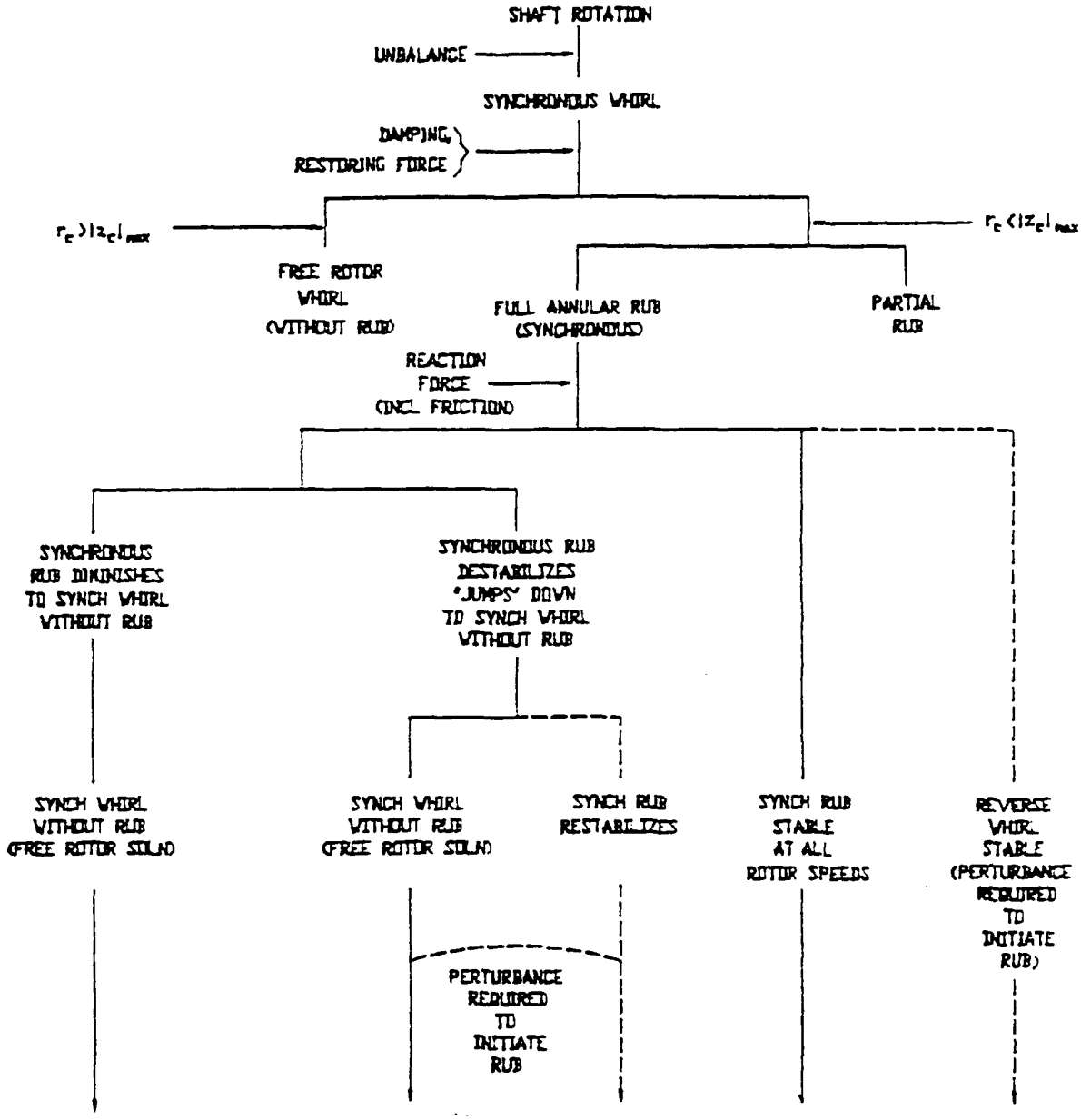

FIGURE 10. ROTOR MODES OF MOTION OUTLINE

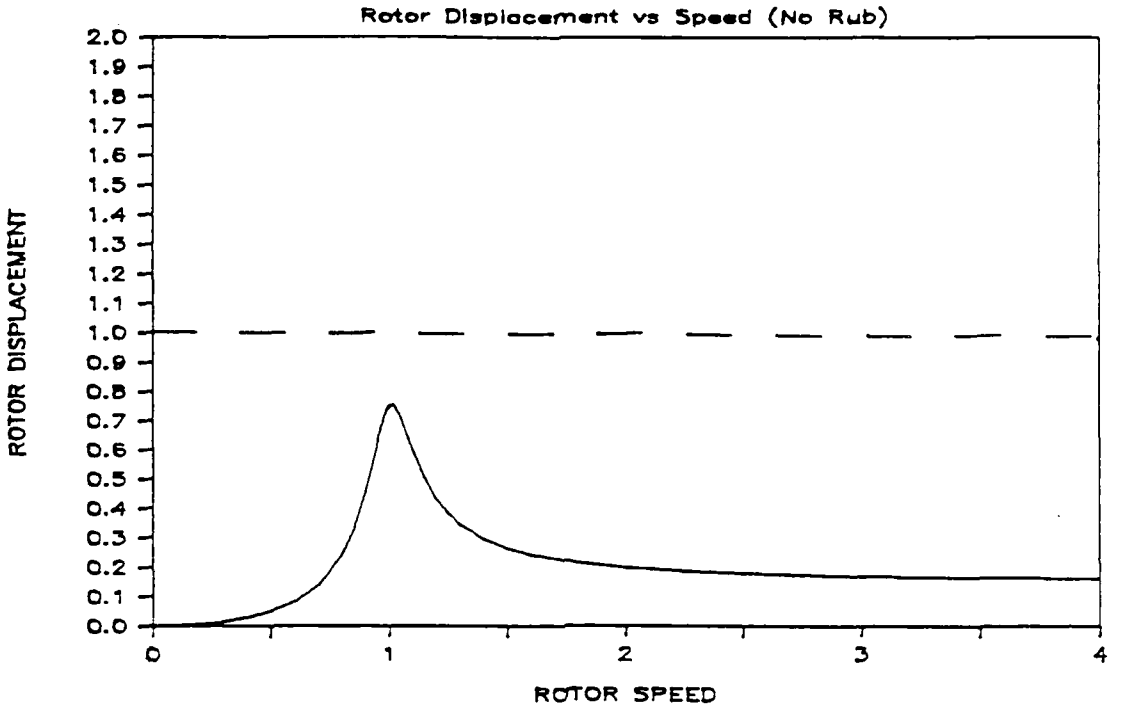

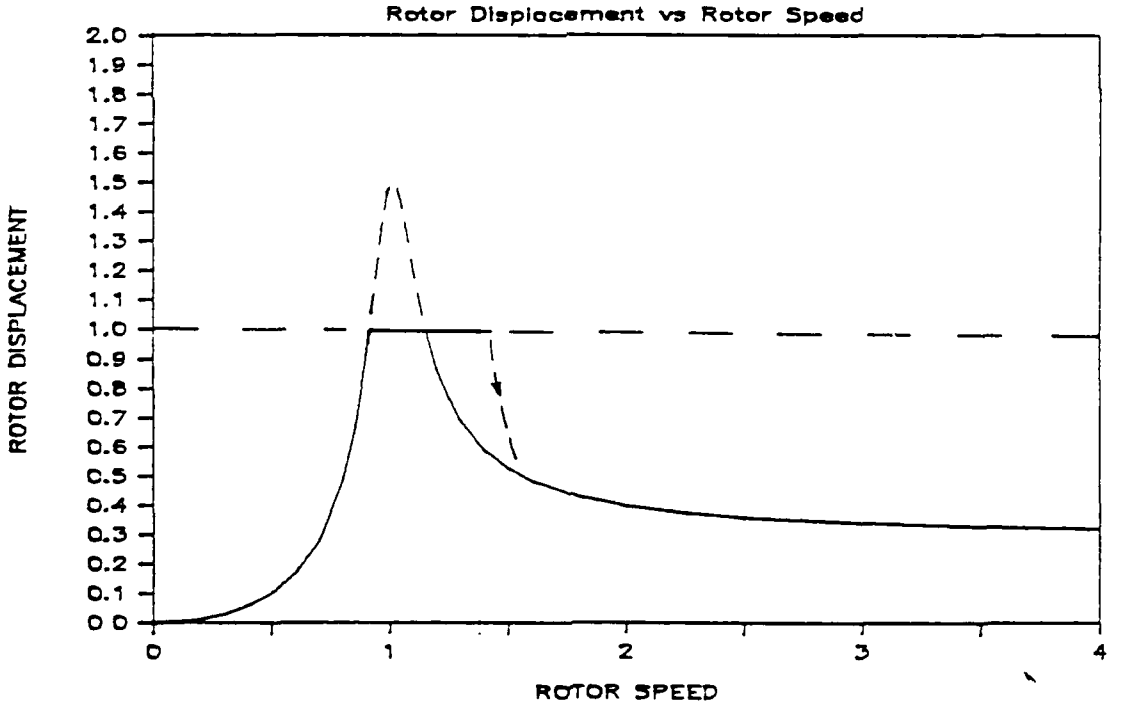

FIGURE 11. AMPLITUDE vs FREQUENCY (No Rub) (Top)
FIGURE 12. AMPLITUDE vs FREQUENCY (Limited Synchronous Rub) (Bottom)

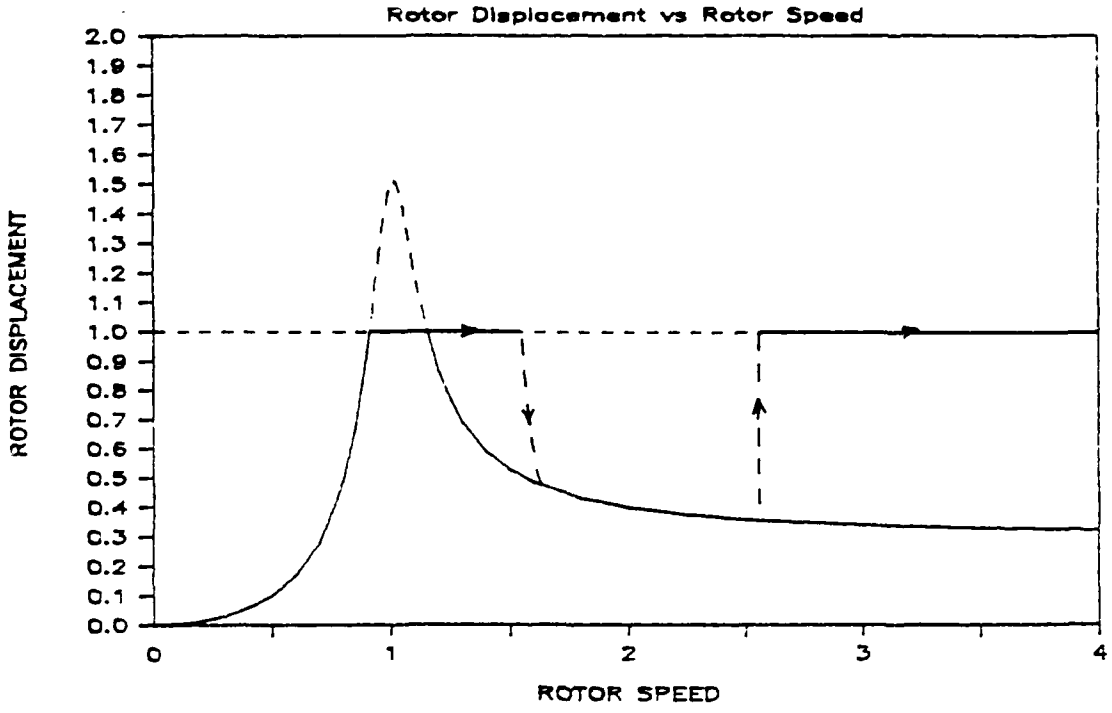

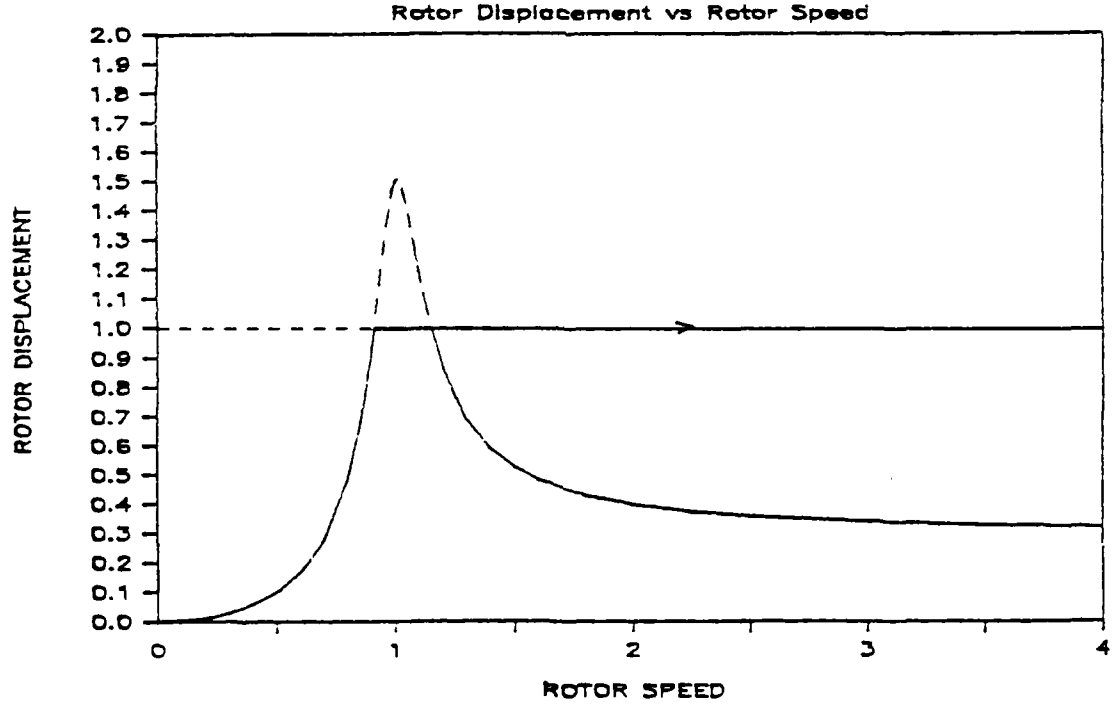

FIGURE 13. AMPLITUDE vs FREQUENCY (Synch Rub-Limited Discontinuity) (Top)
FIGURE 14. AMPLITUDE vs FREQUENCY (Continuous Synch Rub) (Bottom)

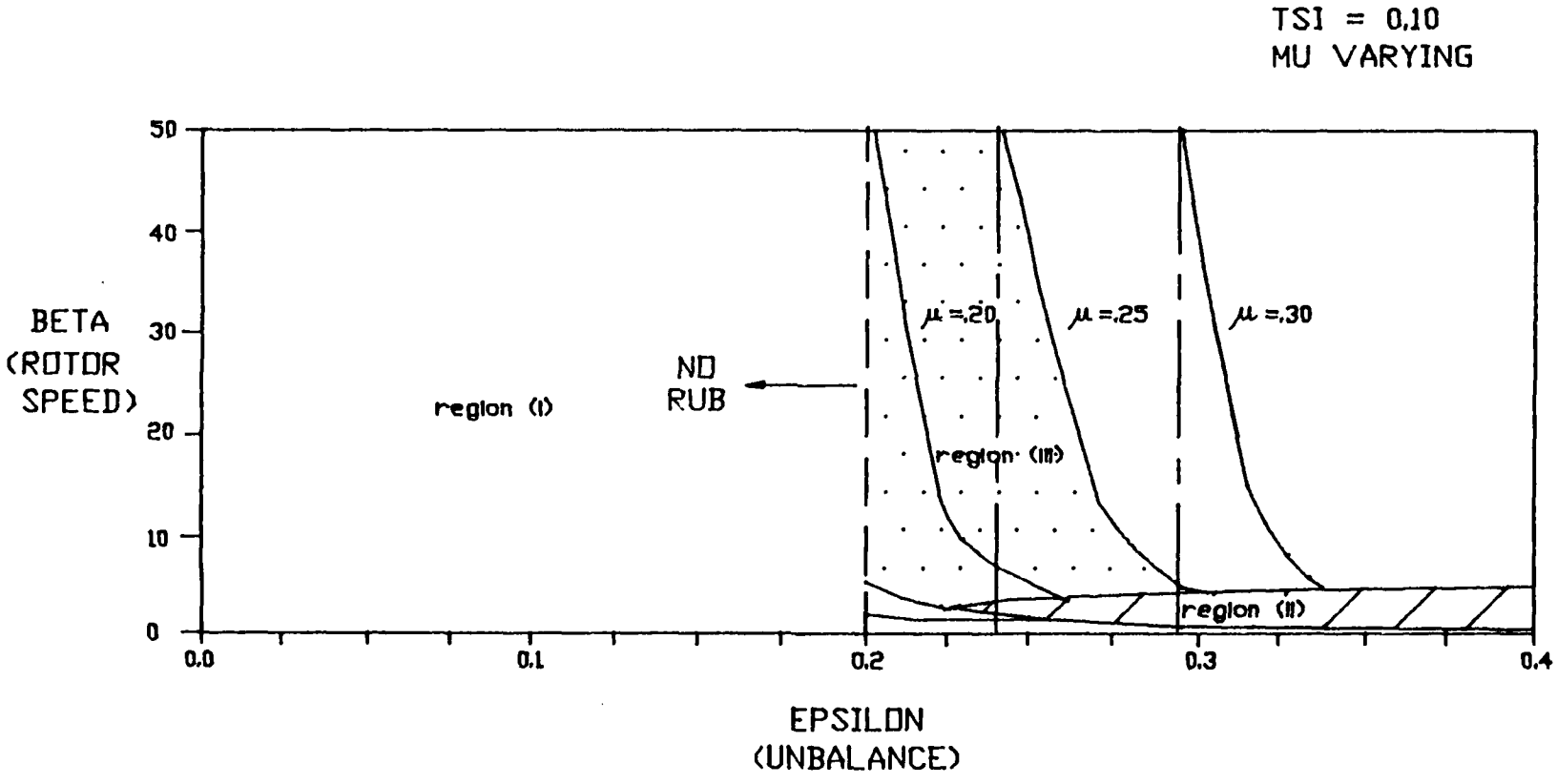

FIGURE 15. ROTOR MOTION MODE DIAGRAM

out of equilibrium. The lower bound to this region is defined by the inequality provided in Equation (15):

$$(\varepsilon\beta^2)^2 - \frac{[\mu(1-\beta^2)+(2\zeta\beta)]^2}{(1+\mu^2)} \leq 0$$

Synchronous rub never re-establishes equilibrium in rotational systems with a value of ε described by the following inequality:

$$\varepsilon < \frac{\mu}{(1+\mu^2)^{1/2}}$$

Otherwise, the speed at which synchronous rub occurs is depicted by the curve labelled "$\mu = 0.25$." This curve is generated similarly to Equation (15) above, but now represents the case:

$$(\varepsilon\beta^2)^2 - \frac{[\mu(1-\beta^2)+(2\zeta\beta)]^2}{(1+\mu^2)} \geq 0$$

Lastly, for any system described by $\zeta = 0.10$ and $\mu = 0.25$; if $\varepsilon \geq (\zeta^2+\mu^2)/[\mu(1+\mu^2)^{1/2}]$, then synchronous rub is a solution to the rotor motion for all speeds, $\beta > \beta_{rub}$. A plot such as in Figure 15 thus clearly outlines rotor motion as a function of speed for any system described by the variables μ, ζ and ε. Specifically, each of the four cases described in this section are delimited according to the system's value of ε:

(i) No rub: $\varepsilon < 2\zeta$

(ii) Limited synchronous rub:

$$2\zeta < \varepsilon \leq \frac{\mu}{(1+\mu^2)^{1/2}}$$

(iii) Synchronous rub - limited discontinuity:

$$\frac{\mu}{(1+\mu^2)^{1/2}} < \varepsilon < \frac{\zeta^2+\mu^2}{\mu(1+\mu^2)^{1/2}}$$

(iv) Continuous synchronous rub:

$$\varepsilon \geq \frac{\zeta^2 + \mu^2}{\mu(1+\mu^2)}^{1/2}$$

The relationships above explicitly indicate the effect on the rotor's mode of motion of altering any of the variables involved.

4. DYNAMICS OF REVERSE WHIRL

Reverse whirl is the state of rotor dynamics wherein the direction of precession of the rotor center about the bearing axis opposes the direction of rotation of the rotor about its own center. It was shown that in the absence of rub, an unbalance in the rotor's mass distribution results in a forward synchronous whirl of the rotor. The presence of damping resists this forward precession and thus creates a phase lag between the rotor center as it precesses and the mass center as it rotates. This damping force though, is linearly related to the whirl speed and so can not by itself destabilize the precessional motion of the rotor. When rub occurs, a frictional force at the interface between the rotor and stator develops which combines with the damping force to oppose the rotor's forward precession. Unlike the damping force though, the frictional force is a non-linear function of rotor speed. If the additional force created by the frictional force opposing the rotor's forward whirl can not be balanced by the tangential component of the centrifugal force associated with the rotor's mass unbalance, then the synchronous whirl assumption breaks down.

The dynamics of the reverse whirl problem are far more complex than for forward synchronous whirl. Since the whirl speed, Ω, is now independent of the rotational speed, ω, it must be introduced as a new variable in the analysis. This then creates the additional complexity of having a phase angle which is now a function of time (more specifically, a function of $(\omega - \Omega)t$). Since the phase angle varies regularly with time though (i.e., constant frequency), a simplifying assumption is that the time averaged, or net position of the mass center of the rotor is located at the centroid of the rotor (i.e., $\delta = 0$). Furthermore, since the whirl and rotational

directions are opposed, then the direction of relative motion at the point of contact (designated point A) between rotor and stator must be determined. The velocity of point A may be written:

$$\vec{V} = \vec{V}_c + \vec{V}_{Ac}$$

where $|\vec{V}_c| = -r_c\Omega$ = linear velocity of the rotor center

$|\vec{V}_{Ac}| = a\omega$ = linear velocity of point A relative to the rotor center

where a = rotor diameter

By assuming $(a\omega) > (r_c\Omega)$, then the linear velocity of the rotor at A may be assumed in the direction of the rotor's rotation and the friction force is thus aligned with the direction of whirl.

The free body diagram may now be analyzed to determine the conditions whereby reverse whirl is possible. Figure 16 displays the forces at work and their assumed orientation for reverse whirl. By considering the balance of forces in the tangential and radial directions, two independent equations are developed. In the tangential direction, the friction force is balanced solely by the damping force:

$$\mu N = D_r(r_c\Omega)$$

By defining $\rho = \Omega/\omega$ and substituting non-dimensional variables:

$$\mu n = 2\zeta\beta\rho \tag{16}$$

In the radial direction, the centrifugal force of the rotor is balanced by the elastic force of the rotor plus the normal force between the rotor and stator:

$$M_r r_c \Omega^2 = N + K_r r_c$$

In non-dimensional form this becomes:

$$\rho^2\beta^2 = n + 1 \tag{17}$$

The rotor rotational speed, ω, and whirl speed, Ω, may be kinematically

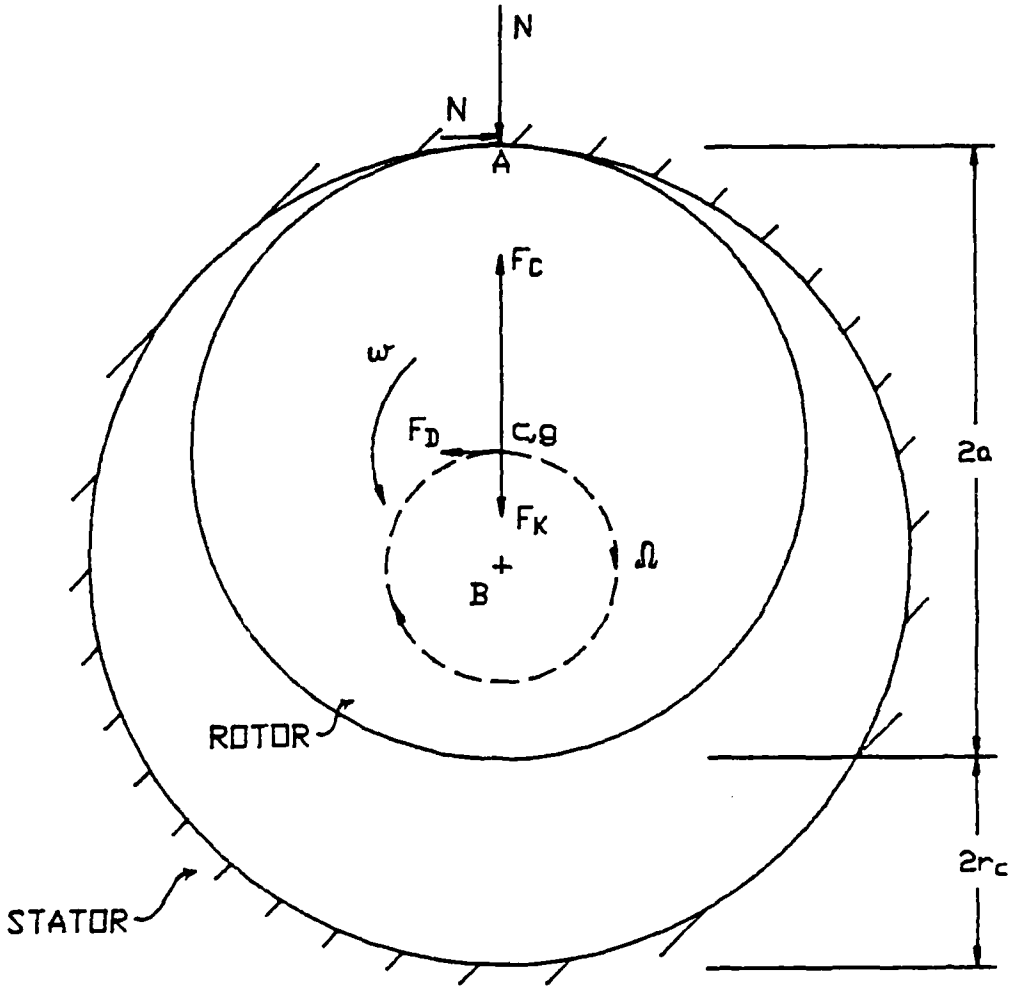

FIGURE 16. REVERSE WHIRL FREE BODY DIAGRAM

related through the slip condition that exists at the rotor-stator interface. A no-slip condition would yield the kinematic relationship common to epicyclic gear trains:

$$\Omega = (a/r_c)\omega$$

If there is slip at the interface, the whirl speed is reduced accordingly. The slip ratio, s, is thus defined as the ratio of the (rotor whirl speed)-to-the- (rotor whirl speed without slip); i.e.,

$$s = \frac{\Omega}{(a/r_c)\omega}$$

Equations (16) and (17) may thus be rewritten:

$$\mu n = 2\zeta\beta[(a/r_c)s] \tag{16a}$$

$$[s(a/r_c)]^2\beta^2 = n + 1 \tag{17a}$$

By substituting (17a) into (16a), the critical condition for reverse whirl is determined:

$$\mu\{[(a/r_c)^2 s^2]\beta^2 - 1\} = 2\zeta\beta[(a/r_c)s]$$

The above condition may be resolved into a quadratic equation in β:

$$\mu[(a/r_c)s]^2\beta^2 - 2\zeta[(a/r_c)s]\beta - \mu = 0 \tag{18}$$

Solving for β yields the critical speed above which reverse whirl is possible:

$$\beta_{rev} = [(\frac{r_c}{a})\frac{1}{s}][\frac{\zeta+(\zeta^2+\mu^2)^{1/2}}{\mu}] \tag{19}$$

The lone unknown variable in the above equation is the slip ratio, s, which may in fact be difficult to determine. The limiting case arises of course when no slip is present (i.e., s = 1.0). If it is assumed that the damping and friction are of the same order of magnitude, then β_{rev} is of the order of r_c/a, which in general is much less than unity. The limiting case thus states that reverse whirl is possible for essentially all rotor speeds

of interest (i.e., within the rub regime). It is not until a significant degree of slip is present (i.e., s is of the order of r_c/a) that the minimum possible speed for reverse whirl may become restrictive on the behavior of a rotor undergoing full annular rub.

Since the rotor first assumes a forward synchronous precession though, it will continue with this motion until either it becomes unstable or is perturbed into another stable mode of motion. As previously developed, the forward synchronous whirl without rub is continuously stable as long as the displacement of the free rotor is less than the constrained rotor's radial clearance. The only mode where synchronous whirl may be destabilized then, is during a synchronous rub. This has been analytically developed and occurs if the reaction force between the rotor and stator becomes imaginary or if the equilibrium state for the rotor-stator is inherently unstable. In this situation, the equations developed based on synchronous whirl are no longer applicable.

A qualitative analysis of the transient state following destabilization of the synchronous rub proves quite meaningful. It may first be reasonably presumed that the rotor will assume either a partial rub or a forward subsynchronous whirl following the destabilization. Considering the latter mode of motion, the impact of the non-synchronicity on the rotor's dynamics is primarily that the phase angle, ϕ, is now a time dependent variable. The centrifugal force which has been pressing the rotor against the stator throughout the full annular rub now has a fluctuating component. As the phase angle approaches 180°, the centrifugal force acting on the rotor center due to the mass unbalance is actually joining with the spring force to drive the rotor center in towards the bearing axis. The normal force rapidly drops to zero and contact is broken between the rotor and stator.

This may be somewhat anticipated by observing the near-vertical negative slope of the corresponding normal force plot at the critical equilibrium speed (see Figure 17). Now that rub is no longer present, there is no force to drive a reverse whirl, and so the rotor will jump down to the stable mode of forward synchronous whirl without rub. Perturbing the rotor back into contact at this speed (or higher) may now provoke a reverse whirl. In the previous section, the possibility for a restabilization of synchronous rub was demonstrated. Under these conditions, either synchronous rub or reverse whirl may result when the rotor is perturbed back into contact with the stator. In general, no smooth transition can occur from a synchronous whirl to a reverse whirl since this would mean transiting through a regime of zero whirl speed. The whirl speed though would not drop below that necessary to maintain rub-contact; for when contact is lost, the rotor either assumes a partial rub whirl or resumes a synchronous whirl without rub.

The behavior of the rotor when transiting from a higher to a lower speed differs markedly from the behavior of the rotor as it is increasing speed. In the absence of some outside perturbation, when reducing speed from a situation of synchronous whirl without rub at a speed, $\beta > 1.0$; no jump phenomenon in the rotor displacement curve would occur, but rather rub would occur only within that region of Figure (5b) where the free-rotor's displacement exceeds the rotor radial clearance.

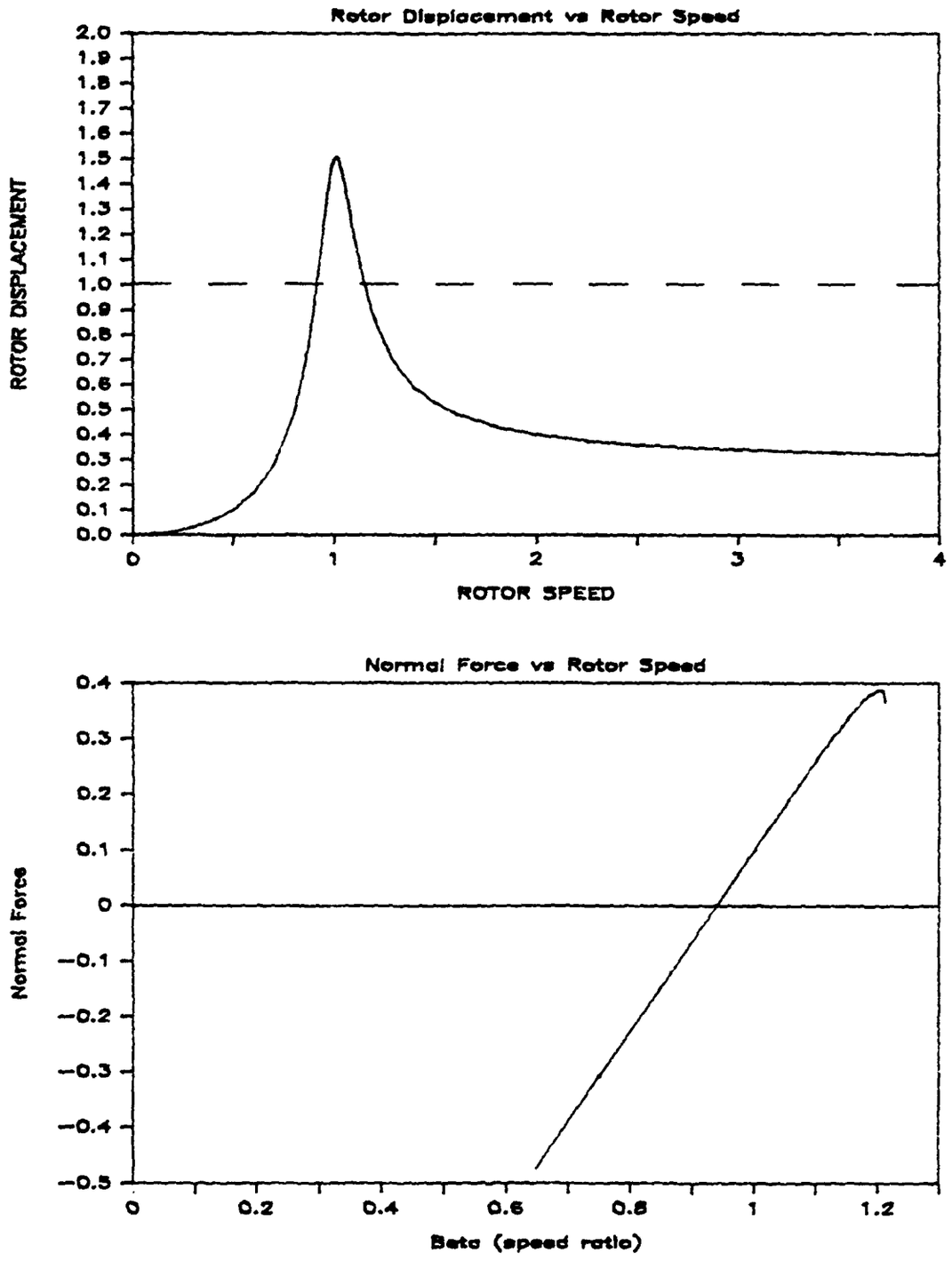

FIGURE 17. NORMAL FORCE PLOT (Limited Synchronous Rub)

5. ROTOR RUB WITH A NON-RIGID STATOR

The assumption of an ideally-rigid stator enclosing the rotating element in this analysis is not feasible, but depending on the stator's dynamic characteristics, such may be an entirely satisfactory assumption for the analysis. In this section, the stator is assigned a finite mass, radial stiffness and damping coefficient. For ease of analysis, these characteristics are assumed to be axisymmetric. Additionally, the stator is assumed to be torsionally rigid. It is often instrumental to investigate the translational system analogous to the rotating system under analysis. This is first accomplished to provide insight to the complex equations developed in the final analysis.

The basic precept in analyzing the coupled rotor-stator system is that once the state of continuous contact is interrupted, the synchronous full annular rub condition will rapidly deteriorate to a partial- or no-rub state; or if sufficiently perturbed, to a reverse whirl. The translational system designed to model the rotor-stator is presented in Figures 18(a) and (b). The rotor and stator are assigned their respective masses, a linear spring and damper to characterize their dynamic characteristics, and are restricted to motion along the horizontal axis. In the rotational system, steady motion of the combined rotor-stator may be depicted by an arc which traces the path of the rotor-stator center of mass. The actual force experienced by the combined mass would have a frequency equal to the rotor's precessional frequency, and a magnitude which depends upon the centrifugal force acting on the rotor and the dynamic characteristics of both the rotor and stator. In the translational system a static pre-load, F_o, is presumed to displace the rotor mass across the radial clearance, r_c, and then further

displaces the combined rotor-stator mass to a static equilibrium position about which the system vibrates. A sinusoidal force then drives the system at the 'synchronous' speed, ω (analogous to the rotor's rotational speed), with a magnitude F_1.

The free body diagrams for the rotor and stator under the static preload are displayed in Figure 18(c).

The force which acts at the interface is given by P_o. Essentially, only the stiffness of the rotor and stator resist the static load. The static equation for the rotor and stator are given by Equations (19) and (20) respectively:

$$F_o - P_o = k_1 x_1 \tag{19}$$

$$P_o = k_2 x_2 \tag{20}$$

Additionally, x_1 and x_2 are related by the kinematic condition:

$$x_1 = r_c + x_2$$

Therefore, a single equation may be written:

$$F_o - P_o = k_1(r_c + P_o/k_2)$$

Solving for the static load at the interface yields:

$$P_o = (F_o - k_1 r_c)k_2/(k_1 + k_2) \tag{21}$$

The equation of motion for the system's dynamic condition is similarly determined by analyzing the forces acting on the rotor and stator. The dynamic condition free body diagrams are provided in Figure 18(d).

Applying Newton's 2nd Law, the balance of forces may be written:

rotor:

$$-k_1 x_1 - D_1 \dot{x}_1 - P_o - P_1 e^{j\omega t} + F_o + F_1 e^{j\omega t} = m_1 \ddot{x}_1 \tag{22}$$

stator:

$$-k_2 x_2 - D_2 \dot{x}_2 + P_o + P_1 e^{j\omega t} = m_2 \ddot{x}_2 \tag{23}$$

where $P_1 e^{j\omega t}$ represents the dynamic reaction force at the rotor-stator

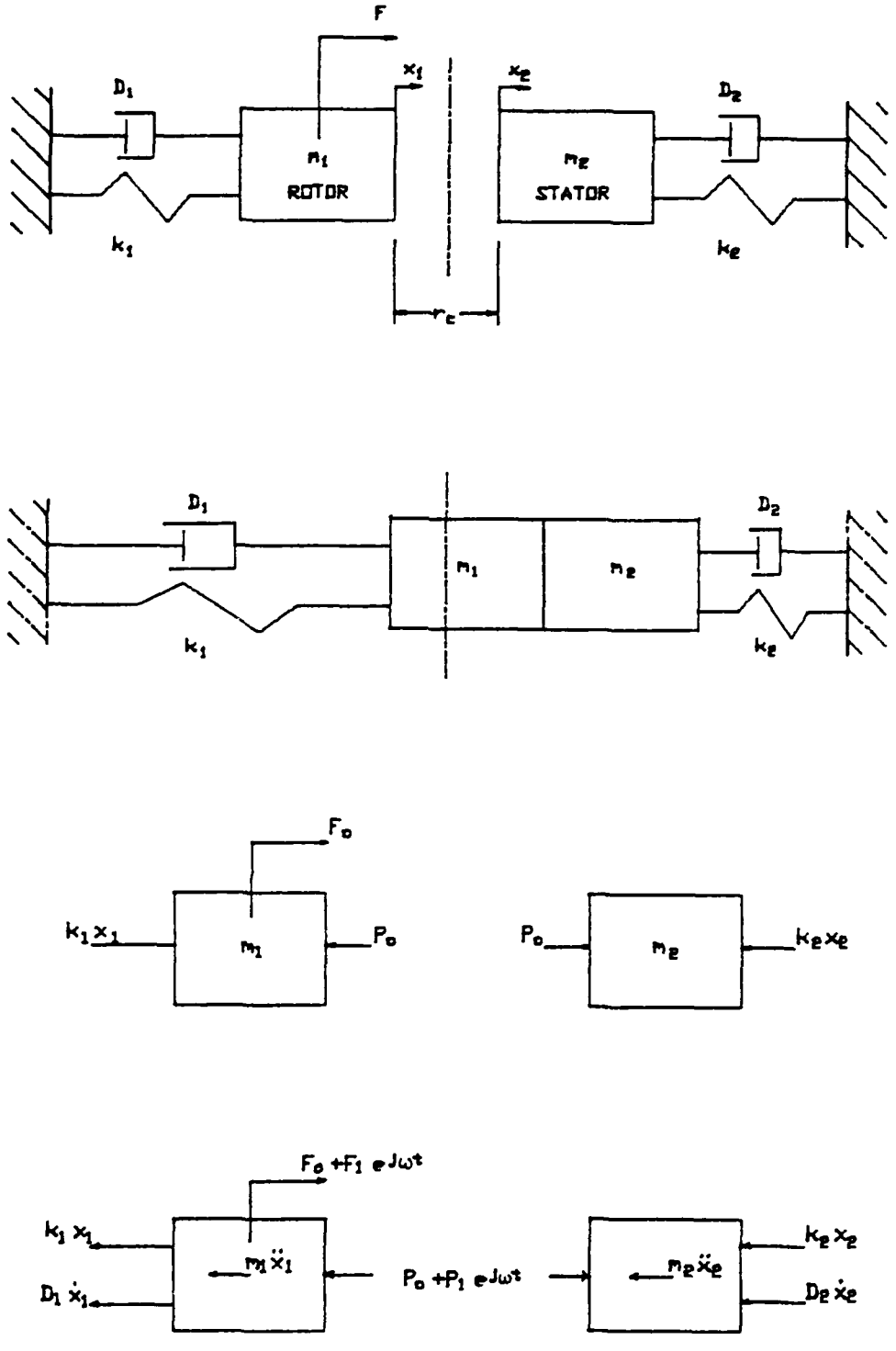

FIGURE 18. TRANSLATIONAL RUB MODEL

interface.

By assuming the coupled system's response is a harmonic motion of magnitude Δ, and recalling the kinematic relationship between x_1 and x_2, the rotor's and stator's displacement variables may be rewritten:

$$x_1 = (r_c + P_o/k_2 + \Delta e^{j\omega t})$$

$$x_2 = (P_o/k_2 + \Delta e^{j\omega t})$$

Making these substitutions into Equations (22) and (23) results in the following equations of motion:

rotor:

$$-k_1(r_c+P_o/\kappa_2+\Delta e^{j\omega t}) - D_1(j\omega)\Delta e^{j\omega t} - P_o - P_1 e^{j\omega t} + F_o + F_1 e^{j\omega t} = -m_1\Delta\omega^2 e^{j\omega t}$$

stator:

$$-k_2(P_o/\kappa_2+\Delta e^{j\omega t}) - D_2(j\omega)\Delta e^{j\omega t} + P_o + P_1 e^{j\omega t} = m_2\Delta\omega^2 e^{j\omega t}$$

These relationships are valid only if the rotor and stator elements maintain continuous contact. Eliminating the static equilibrium relationships from the above equations and solving each equation for the dynamic reaction at the interface yields equivalent relationships:

$$P_1 = F_1 + \Delta(-k_1 - j\omega D_1 + m_1\omega^2)$$

$$P_1 = \Delta(k_2 + j\omega D_2 - m_2\omega^2)$$

These two relationships may be reduced to a single equation and solved for the magnitude of the vibrational response:

$$\Delta = \frac{F_1}{[(k_1 + k_2) - \omega^2(m_1 + m_2)] + j\omega(D_1 + D_2)} \qquad (24)$$

The criterion that 'synchronous rub' (as portrayed by this model) remains in equilibrium is evidenced through the model by a positive reaction force at the interface, i.e., that the magnitude of the dynamic reaction force be less than the static reaction force:

$$|P_1| < P_o$$

disregarded since only the magnitudes involved affect the "equilibrium criterion". Rearranging terms results in the final criterion dictating the equilibrium of synchronous rub:

$$\frac{|F_1|}{\left[\left(1 - \frac{\omega^2}{\omega_N^2}\right)^2 + \left(2\zeta_o \frac{\omega}{\omega_N}\right)^2\right]^{1/2}} < \frac{(F_o - k_1 r_c)}{\left[\left(1 - \frac{\omega^2}{\omega_{N2}^2}\right)^2 + \left(2\zeta_2 \frac{\omega}{\omega_{N2}}\right)^2\right]^{1/2}} \qquad (26a)$$

The inter-relationships of the various terms: $|F_1|$ relative to $(F_o - k_1 r_c)$, and $\{[1 - (\omega^2/\omega_N^2)]^2 + [2\zeta_o(\omega/\omega_N)]^2\}^{1/2}$ relative to $\{[1 - (\omega^2/\omega_{N2}^2)]^2 + [2\zeta_2(\omega/\omega_{N2})]^2\}^{1/2}$ outline various regimes in the plot of (force vs. frequency) where synchronous rub is in equilibrium. Four fundamental cases are depicted graphically in Figures (19) through (22):

(i) $(F_o - k_1 r_c) > |F_1|$ and $\omega_{N2} > \omega_N$

(ii) $(F_o - k_1 r_c) < |F_1|$ and $\omega_{N2} > \omega_N$

(iii) $(F_o - k_1 r_c) > |F_1|$ and $\omega_{N2} < \omega_N$

(iv) $(F_o - k_1 r_c) < |F_1|$ and $\omega_{N2} < \omega_N$

Throughout tnese figures, the shaded region indicates the speed regime wherein synchronous rub does not satisfy dynamic equilibrium in accordance with the condition provided by Equation (26a). The artificialities of the translational model are evidenced by the awkward low frequency behavior of the graphs. In particular, there is no clear correlation between the terms $(F_o - k_1 r_c)$ and F_1, and similar functions in the rotational system. A single most prominent observation in all four cases though, is that synchronous rub is not in equilibrium in the vicinity of the combined rotor-stator natural frequency. This supports earlier statements that it is the characteristics of the combined rotor-stator which govern the stability of synchronous rub.

Combining Equations (22), (23) and (24), this criterion becomes:

$$|F_1 - \Delta[(k_1 - \omega^2 m_1) + j\omega D_1]| < (F_o - k_1 r_c)k_2/(k_1 + k_2) \qquad (25)$$

$$|\Delta[(k_2 - \omega^2 m_2) + j\omega D_2]| < (F_o - k_1 r_c)k_2/(k_1 + k_2) \qquad (26)$$

Substituting for the variable Δ using Equation (24), this condition becomes:

$$\left|F_1 - \frac{F_1[(k_1 - \omega^2 m_1) + j\omega D_1]}{[(k_1 + k_2) - \omega^2(m_1 + m_2)] + j\omega(D_1 + D_2)}\right| < (F_o - k_1 r_c)\left(\frac{k_2}{k_1 + k_2}\right)$$

It is convenient to employ the following definitions when referring to the rotor, stator and combined rotor-stator:

$$\omega_N = [(k_1 + k_2)/(m_1 + m_2)]^{1/2}$$

$$\omega_{N1} = (k_1/m_1)^{1/2}$$

$$\omega_{N2} = (k_2/m_2)^{1/2}$$

$$\zeta_o = (D_1 + D_2)/2[(k_1 + k_2)(m_1 + m_2)]^{1/2}$$

$$\zeta_1 = D_1/2[k_1 m_1]^{1/2}$$

$$\zeta_2 = D_2/2[k_2 m_2]^{1/2}$$

The condition that "full annular synchronous rub" be a solution to system motion now becomes:

$$\left|F_1 \cdot \frac{k_2}{k_1 + k_2} \cdot \frac{[(1 - \frac{\omega^2}{\omega_{N2}^2}) + j(2\zeta_2 \frac{\omega}{\omega_{N2}})]}{[(1 - \frac{\omega^2}{\omega_N^2}) + j(2\zeta_o \frac{\omega}{\omega_N})]}\right| < (F_o - k_1 r_c)\frac{k_2}{k_1 + k_2}$$

This inequality may be further simplified by eliminating common factors and by writing the two complex dimensionless impedances in terms of their magnitude and phase. The phase relationships which evolve may be

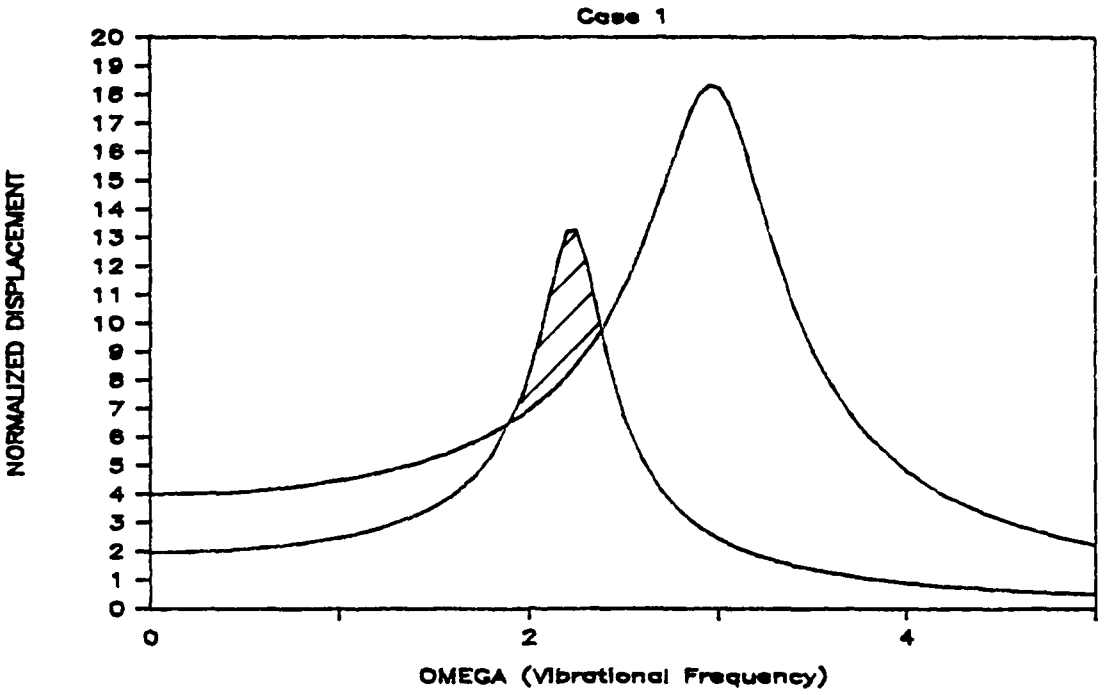

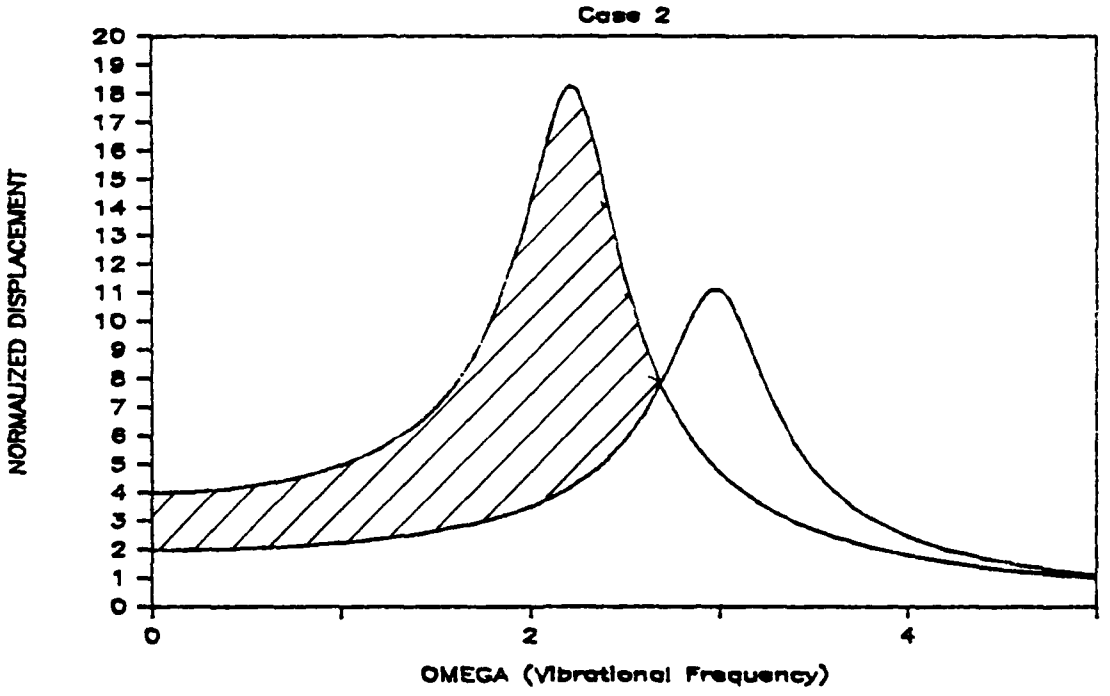

FIGURE 19 RUB CONDITION - CASE 1 (Top)
FIGURE 20. RUB CONDITION - CASE 2 (Bottom)

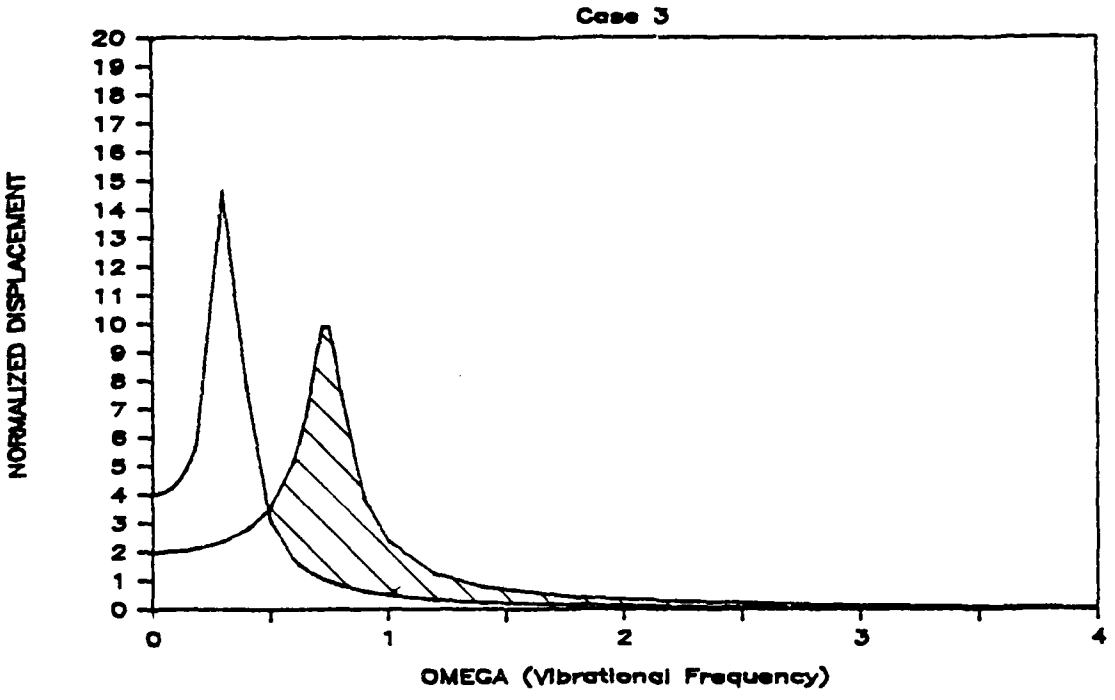

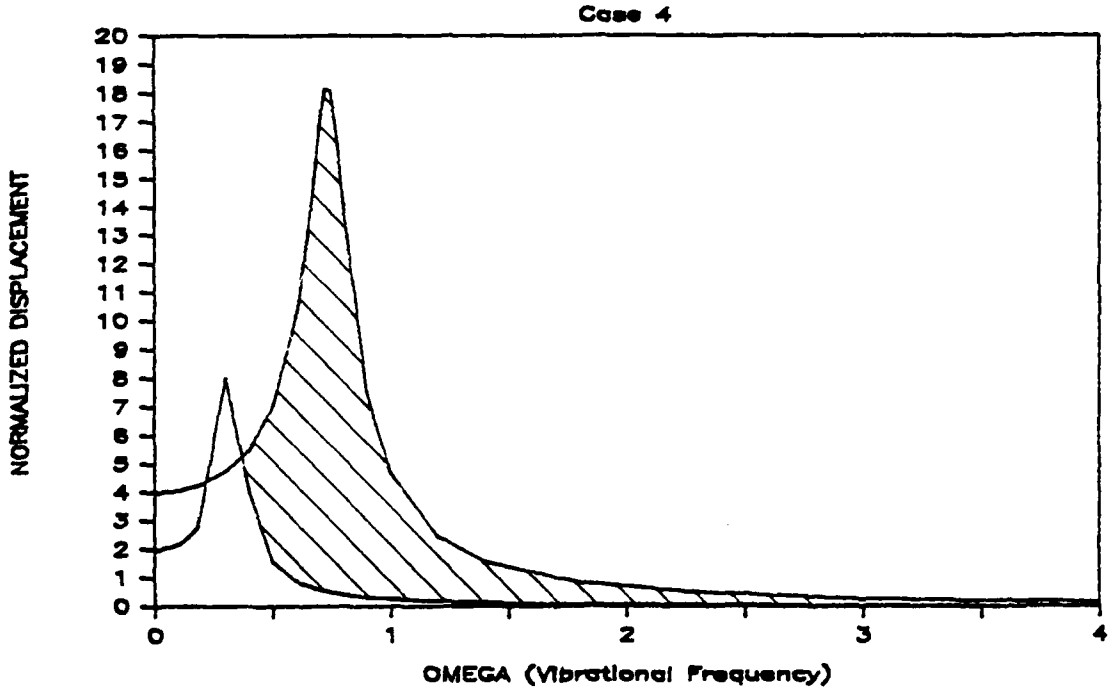

FIGURE 21. RUB CONDITION - CASE 3 (Top)
FIGURE 22. RUB CONDITION - CASE 4 (Bottom)

The more exact analysis of the rotor-stator dynamics requires the assignment of finite mass, radial stiffness and damping characteristics to the stator in Figure 2. As earlier stated, these characteristics are assumed axisymmetric. The reference position for both the rotor and stator displacements remains the imaginary bearing axis, B, which marks the rest position for the rotor and stator. Figure 23 depicts the rotor in contact with the stator; with the free body diagrams for each element provided in Figures 24(a) and (b). The equations of motion for the rotor and stator are developed according to the balance of forces in the free body diagrams. The forces acting on the rotor are identical in nature to the forces present in the rigid stator case. The balance of forces for the rotor is written:

$$-K_r\vec{z}_c - D_r\dot{\vec{z}}_c - \vec{R}(t) = M_r(\ddot{\vec{z}}_g) \qquad (27)$$

The reaction force which acts at the rotor-stator interface though, is now a variable which depends on both the rotor's and stator's dynamic characteristics. Since the stator is non-rigid, the reaction force drives the stator out of line with the bearing center-rotor center axis. The resultant phase relationship between the rotor displacement and the rub location may be described by the angle λ, which is a function of the rotor displacement, stator displacement and reaction force lines of action. Tne reaction force may thus be broken down into its normal and tangential (friction) components with a periodic time dependence characterized by the synchronous speed, ω, and the phase angle λ:

$$\vec{R}(t) = (N + j\mu N)e^{j(\omega t + \lambda)}$$

or

$$\vec{R}(t) = N(1 + \mu^2)^{1/2}\, e^{j(\omega t + \lambda + \psi)}$$

where $\psi = \tan^{-1}\mu$

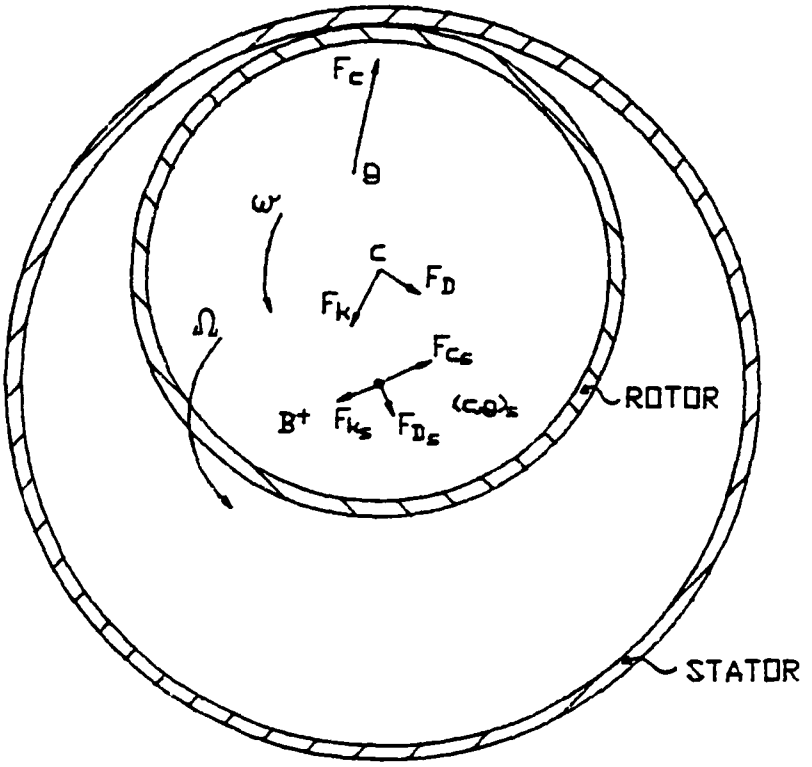

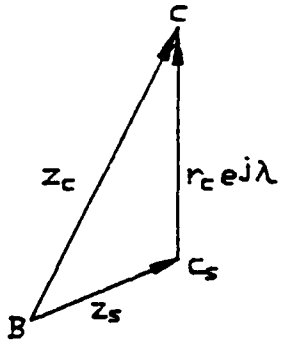

FIGURE 23(a). ROTOR-STATOR LOAD DIAGRAM (Top)
FIGURE 23(b). ROTOR-STATOR DISPLACEMENT VECTOR DIAGRAM

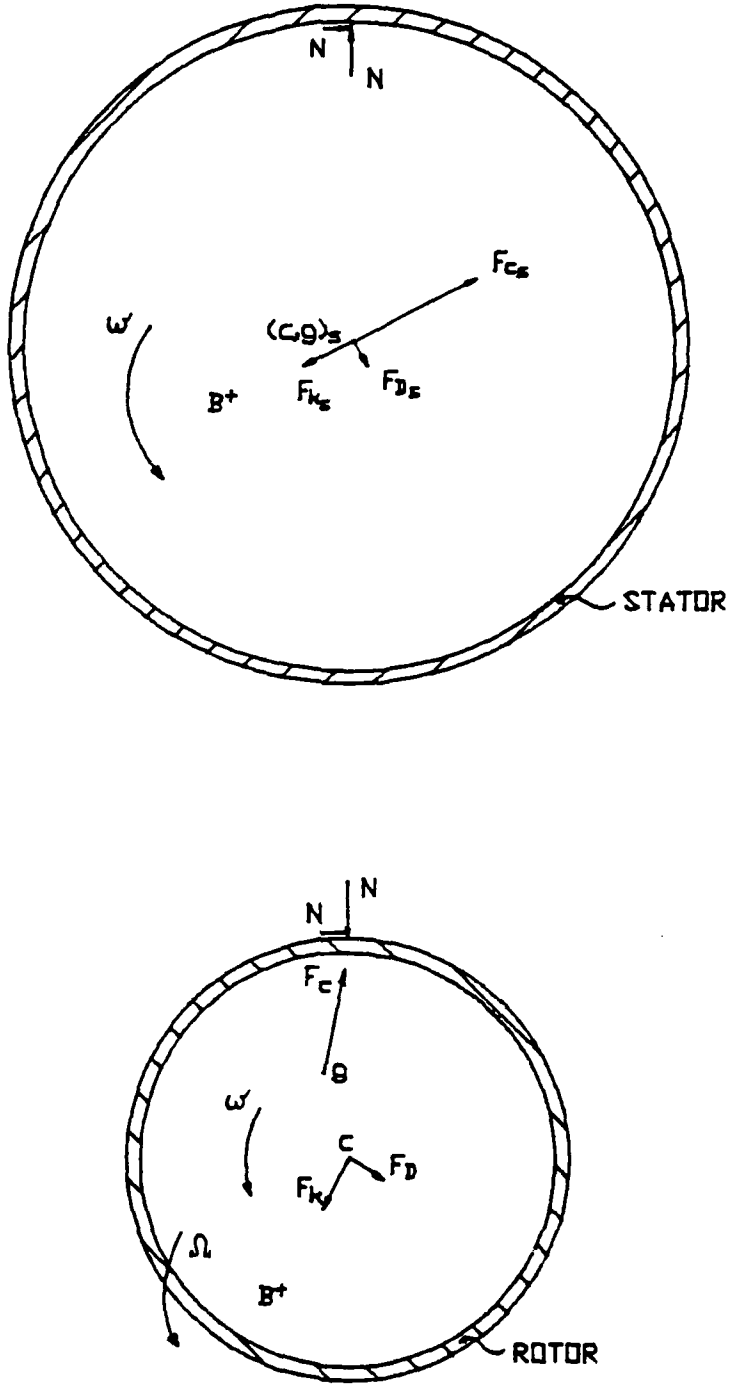

FIGURE 24. ROTOR AND STATOR FREE BODY DIAGRAMS

Additionally, the displacement of the rotor's center of gravity may be expressed:

$$\vec{z}_g = |\vec{z}_g| e^{j\omega t} + \delta e^{j(\omega t+\theta)}$$

θ is the phase angle which accounts for the lag between the rotor center and its forcing function. This forcing function now comprises both the centrifugal force due to unbalance, $\vec{F}_c$, and the reaction force, $\vec{R}(t)$. The resulting expression for θ is thus a function of three phase angles: ϕ, the phase angle due to rotor damping; ψ, the phase angle describing the line of action of the reaction force at the rub location; and λ, the phase difference between the rub location and the rotor center's displacement:

$$\theta = \tan^{-1}[\omega D_r + N(1+\mu^2)^{1/2}\sin(\psi+\lambda)]/[(K_r - \omega^2 M_r) + N(1+\mu^2)^{1/2}\cos(\psi+\lambda)]$$

Making these substitutions, the force balance equation for the rotor may now be written:

$$-K_r\vec{z}_c - D_r\dot{\vec{z}}_c - N(1+\mu^2)^{1/2}e^{j(\omega t+\lambda+\psi)} = M_r \frac{d^2}{dt^2}(\vec{z}_c + \delta e^{j(\omega t+\theta)}) \quad (28)$$

Equation (28) may be solved for the displacement of the rotor center:

$$\vec{z}_c = \frac{\omega^2 M_r \delta e^{j(\omega t+\theta)} - N(1+\mu^2)^{1/2}e^{j\omega t+\lambda+\psi)}}{[(K_r - \omega^2 M_r) + (j\omega D_r)]}$$

Breaking the rotor's impedance down to its magnitude and phase yields:

$$\vec{z}_c = \frac{\omega^2 M_r \delta e^{j(\omega t+\theta)} - N(1+\mu^2)^{1/2}e^{j(\omega t+\lambda+\psi)}}{[(K_r - \omega^2 M_r)^2 + (\omega D_r)^2]^{1/2}} e^{-j\phi} \quad (29)$$

Dividing through by the term $r_c e^{j\omega t}$ and substituting non-dimensional variables, the rotor displacement may be finally written:

$$\frac{\vec{z}_c}{r_c e^{j\omega t}} = \frac{\varepsilon\beta^2 e^{j\theta} - n(1+\mu^2)^{1/2} e^{j(\psi+\lambda)}}{[(1-\beta^2)^2 + (2\zeta\beta)^2]^{1/2}} e^{-j\phi} \quad (29a)$$

Whereas the centrifugal force due to unbalance drives the rotor's motion, it is the synchronous rub force (i.e., the reaction force, $\vec{R}(t)$) which acts as the input driving force for the stator's motion. The forces which respond to this driving force are the stator's inertial, elastic and damping responses. The force balance for the stator is derived from the free body diagram:

$$-K_s\vec{z}_s - D_s\dot{\vec{z}}_s - \vec{R}(t) = M_s\ddot{\vec{z}}_s \tag{30}$$

By assuming a synchronous whirl response by the stator, $\vec{z}_s = |\vec{z}_s|e^{j(\omega t+\eta)}$ and solving for $\vec{z}_s$, the stator's equation of motion is determined:

$$\vec{z}_s = \frac{\vec{R}(t)}{[(K_s - \omega^2 M_s) + (j\omega D_s)]}$$

Reducing the stator's receptance to a magnitude and phase, τ, and substituting for the reaction force, the stator's equation of motion becomes:

$$\vec{z}_s = \frac{N(1+\mu^2)e^{j(\omega t+\psi+\lambda)}}{[(K_s - \omega^2 M_s)^2 + (\omega D_s)^2]^{1/2}} e^{-j\tau}$$

where $\tau = \tan^{-1}\dfrac{\omega D_s}{K_s - \omega^2 M_s}$

This equation may be expressed in non-dimensional terms by utilizing the following definitions:

$$\omega_{Ns} = \sqrt{K_s/M_s}$$

$$\beta_s = \omega/\omega_{Ns}$$

$$\zeta_s = D_s/[2\sqrt{K_s M_s}]$$

Now dividing through by the term $r_c e^{j\omega t}$ and factoring out the ratio (K_r/K_s), the non-dimensional relation for the stator's displacement becomes:

$$\frac{\vec{z}_s}{r_c e^{j\omega t}} = \frac{(\frac{K_r}{K_s})n(1+\mu^2)^{1/2} e^{j(\psi+\lambda-\tau)}}{[(1-\beta_s^2)^2 + (2\zeta_s\beta_s)^2]^{1/2}} \tag{31}$$

Two variables of interest in this analysis are the rotor's displacement and the reaction force at the rotor-stator interface. To determine the rotor's displacement $\vec{z}_c$, Equations (27) and (30) are utilized. The reaction force acting upon the stator is equal in magnitude but opposite in direction to that acting upon the rotor, so Equations (27) and (30) may be combined with the force term $\vec{R}(t)$ eliminated:

$$-K_r\vec{z}_c - K_s z_s - D_r\dot{\vec{z}}_c - D_s\dot{\vec{z}}_s = M_r\ddot{\vec{z}}_g + M_s\ddot{\vec{z}}_s \tag{32}$$

Figure 23(b) provides the vector triangle relating the stator displacement, rotor displacement and radial clearance. The kinematic condition which arises from the geometry presented here is given by:

$$\vec{z}_c - \vec{z}_s = r_c e^{j(\omega t+\lambda)}$$

The implication here is twofold:

(i) The magnitude of the rotor displacement relative to the stator displacement equals the radial clearance between the two elements.

(ii) The point of contact between the two elements must be in line with the centers of the displaced rotor and stator.

Applying this kinematic relationship and the previously derived condition, $\vec{z}_g = \vec{z}_c + \delta e^{j(\omega t+\phi)}$, results in the following equation of motion for the rotor:

$$(M_r + M_s)\ddot{\vec{z}}_c + (D_r + D_s)\dot{\vec{z}}_c + (K_r + K_s)\vec{z}_c = M_r \frac{d^2}{dt^2}(\delta e^{j(\omega t+\phi)}) + K_s r_c e^{j(\omega t+\lambda)}$$

The synchronous whirl solution is thus given by:

$$\vec{z}_c = \frac{[\omega^2 M_r \delta e^{j\phi} + K_s r_c e^{j\lambda}] e^{j\omega t}}{[(K_r + K_s) - \omega^2(M_r + M_s)] + j[\omega(D_r + D_s)]} \tag{33}$$

The time-independent, non-dimensional solution for the rotor displacement is obtained by dividing each side by the quantity $r_c e^{j\omega t}$ and factoring out K_r on the right hand side. The resulting expression is:

$$\frac{\vec{z}_c}{r_c e^{j\omega t}} = \frac{\varepsilon\beta^2 e^{j\phi} + \frac{K_s}{K_r} e^{j\lambda}}{\{[(1-\beta^2) + \frac{K_s}{K_r}(1-\beta^2 \frac{\omega_{Nr}}{\omega_{Ns}}^2)]^2 + [2\zeta\beta + 2\zeta\beta \frac{\omega_{Nr}}{\omega_{Ns}}]^2\}^{1/2}} e^{-j\kappa} \tag{33a}$$

$$\text{where } \kappa = \tan^{-1} \frac{\omega(D_r + D_s)}{(K_r + K_s) - \omega^2(M_r + M_s)}$$

This equation is further reduced to a single magnitude and phase in the following:

$$\frac{\vec{z}_c}{r_c e^{j\omega t}} = \frac{[(\varepsilon\beta^2\cos\phi + \frac{K_s}{K_r}\cos\lambda)^2 + (\varepsilon\beta^2\sin\phi + \frac{K_s}{K_r}\sin\lambda)^2]^{1/2}}{\{[(1-\beta^2) + \frac{K_s}{K_r}(1-\beta^2 \frac{\omega_{Nr}}{\omega_{Ns}}^2)]^2 + [2\zeta\beta + 2\zeta\beta \frac{\omega_{Nr}}{\omega_{Ns}}]^2\}^{1/2}} e^{j(\nu-\kappa)} \tag{33b}$$

$$\text{where } \nu = \tan^{-1} \frac{(\varepsilon\beta^2\sin\phi + \frac{K_s}{K_r}\sin\lambda)}{(\varepsilon\beta^2\cos\phi + \frac{K_s}{K_r}\cos\lambda)}$$

The reaction force is more difficult to solve than the rotor displacement, but provides much meaningful information regarding the rub motion. A positive reaction force indicates full annular synchronous rub is in equilibrium. Conversely, a negative reaction force indicates a no-rub action, while an imaginary reaction force indicates full annular synchronous rub is not in equilibrium (i.e., not a solution to the rub equation). In

order to solve for the reaction force as a function of the rotor speed, the kinematic condition relating the rotor and stator motion must once again be applied:

$$\frac{\vec{z}_c - \vec{z}_s}{r_c e^{j\omega t}} = e^{j\lambda}$$

The rotor's displacement relative to the stator is derived from Equations (29a) and (31):

$$\frac{\vec{z}_c - \vec{z}_s}{r_c e^{j\omega t}} = \frac{\varepsilon\beta^2 e^{j(\theta-\phi)}}{R_r^{1/2}} - n(1+\mu^2)^{1/2} e^{j(\psi+\lambda)}\left[\frac{e^{-j\phi}}{R_r^{1/2}} + \frac{(\frac{K_r}{K_s})e^{-j\tau}}{R_s^{1/2}}\right]$$

where $R_r = [(1-\beta^2)^2 + (2\zeta\beta)^2]$

and $R_s = [(1-\beta_s^2)^2 + (2\zeta_s\beta_s)^2]$

Applying the above kinematic condition, this equation may be written:

$$\frac{\varepsilon\beta^2 e^{j(\theta-\phi)}}{R_r^{1/2}} - n(1+\mu^2)^{1/2}\left[\frac{e^{j(\psi-\phi)}}{R_r^{1/2}} + \frac{(\frac{K_r}{K_s})e^{j(\psi-\tau)}}{R_s^{1/2}}\right]e^{j\lambda} = e^{j\lambda}$$

Solving for the phasor $e^{j\lambda}$ yields:

$$e^{j\lambda} = \{R_s^{1/2}\varepsilon\beta^2 e^{j(\theta-\phi)}\}/$$

$$\{(R_r R_s)^{1/2} + n(1+\mu^2)^{1/2}[R_s^{1/2}\cos(\psi-\phi) + (\frac{K_r}{K_s})R_r^{1/2}\cos(\psi-\tau)] +$$

$$jn(1+\mu^2)^{1/2}[R_s^{1/2}\sin(\psi-\phi) + (\frac{K_r}{K_s})R_r^{1/2}\sin(\psi-\tau)]\}$$

By defining

$$\sigma = \tan^{-1}\left\{\frac{n(1+\mu^2)^{1/2}[R_s^{1/2}\sin(\psi-\phi) + (\frac{K_r}{K_s})R_r^{1/2}(\psi-\tau)]}{(R_rR_s)^{1/2} + n(1+\mu^2)^{1/2}[R_s^{1/2}\cos(\psi-\phi) + (\frac{K_r}{K_s})R_r^{1/2}\cos(\psi-\tau)]}\right\}$$

then the relationship becomes:

$$e^{j\lambda} = \{R_s^{1/2}\varepsilon\beta^2 e^{j(\theta-\phi-\sigma)}\}/$$

$$(\{(R_rR_s)^{1/2} + n(1+\mu^2)^{1/2}[R_s^{1/2}\cos(\psi-\phi) + (\frac{K_r}{K_s})R_r^{1/2}\cos(\psi-\tau)]\}^2 +$$

$$+\{n(1+\mu^2)^{1/2}[R_s^{1/2}\sin(\psi-\phi) + (\frac{K_r}{K_s})R_r^{1/2}\sin(\psi-\tau)]\}^2)^{1/2} \quad (34)$$

Therefore, the phase angle may be defined in terms of known variables:

$$\lambda = (\theta - \phi - \sigma) \ ,$$

with the magnitude of Equation (32) being equal to unity. The square of the magnitude may also be equated to unity, yielding:

$$R_s(\varepsilon\beta^2)^2/(\{(R_rR_s)^{1/2} + n(1+\mu^2)^{1/2}[R_s^{1/2}\cos(\psi-\phi) + (\frac{K_r}{K_s})R_r^{1/2}\cos(\psi-\tau)]\}^2 +$$

$$+ \{n(1+\mu^2)^{1/2}[R_s^{1/2}\sin(\psi-\phi) + (\frac{K_r}{K_s})R_r^{1/2}\sin(\psi-\tau)]\}^2) = 1 \quad (34a)$$

Equation (34a) is resolved into a quadratic equation in the variable n in the following expression:

$$n^2(1+\mu^2)^{1/2}[1+2(\frac{K_r}{K_s})\frac{R_r^{1/2}}{R_s^{1/2}}\cos(\tau-\phi) + (\frac{K_r}{K_s})^2\frac{R_r}{R_s}] +$$

$$+ 2n[R_r^{1/2}\cos(\psi-\theta) + (\frac{K_r}{K_s})\frac{R_r}{R_s^{1/2}}\cos(\psi-\tau)] + \frac{(R_r - \varepsilon^2\beta^4)}{(1+\mu^2)^{1/2}} = 0$$

Solving this equation for the normal force, n, yields the lengthy expression:

$$n = (-[R_r^{1/2}\cos(\psi-\theta) + (\frac{K_r}{K_s})\frac{R_r}{R_s}^{1/2}\cos(\psi-\tau)] \pm$$

$$\pm \{[R_r^{1/2}\cos(\psi-\phi) + (\frac{K_r}{K_s})\frac{R_r}{R_s}^{1/2}\cos(\psi-\tau)]^2 -$$

$$- [1+2\frac{K_r}{K_s}\frac{R_r}{R_s}^{1/2}\cos(\tau-\phi) + (\frac{K_r}{K_s})^2\frac{R_r}{R_s}][R_r - \varepsilon^e\beta^4]\}^{1/2})/$$

$$\{(1+u^2)^{1/2}[1+2\frac{K_r}{K_s}\frac{R_r}{R_s}^{1/2}\cos(\tau-\phi) + (\frac{K_r}{K_s})^2\frac{R_r}{R_s}]\} \qquad (35)$$

An alternative expression is derived by applying the following relationships:

$$\cos(\psi - \phi) = \frac{[(1-\beta^2) + 2\zeta\beta\mu]}{(1+\mu^2)^{1/2}\,R_r^{1/2}}$$

$$\cos(\psi - \tau) = \frac{[(1-\beta_s^2) + 2\zeta_s\beta_s\mu]}{(1+\mu^2)^{1/2}\,R_s^{1/2}}$$

$$\cos(\tau - \theta) = \frac{(1-\beta^2)(1-\beta_s^2) + (2\zeta\beta)(2\zeta_s\beta_s)}{R_r^{1/2}R_s^{1/2}}$$

Making these substitutions:

$$n = (-[(1-\beta^2 + 2\zeta\beta\mu) + \frac{K_r}{K_s}\frac{R_r}{R_s}(1-\beta_s^2 + 2\zeta_s\beta_s\mu)] \pm$$

$$\pm \{[(1-\beta^2 + 2\zeta\beta\mu) + \frac{K_r}{K_s}\frac{R_r}{R_s}(1-\beta_s^2 + 2\zeta_s\beta_s\mu)]^2$$

$$- [1+2\frac{K_r}{K_s}\frac{(1-\beta^2)(1-\beta_s^2)+(2\zeta\beta)(2\zeta_s\beta_s)}{R_s} + (\frac{K_r}{K_s})^2\frac{R_r}{R_s}](1+\mu^2)[R_r - \varepsilon^2\beta^4]\}^{1/2})/$$

$$\{(1+\mu^2)[1+2\frac{K_r}{K_s}\frac{(1-\beta^2)(1-\beta_s^2) + (2\zeta\beta)(2\zeta_s\beta_s)}{R_s} + (\frac{K_r}{K_s})^2\frac{R_r}{R_s}]\} \qquad (36)$$

It should be noted that the expression above reduces to the earlier derived result for rub against a rigid stator (Equation 11)) by employing the corresponding conditions:

$K_s = \infty$, therefore $K_r/K_s = 0$

$$\omega_{Ns} = \infty$$

$$\zeta_s = 0$$

$$\beta_s = 0$$

$$R_s = 1.0$$

The impact of releasing restrictions on the stator's dynamic behavior is particularly complex due to the numerous variables involved. By comparing Equations (11) and (35) though, qualitative conclusions may be drawn. There are three dynamic 'elements' significant to this system: the rotor, the stator and the combined rotor-stator. The character of the response of each element is dependent on the speed of excitation and the element's natural frequency. By considering the magnitude of a generic element's mechanical impedance, $[(K - \omega^2 M)^2 + (\omega D)^2]^{1/2}$, then it is apparent that at low excitation frequencies, the response is as a stiff spring, characterized by the value of K. At high frequencies, the response is as a massive element; characterized by the value of M. The response is a maximum in the vicinity of the natural frequency, $\sqrt{K/M}$, (specifically at $\omega = [\omega_N^2 - D^2/2M]^{1/2}$). These simple principles may be applied to help explain the dynamics of the rotor-stator system.

Given the rotor's and stator's characteristic mass and stiffness; the composite element's natural frequency, ω_N, occurs between ω_{Nr} and ω_{Ns}:

$$\omega_N = \sqrt{\frac{K_r + K_s}{M_r + M_s}}$$

Three simple relationships thus exist between the rotor and stator:

(i) the stator's natural frequency is greater than the rotor's natural frequency

(ii) the stator's natural frequency is less than the rotor's natural frequency

(iii) the stator's natural frequency is of the order of the rotor's natural frequency

Each of these relationships may be satisfied by several conditions relating the elements' mass and stiffness. For example, $\omega_{Ns} > \omega_{Nr}$ is unconditionally true when $K_s > K_r$ and $M_s = M_r$ or when $K_s = K_r$ and $M_s < M_r$. It is conditionally true when $K_s > K_r$ and $M_s > M_r$ or when $K_s < K_r$ and $M_s < M_r$. It is evident that a large number of cases may be analyzed based on the relative masses and stiffnesses alone. This is exacerbated when variations in unbalance, friction and damping are investigated.

If ω_{Ns} is sufficiently greater than ω_{Nr}, then when rub first initiates, the stator response resembles the infinitely stiff case; with the resulting reaction force depending directly on K_s. In general, since it is the stator's stiffness which keeps it pressed against the precessing rotor at speeds below ω_N, then continuous synchronous rub becomes a less stable mode of motion as K_s decreases. As rotor speed approaches ω_N, the rotor-stator system becomes very compliant and continuous synchronous rub will cease (i.e., the radical term in Equation (36) becomes negative). As the rotor speed further increases and reaches ω_{Ns}, the stator alone is extremely

compliant. Since a small push by the rotor thus brings a disproportionately large response by the stator, then continuous contact may rapidly diminish. (This is evident in Equation (36) since the value of R_s tends toward zero as β_s approaches 1.0 and the negative term within the radical, $-(K_r/K_s)^2(R_r/R_s)$, becomes dominant). Throughout this speed regime, the rotor's motion (if unperturbed) is identical to that of the free rotor. At yet higher speeds, the stator's mass dominates the character of its response. Using limit analysis, the stator's behavior once again approaches the rigid response at very high speeds ($\beta >> \beta_s$). The criterion for stability of synchronous rub at very high speeds is identical to that for an infinitely stiff stator; i.e.,

$$\text{if } \varepsilon > \frac{\mu}{(1+\mu^2)^{1/2}}$$

then synchronous rub is stable for $\beta >> \beta_s$

At this speed though, the rotor must be perturbed to initiate the rub.

If ω_{Ns} and ω_{Nr} are equal, then the stator's response resembles the rotor's response for any particular excitation frequency. Therefore, the speed at which the combined rotor-stator is most compliant coincides with the speed at which the free-rotor's runout is greatest. This similarity in response tends to nullify the stator's non-rigid character if (K_r/K_s) and (M_r/M_s) are greater than 1.0. As K_s and M_s are increased, the response rapidly approaches the rigid stator case. When the stator's dynamic characteristics equal the rotor's, then the speed regime in which continuous synchronous rub is a solution to rotor motion is identical to the rigid stator case and the reaction force is exactly half that which would result if the stator were rigid. As the stator becomes less stiff and less massive, synchronous rub becomes less stable. In the limit, for low values

of (K_s/K_r), the system is unable to sustain a continuous rub with the precessing rotor.

If the stator's natural frequency is measurably less than the rotor's, then the speed regime in which the stator is most compliant occurs prior to the initiation of rub. When the rotor first gains contact, the stator's impedance and that of the combined rotor-stator are increasing with the square of the speed. The response of the system rapidly approaches that of the rigid stator case as M_s increases and thus either ω_{Ns} decreases or, for a constant ω_{Ns}, K_s increases. If in fact a low value of ω_{Ns} is due to low values of both K_s and M_s, then ω_N may be approximated by ω_{Nr} and the rub response is as described previously for $\omega_N = \omega_{Nr}$.

The impact of the stator's damping characteristics are straightforward. Independent of the natural frequencies, stiffnesses or masses of the rotor and stator; any increase in the stator's damping coefficient tends to diminish the equilibrium of synchronous rub. Assuming light damping for both rotor and stator, variations in stator damping has little effect on the magnitude of the reaction force during rub.

In summary, if the stator's natural frequency is greater than the rotor's natural frequency, then synchronous rub is not in equilibrium throughout a speed regime which encompasses the stator's and the combined rotor-stator's natural frequencies (ω_{Ns} and ω_N respectively). This speed regime widens for a given value of ω_{Ns} as the stator stiffness, K_s, and stator mass, M_s, are decreased. Similarly, the reaction force experienced during continuous rub for a given value of ω_{Ns} decreases as K_s and M_s are decreased. As the stator's natural frequency is reduced towards the rotor's natural frequency, this particular speed regime where synchronous rub is not viable diminishes accordingly. When $\omega_{Ns} = \omega_{Nr}$, the stability of synchronous

rub resembles that of the rotor against a rigid stator; being more stable if (K_r/K_s) (and thus (M_r/M_s)) is less than unity and vice versa. As may be expected, the reaction force in this case increases as K_s and M_s increase. As the values of ω_N and ω_{Ns} are reduced below ω_{Nr} the synchronous rub system response becomes as stable as if the rotor were rubbing against a rigid stator. This is true since the stator's impedance rapidly increases with the square of the excitation frequency. Regarding stator damping, any increase in the damping coefficienct, D_s, reduces the speed regime in which synchronous rub may occur. In general, the stator's finite mass, stiffness and damping characteristics serve to abate the negative characteristics of rotor rub. In no case do these characteristics intensify the reaction forces between the two elements (when compared with rub against a rigid stator), but rather they tend to reduce the reaction forces, often sufficient enough to create a dynamic relationship less favorable for full annular synchronous rub (and too, reverse whirl).

Appendix A presents a numerical investigation of the impact of varying the parameters discussed in this section. Through the efforts of Professor Udo Fischer of the University of Magdeburg, Magdeburg, East Germany, a Fortran program has been developed which clearly demonstrates the time dependent response of the rotor and stator in accordance with the equations of motion developed here. The stability of the synchronous rub precession in those speed regimes where this mode of rotor motion is in equilibrium is clearly demonstrated.

6. CONCLUSIONS AND RECOMMENDATIONS FOR FUTURE WORK

Mechanical vibrations in rotating machinery result from any mass unbalance present in the rotating element. Should rotor rub occur as a result of these vibrations, the integrity of the system may be significantly impaired. Two direct solutions to this problem are immediately apparent:

(i) Reduce the mass unbalance which drives the vibrations in the system, or

(ii) Increase the radial clearance between the rotating element and the stationary element.

Both of these solutions are costly, either through the precision required in the manufacturing phase or efficiency lost throughout the operational life of the system.

The dynamics of rotor rub are quite complex, but in general a system may be resolved to one of four behavioral types dependent on the system's parameters:

(i) Synchronous precession without rub

(ii) Partial rotor rub

(iii) Full annular rotor rub

(iv) Reverse whirl

Most rotating machinery are designed for the no-rub condition. Analytically, rub may be anticipated if the ratio of the mass eccentricity-to-the-

radial clearance exceeds twice the damping ratio for the system. Should rub occur, the equilibrium of full annular rub is then dependent on both the rotor's and stator's dynamic characteristics, the system's unbalance, the radial clearance and friction experienced between the two contacting surfaces, and the rotor's speed.

Initial analysis was conducted with the assumption that the system's stator is infinitely rigid. Dependent upon the system's damping ratio, displacement-to-clearance ratio and frictional coefficient; the rotor's response as a function of speed can then be characterized according to one of the following:

(i) Limited synchronous rub: Synchronous rub is in equilibrium up to a "critical speed" (unique to each system) above which equilibrium is never regained.

(ii) Synchronous rub - limited discontinuity: Similar to the limited rub case, equilibrium is lost at some critical speed, but is then regained at a higher speed.

(iii) Continuous synchronous rub: As the description implies, this type system is able to find an equilibrium position for all rotor speeds.

Speed regimes where full annular rub is either not in equilibrium or not stable may fall into a partial rub (if this mode is in stable equilibrium at this rotor speed) or jump down to a synchronous whirl without rub. An alternative mode of rotor motion which may be stable under these conditions is a reverse whirl driven by the counter-torque produced by the frictional forces acting on the rotor. Some disturbance is necessary to perturb the system into the reverse whirl, but such may occur through a

transient partial rub motion following the deterioration of full annular rub.

Expanding the analysis to investigate the impact of the stator being non-rigid results in extremely detailed equations describing the motion of the system and the forces at work between the rotating and stationary element. In contrast to the rigid-stator system, the stator now joins with the rotor in responding to the unbalance driving the vibrations. In general, equilibrium of the full annular rub diminishes in the vicinity of the combined rotor-stator natural frequency (which previously was infinite). Additionally, the amplitude of the motion varies greatly now that the stator is not absolutely constraining. If the stator natural frequency is greater than the rotor natural frequency, then the recurrence of rub at speeds above this requires some perturbation to initiate contact. In general, the finite dynamic characteristics assigned to the stator which make it non-rigid diminish the reaction forces experienced by the rotor and stator (as compared to the rigid stator case) and in fact may create a dynamic relationship less favorable for full annular synchronous rub.

Much work remains to be accomplished in the study of rotor rub. Experimental investigation of the results presented here would prove particularly meaningful in validating the results and justifying the assumptions made. An analytical investigation of the equilibrium conditions for partial rotor rub would be very complementary to this study on the full annular rub problem. Of particular significance would be work which contributes to the analytical determination of the stability of full annular rub, partial rub and reverse whirl for a rotational system as a function of the excitation frequency.

REFERENCES

1. Ehrich, F.F., "The Dynamic Stability of Rotor-Stator Radial Rubs in Rotating Machinery," Paper, ASME, 56, No. 6, 1969.
2. Muszynska, Agnes, "Rub -- An Important Malfunction in Rotating Machinery," Proc. Senior Mechanical Engineering Seminar, Bently Nevada Corporation, Carson City, Nevada, June 1983.
3. Muszynska, A., "Partial Lateral Rotor to Stator Rubs," Third International Conference: Vibrations in Rotating Machinery, York, United Kingdom, 1984.
4. Bently, D.E., "Forced Subrotative Speed Dynamic Action of Rotating Machinery," ASME Publication, 74-Pet-16, Petroleum Mechanical Engineering Conference, Dallas, TX, September 1974.
5. Kascak, A.F., "The Response of Turbine Engine Rotors to Interference Rubs," NASA Technical Memorandum 81518, Technical Report 80-C-14, 1980.
6. Muszynska, A., "Modal Analysis and Vibration Diagnostics in Machinery," Proc. Eighth Machinery Dynamics Seminar, Halifax, Nova Scotia, Canada, October, 1984.
7. Rabinowicz, Ernest, Friction and Wear of Materials, John Wiley & Sons, New York, N.Y., 1965.
8. den Hartog, J.P., Mechanics, McGraw Hill, New York, N.Y., 1948.
9. Black, H.F., "Interaction of a Whirling Rotor with a Vibrating Stator Across a Clearance Annulus," Journal, Mechanical Engineering Science, V.10, No. 1, 1968.
10. Johnson, D.C., "Synchronous Whirl of a Vertical Shaft Having Clearance in One Bearing," Journal, Mechanical Engineering Science, Vo.85, No. 1, 1962.

11. Billett, R.A., "Shaft Whirl Induced by Dry Friction," Engineer, V.220, No. 5727, 1965.

12. Childs, D.W., "Fractional-Frequency Rotor Motion Due to Non-symmetric Clearance Effects," ASME Publication, 81-GT-145, International Gas Turbine Conference and Products Show, Houston, TX, March 1981.

13. Morris, J., "The Impact of Bearing Clearances on Shaft Stability: A New Approach to Shaft Balancing," Aircraft Engineering, V.29, December 1957.

14. den Hartog, J.P., Mechanical Vibration, 2nd ed., McGraw Hill, New York, N.Y., 1940.

APPENDIX A

It is the intent in this Appendix to investigate the dynamics of several exemplary rotor-stator systems in accordance with the analysis thus far conducted for rotor-rub. Unlimited combinations of rotor and stator dynamic characteristics are possible, but here a limited number are studied to demonstrate the impact on system behavior of varying key parameters. In particular, variations in rotor and stator natural frequencies, stiffnesses, masses and damping characteristics are investigated. Similarly, the effects of varying the magnitude of the unbalance and friction are studied. The indicators for system behavior deemed here to convey the most information are:

(i) Rotor Amplitude vs. Speed

(ii) Normal Force vs. Speed

(iii) Rotor and Stator Displacement History

Synchronous rub is presumed in the analysis, and is indicated by stable rotor displacement solutions (aside from the fundamental free-rotor solution) in conjunction with a real, positive reaction (or normal) force at the rotor-stator interface.

The plot of rotor amplitude (z_c/r_c) vs. frequency ratio (ω/ω_{Nr}) is presented for the two solutions to Equation (29) as well as the free-rotor solution to Equation (4). The free-rotor solution (depicted by the broken-line) is the only stable solution below the rub speed, β_{rub}, and is again stable at speeds greater than β' (described in section 3). Both equilibrium solutions to Equation (29) are presented (depicted by the solid lines

labelled 1 and 2), but it is only curve 1, that solution initiating at the rub speed, which provides stable equilibrium. This is somewhat intuitive by analyzing the geometry of the rotor and stator equilibrium conditions (such as Figure 23) corresponding to a particular speed of interest. Where the solution is discontinuous, the recurrence of this stability is not assured.

The normal force is also plotted for the stable solution as a function of rotor speed. Regions where the normal force is negative indicates rub is not in action. It is immediately apparent that no solution exists for synchronous rub in the vicinity of the combined rotor-stator and the stator natural frequencies. Stability of equilibrium is determinable using a simulation program provided by Professor Udo Fischer which traces both the rotor's and stator's displacement as a function of time. Several examples of both stable and unstable equilibrium are provided throughout this appendix. A stable equilibrium is indicated by the constant orbit of both the rotor and stator. This solution may be artificially perturbed (through initial conditions to the program), but still returns to the equilibrium condition. Unstable equilibrium is evidenced by varying amplitude of both rotor and stator displacement, typically ending in the rotor undergoing a synchronous whirl without rub while the stator returns to the rest position.

Two primary groupings are analyzed: $\omega_{Ns} > \omega_{Nr}$ and $\omega_{Ns} < \omega_{Nr}$. A total of 18 cases are presented with their key parameters outlined in Table A1. Rotor characteristics are indicated by subscript 1 while stator characteristics are indicated by subscript 2. One baseline case for each of the primary groupings is analyzed, with comments regarding each subsequent case within the grouping being referenced to the baseline case (unless specifically stated otherwise).

These cases, as described in the following, clearly demonstrate the impact of varying the system's parameters as previously discussed:

Case 1: This case provides the baseline for the condition $\omega_{ns} > \omega_{Nr}$. As an example of limited synchronous rub, only a limited speed regimes exists wherein synchronous rub is in equilibrium.

Case 2: This case demonstrates the impact of an increase in the mass unbalance. As an example of synchronous rub-limited mass unbalance. As an example of synchronous rub-limited discontinuity, synchronous rub is in equilibrium for all speeds greater than the rub speed, except for a limited region demarked by the combined rotor-stator and the stator natural frequencies. Additionally, the amplitude of displacement is increased above the baseline while the reaction force increases severely.

Case 3: A reduction in friction increases the speed regime wherein synchronous rub is in equilibrium. Concurrent with this is a large increase in the reaction force.

Case 4: Similar to Case 3, a reduction in stator damping leads to establishing the equilibrium of synchronous rub over all speeds outside of the combined rotor-stator and stator natural frequencies. As well, there is an increase in the reaction force.

Case 5: Reducing the rotor's damping results in a large increase in the amplitude of displacement (above the baseline) and a slight increase in the speed region for synchronous rub. No recurrence of rub occurs though above the stator natural frequency.

Case 6: An increase in excitation and damping on the rotor and stator demonstrates how the damping reduces the displacement and reaction force at low speeds (in comparison to Case 2), but has little impact at high speeds ($\omega > \omega_{Ns}$).

Case 7: Reducing stator rigidity while maintaining the same stator natural frequency results in a reduced region of synchronous rub and a reduced reaction force.

Case 8: Converse to Case 7, increasing stator rigidity increases the region of synchronous rub and results in increased reaction forces.

Case 9: Increasing stator stiffness and so the stator natural frequency extends the speed regime for synchronous rub while causing an increase in the reaction force and a reduction in displacement.

Case 10: Increasing stator stiffness and the excitation demonstrates the large displacements and severe reaction forces that may develop. Once again, synchronous rub is re-established above the stator natural frequency.

Case 11: This case represents the baseline for the condition $\omega_{Ns} < \omega_{Nr}$. A limited synchronous rub occurs with a displacement less than the radial clearance.

Case 12: Increasing excitation results in a continuous synchronous rub with significant reaction forces developing at high speeds.

Case 13: Reducing friction also causes a continuous synchronous rub to occur similar to the previous case.

Case 14: Reducing the stator's damping has only a slight impact on the reaction force and equilibrium range for synchronous rub at speeds much greater than the stator natural frequency.

Case 15: Reducing rotor damping results in a continuous synchronous rub similar to Case 12.

Case 16: Increasing stator rigidity, while maintaining constant natural frequency reduces the speed regime of synchronous rub in this case while causing the amplitude to approach the radial clearance.

Case 17: Converse to the previous case reducing stator rigidity for a given ω_{Ns}, causes a reduction in amplitude with a slight increase in the speed regime for synchronous rub.

Case 18: Increasing stator mass (and thus reducing ω_{Ns}) has little effect on the speed regime or reaction force of the synchronous rub, but does drive the displacement toward the radial clearance (i.e., the rigid stator condition).

The stability of the solutions represented by displacement curves 1 and 2 is analyzed for the three rub behavior types: limited synchronous rub (Cases 1 and 11), synchronous rub-limited discontinuity (Case 2) and continuous synchronous rub (Case 12). Within these examples, several speeds are investigated in order to study the stability of each speed regime wherein synchronous rub is in equilibrium and too the stability of the two solutions at those speeds. These examples demonstrate the inherent instability of curve 2 solutions as well as the variability of stability associated with curve 1 solutions. In particular, curve 1 appears stable for both the limited rub and continuous rub conditions, but there is a speed range within the synchronous rub-limited discontinuity equilibrium solutions wherein stability is lost.

TABLE A1

Case No.	K2/K1	M2/M1	D1	D2	ϵ	μ
1	4.0	1.0	0.2	0.2	0.3	0.3
2	4.0	1.0	0.2	0.2	0.5	0.3
3	4.0	1.0	0.2	0.2	0.3	0.2
4	4.0	1.0	0.2	0.0	0.3	0.3
5	4.0	1.0	0.0	0.2	0.3	0.3
6	4.0	1.0	0.4	0.4	0.3	0.3
7	1.0	0.25	0.2	0.2	0.3	0.3
8	8.0	2.0	0.2	0.2	0.3	0.3
9	16.0	1.0	0.2	0.2	0.3	0.3
10	16.0	1.0	0.2	0.2	0.5	0.3
11	1.0	4.0	0.2	0.2	0.3	0.3
12	1.0	4.0	0.2	0.2	0.5	0.3
13	1.0	4.0	0.2	0.2	0.3	0.2
14	1.0	4.0	0.2	0.0	0.3	0.3
15	1.0	4.0	0.0	0.2	0.3	0.3
16	2.0	8.0	0.2	0.2	0.3	0.3
17	0.25	1.0	0.2	0.2	0.3	0.3
18	1.0	9.0	0.2	0.2	0.3	0.3

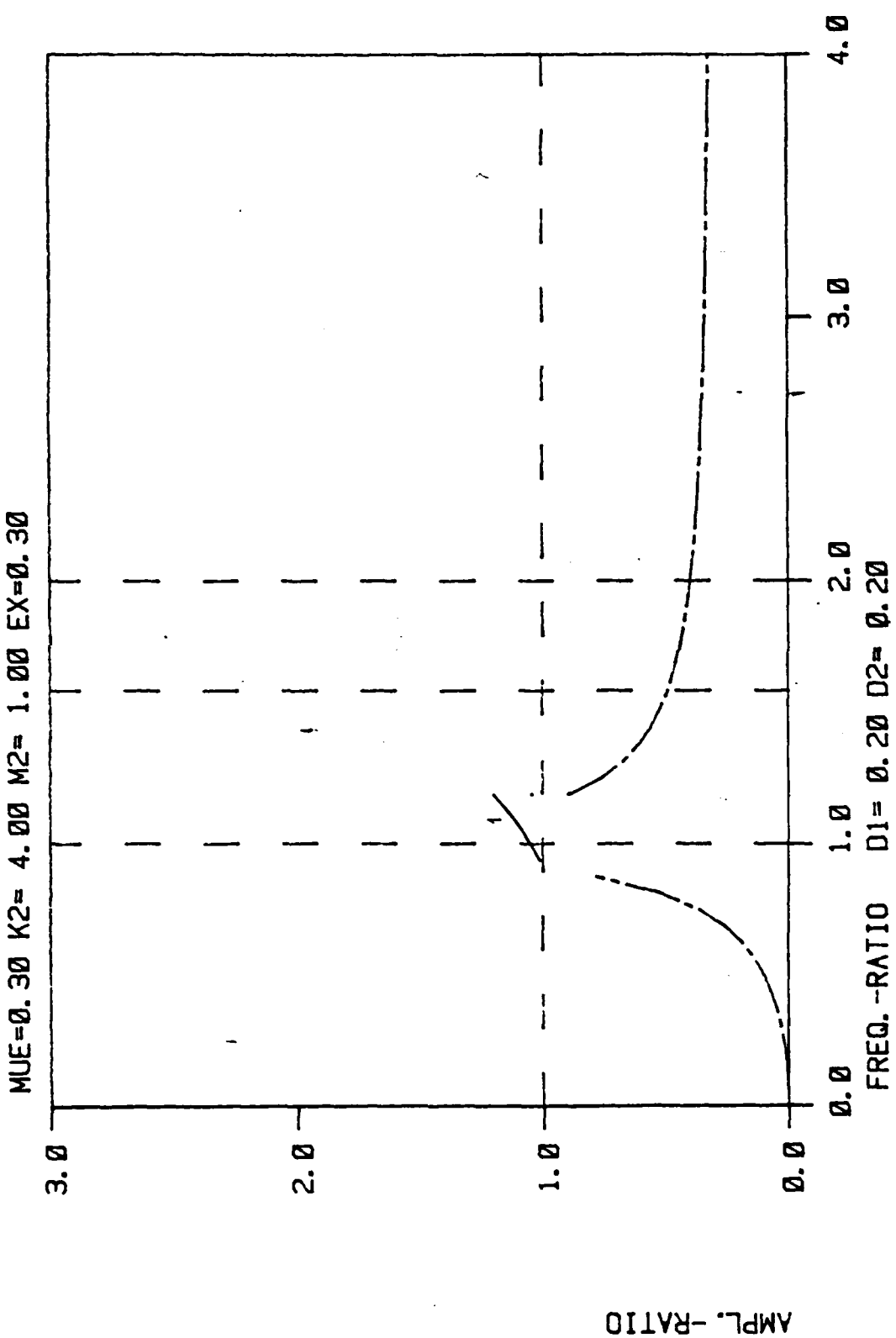
MUE=0.30 K2= 4.00 M2= 1.00 EX=0.30
AMPL.-RATIO
3.0
2.0
1.0
0.0
0.0
1.0
2.0
3.0
4.0
FREQ.-RATIO D1= 0.20 D2= 0.20

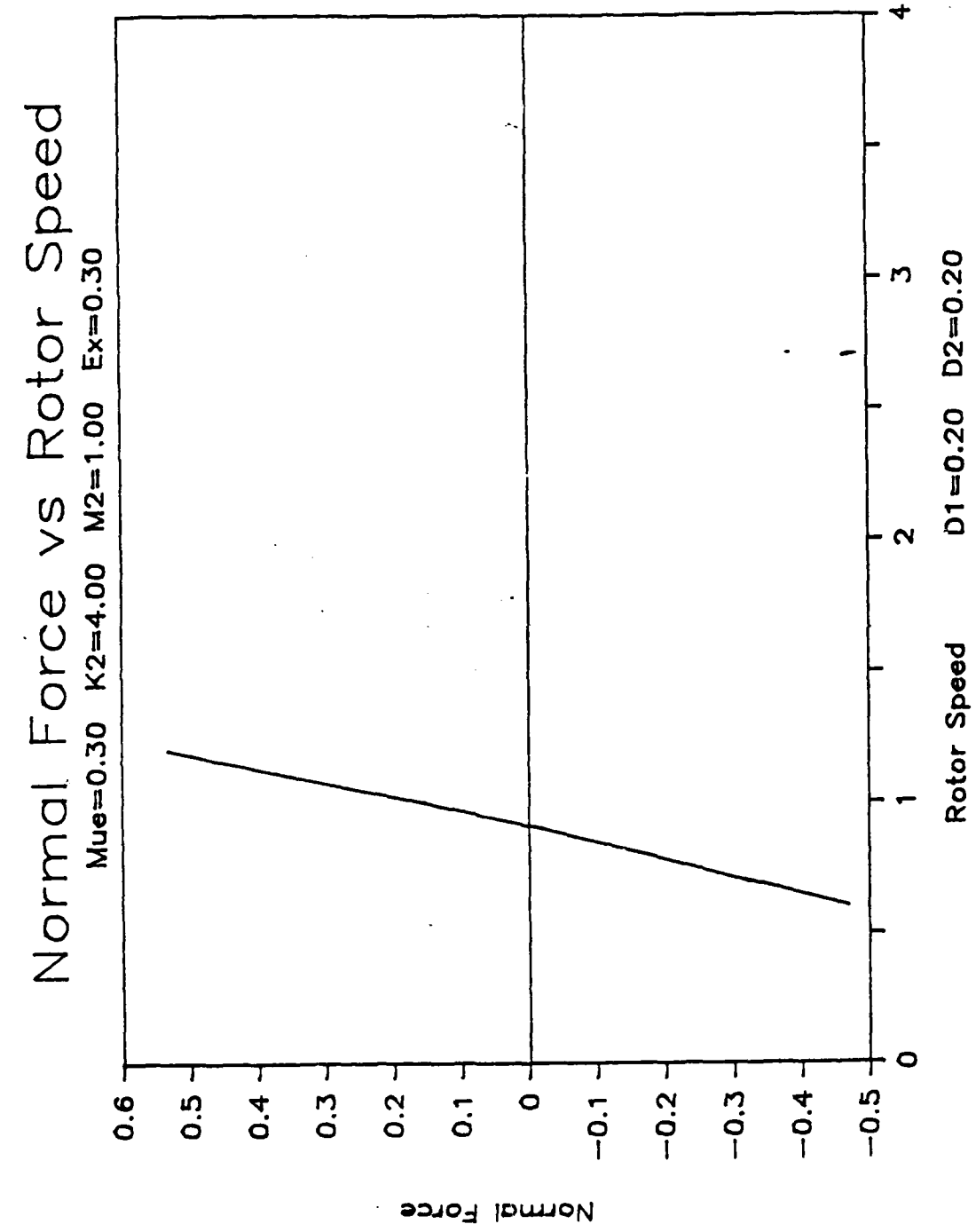
Normal Force vs Rotor Speed
Mue=0.30 K2=4.00 M2=1.00 Ex=0.30
D1=0.20 D2=0.20
Rotor Speed
Normal Force
0.6
0.5
0.4
0.3
0.2
0.1
0
−0.1
−0.2
−0.3
−0.4
−0.5
0
1
2
3
4

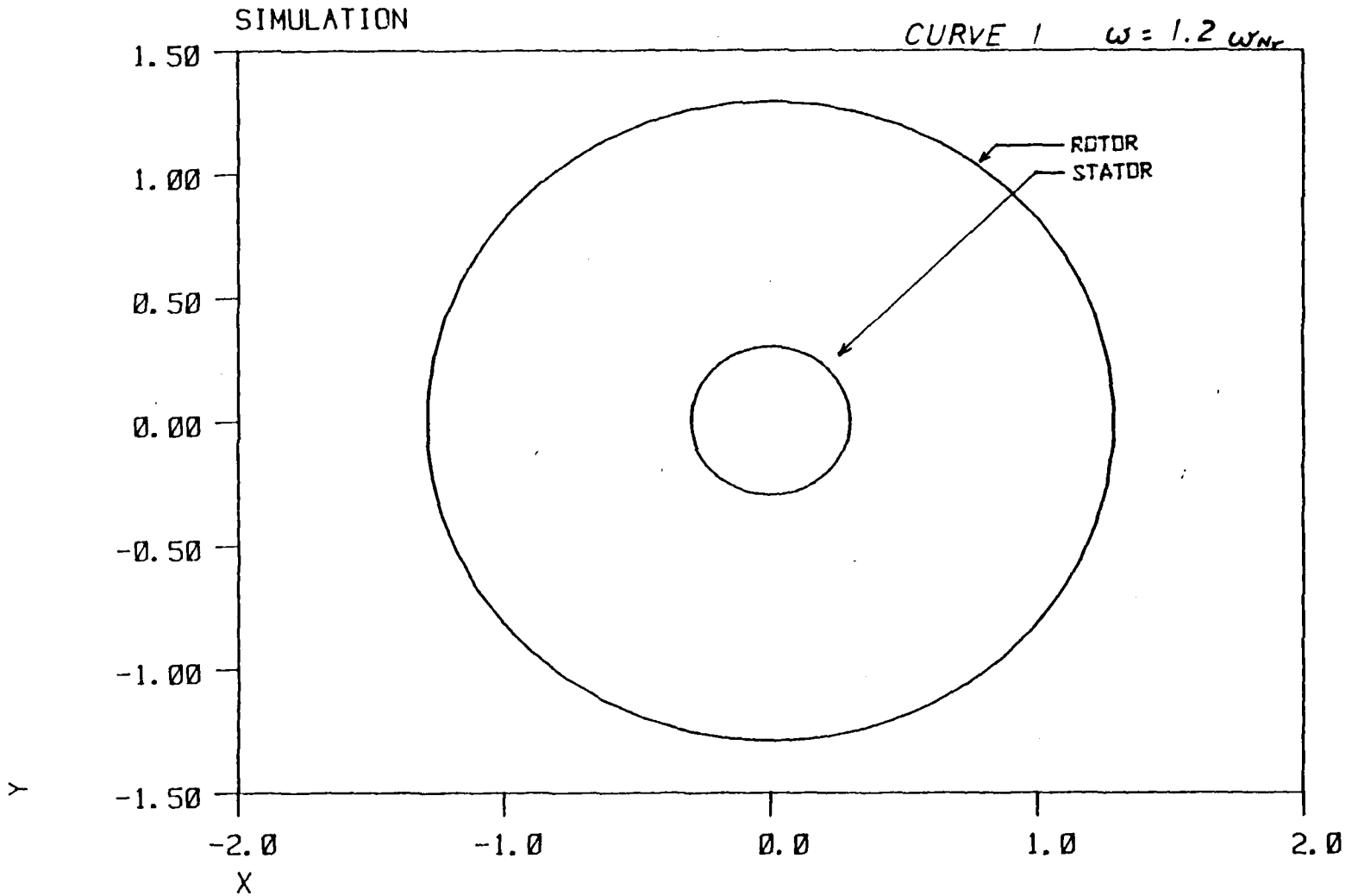
SIMULATION
CURVE 1 ω = 1.2 ω_Nr
ROTOR
STATOR
1.50
1.00
0.50
0.00
-0.50
-1.00
-1.50
Y
-2.0
-1.0
0.0
1.0
2.0
X

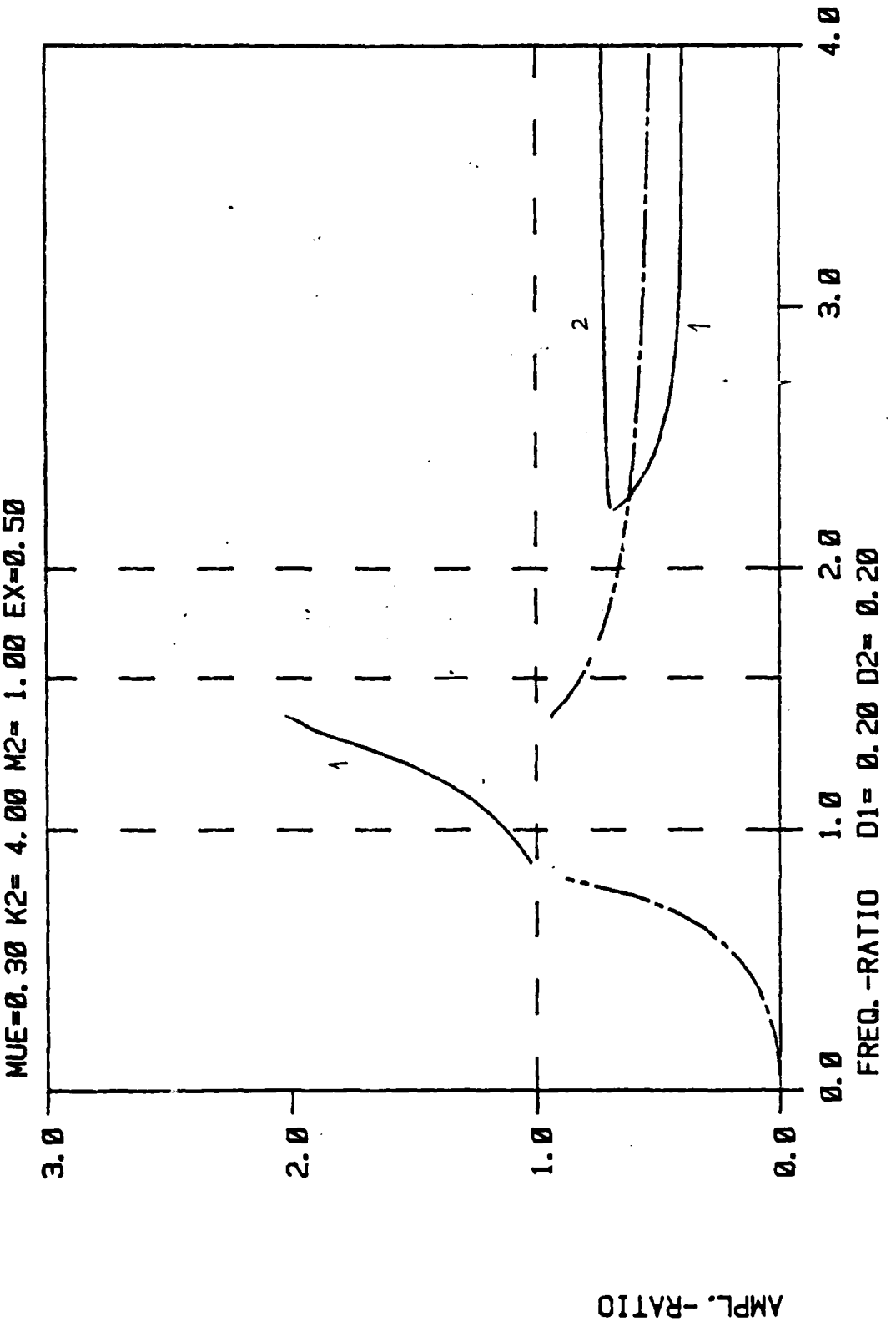
MUE=0.30 K2= 4.00 M2= 1.00 EX=0.50
AMPL.-RATIO
FREQ.-RATIO D1= 0.20 D2= 0.20
0.0
1.0
2.0
3.0
4.0
1
2

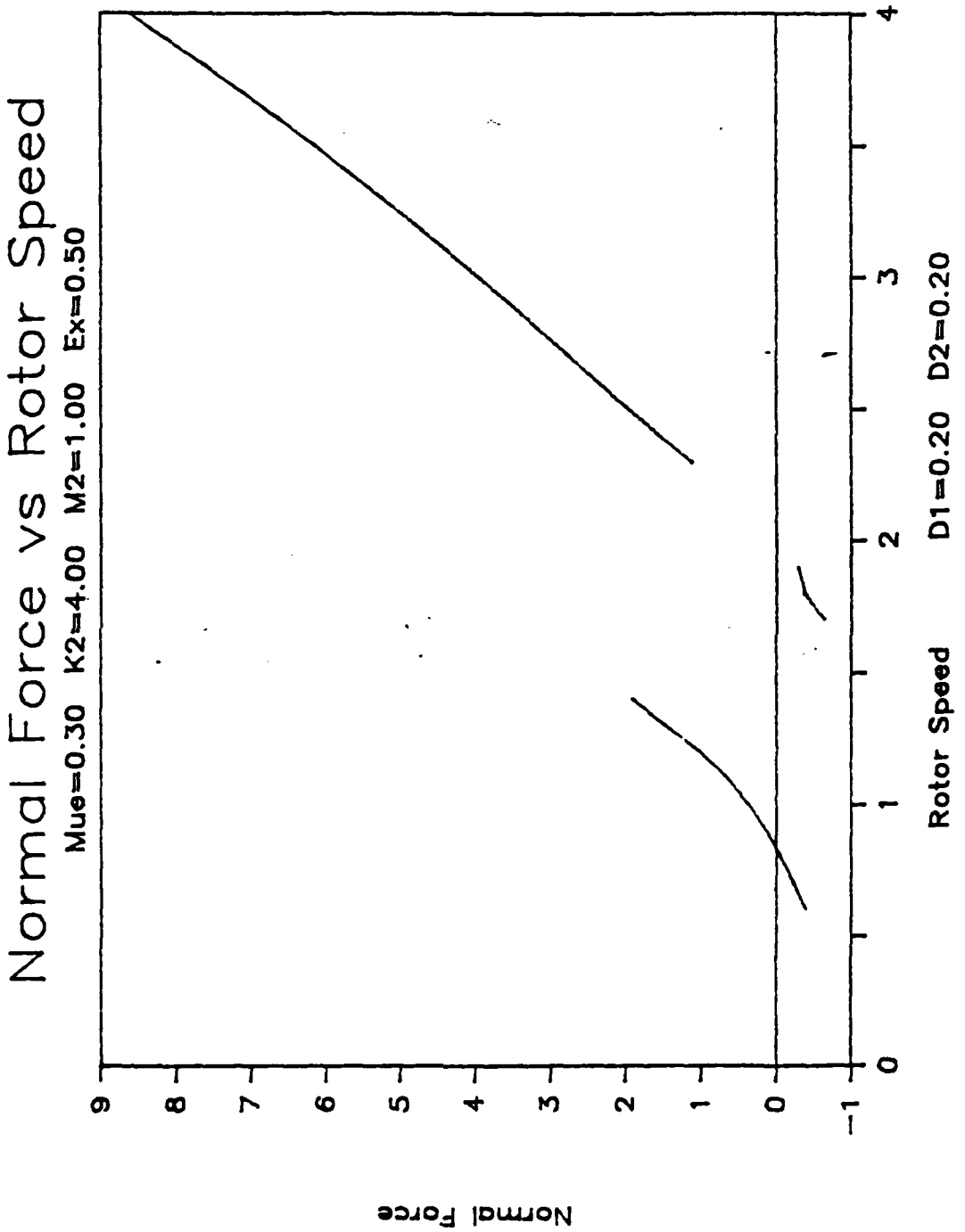
Normal Force vs Rotor Speed
Mue=0.30 K2=4.00 M2=1.00 Ex=0.50
Normal Force
9
8
7
6
5
4
3
2
1
0
-1
0
1
2
3
4
Rotor Speed
D1=0.20 D2=0.20

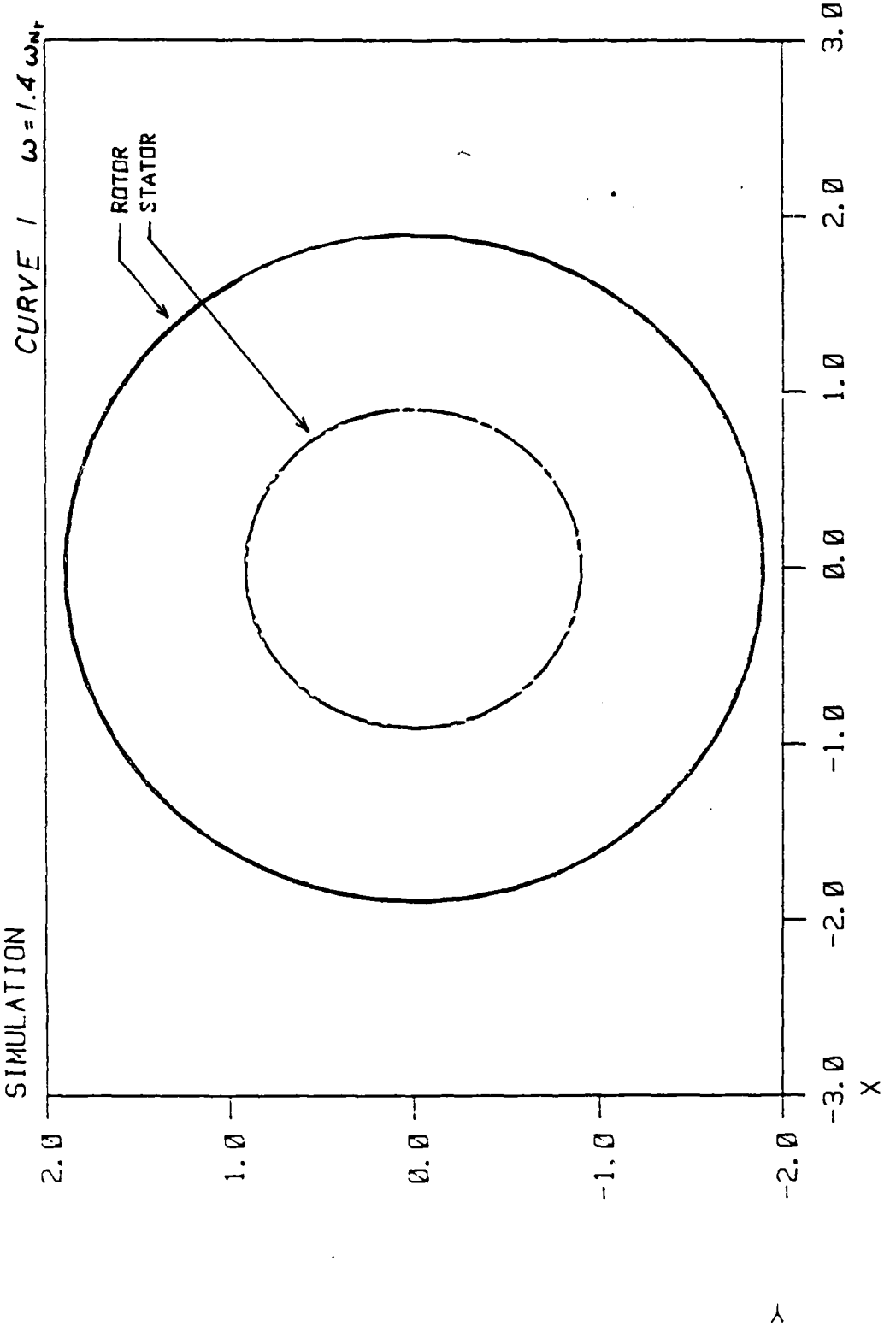
SIMULATION
CURVE 1 ω = 1.4 ωNr
ROTOR
STATOR
2.0
1.0
0.0
-1.0
-2.0
-3.0
-2.0
-1.0
0.0
1.0
2.0
3.0
X
Y

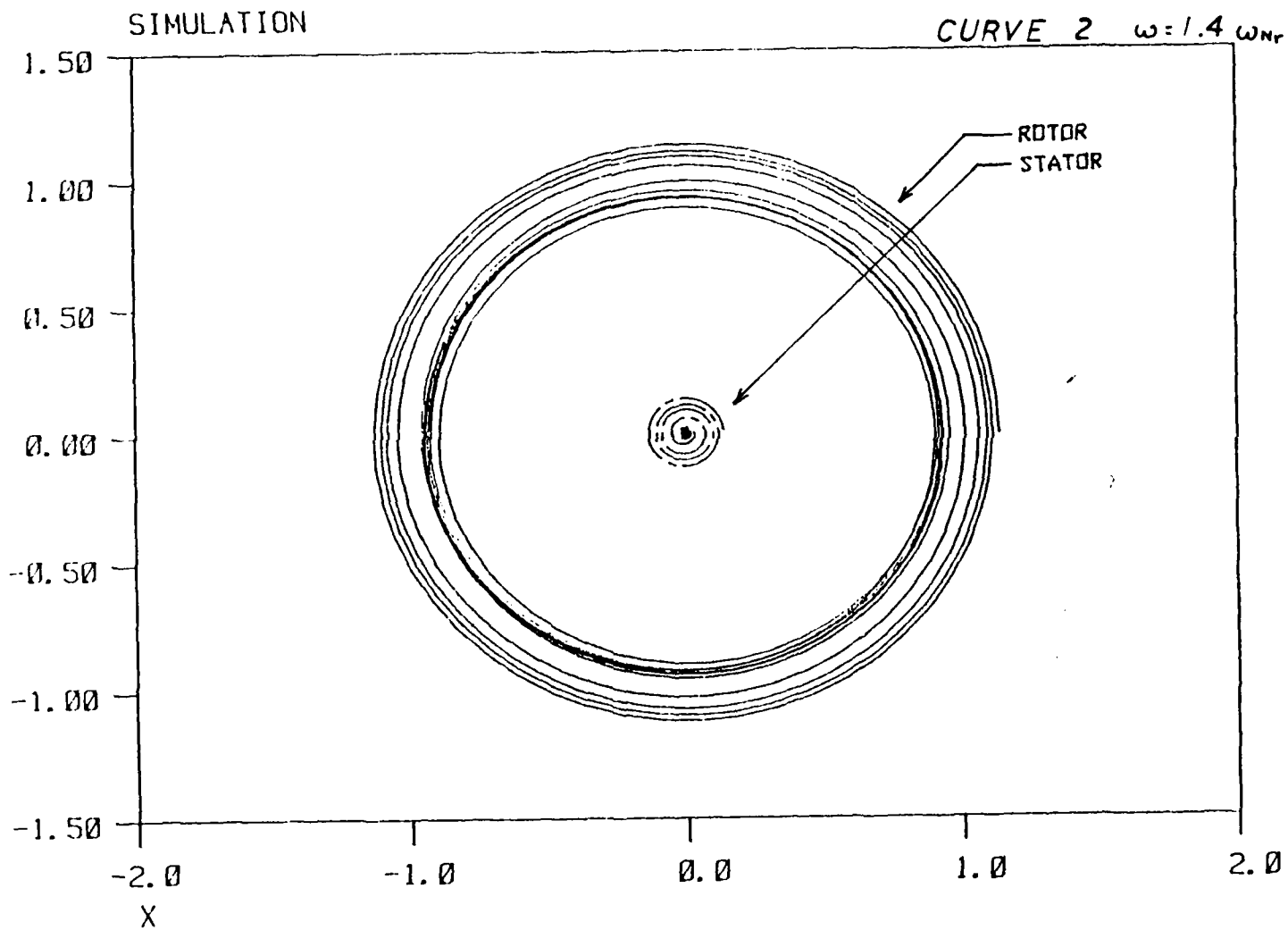
SIMULATION
CURVE 2 ω=1.4 ωNr
ROTOR
STATOR
1.50
1.00
0.50
0.00
-0.50
-1.00
-1.50
Y
-2.0
-1.0
0.0
1.0
2.0
X

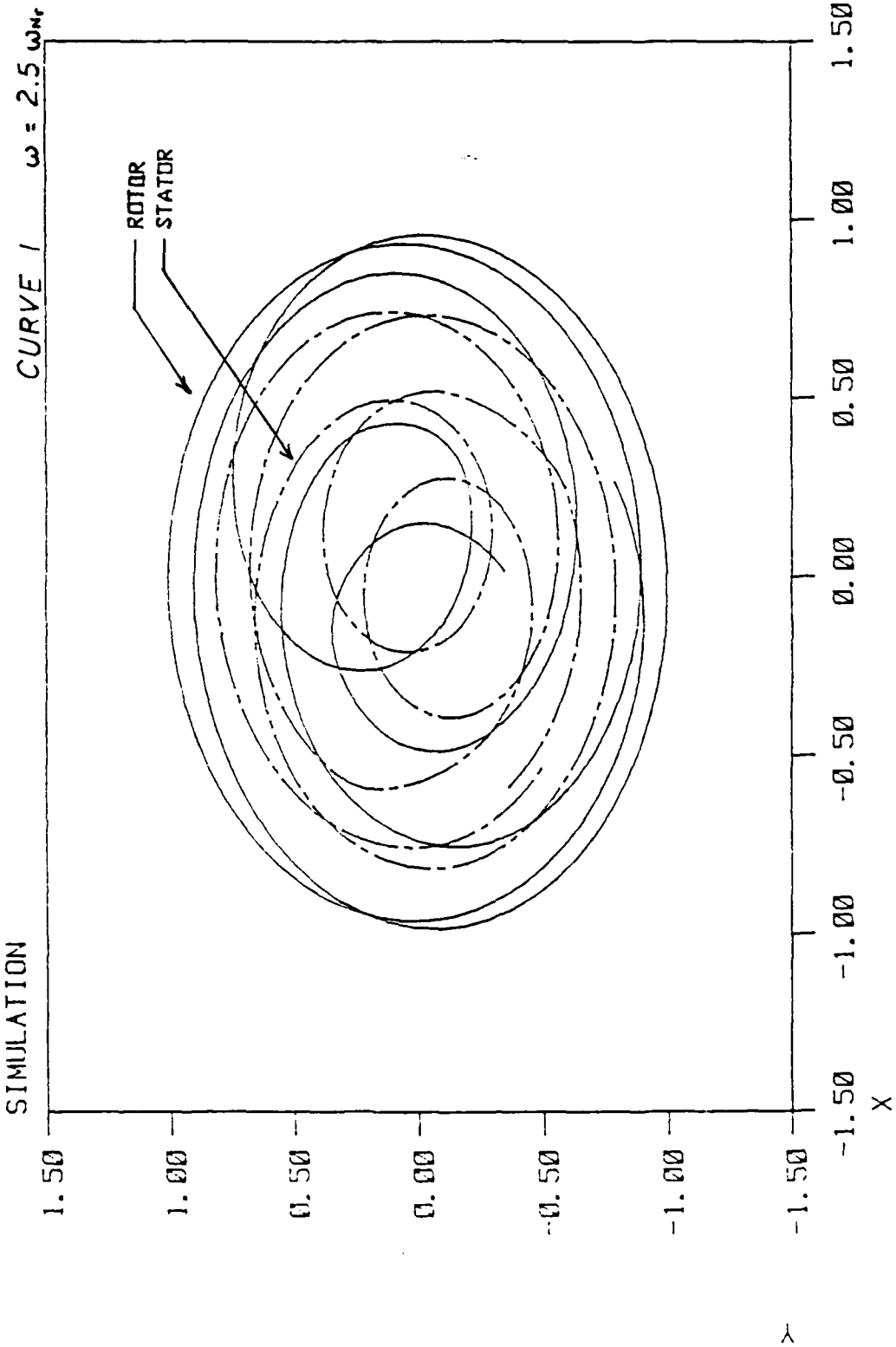
SIMULATION
CURVE 1
ω = 2.5 ω_Nr
ROTOR
STATOR
1.50
1.00
0.50
0.00
-0.50
-1.00
-1.50
-1.50
-1.00
-0.50
0.00
0.50
1.00
1.50
X
Y

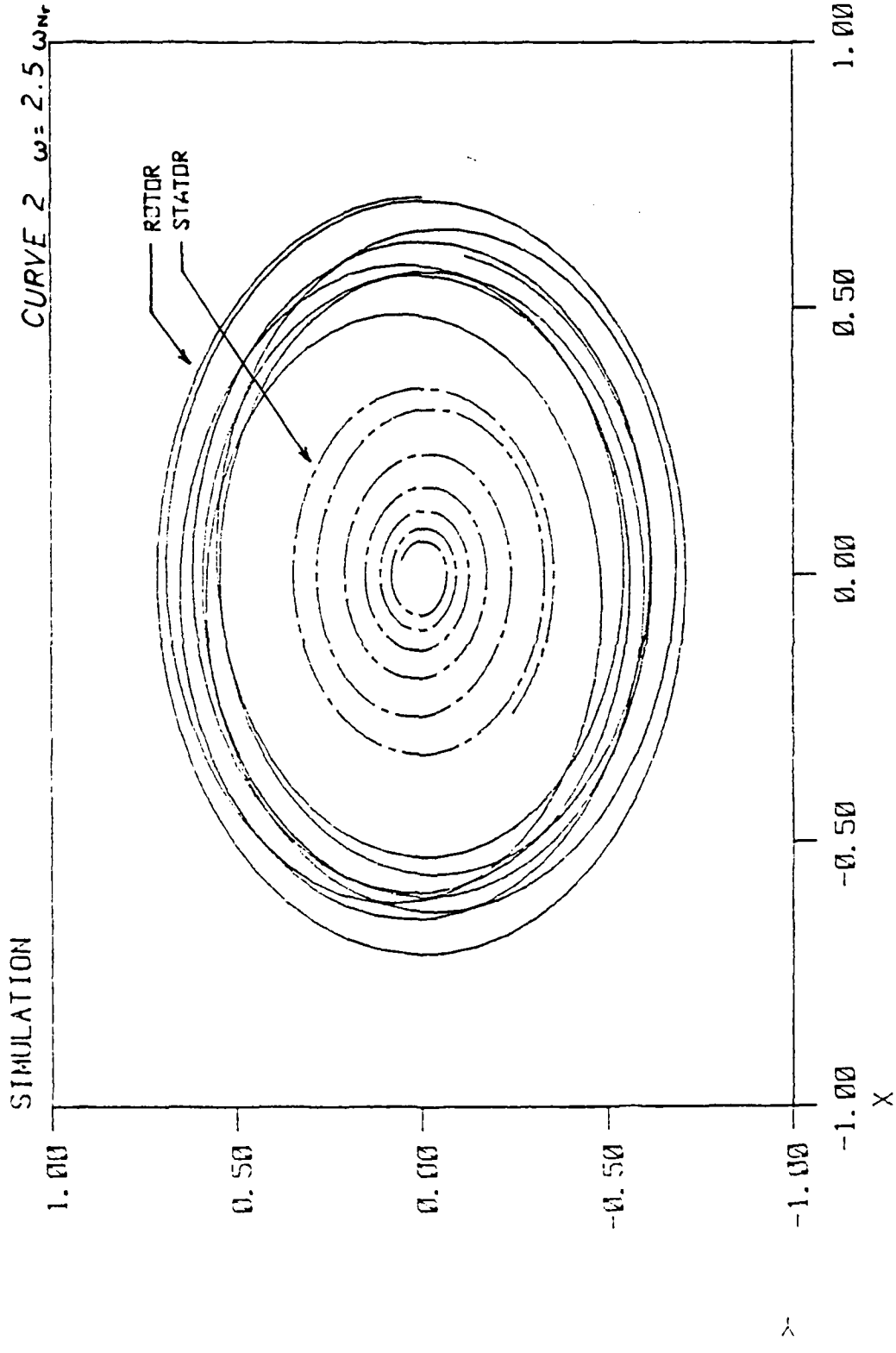
SIMULATION
CURVE 2 ω= 2.5 ω_Nr
ROTOR
STATOR
1.000
0.50
0.00
-0.50
-1.00
-1.00
-0.50
0.00
0.50
1.00
X
Y

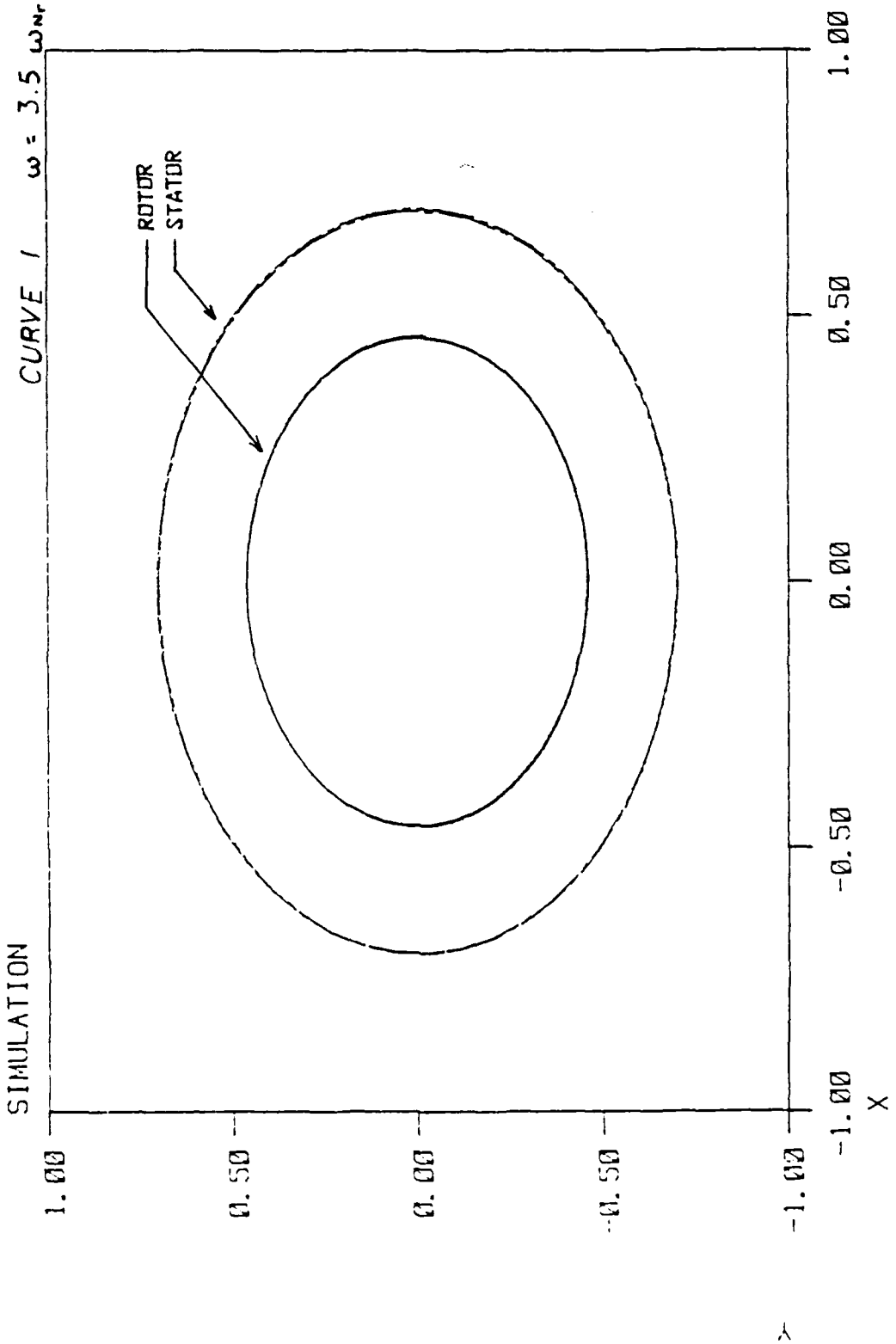
SIMULATION
CURVE 1 ω = 3.5 ω_Nr
ROTOR
STATOR
1.00
0.50
0.00
-0.50
-1.00
-1.00
-0.50
0.00
0.50
1.00
X
Y

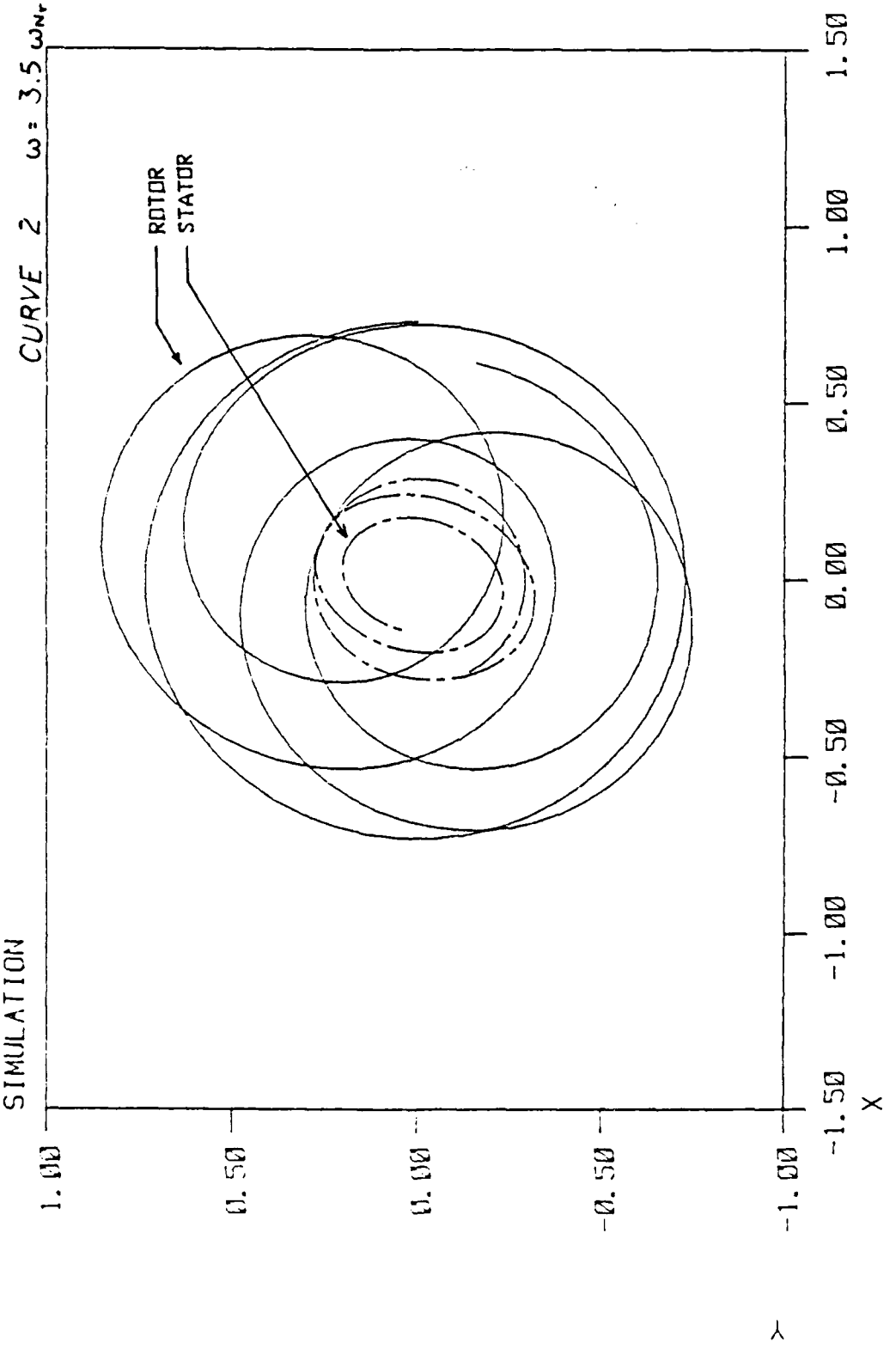
SIMULATION
CURVE 2 ω = 3.5 ωNr
ROTOR
STATOR
1.00
0.50
0.00
-0.50
-1.00
-1.50
-1.00
-0.50
0.00
0.50
1.00
1.50
X
Y

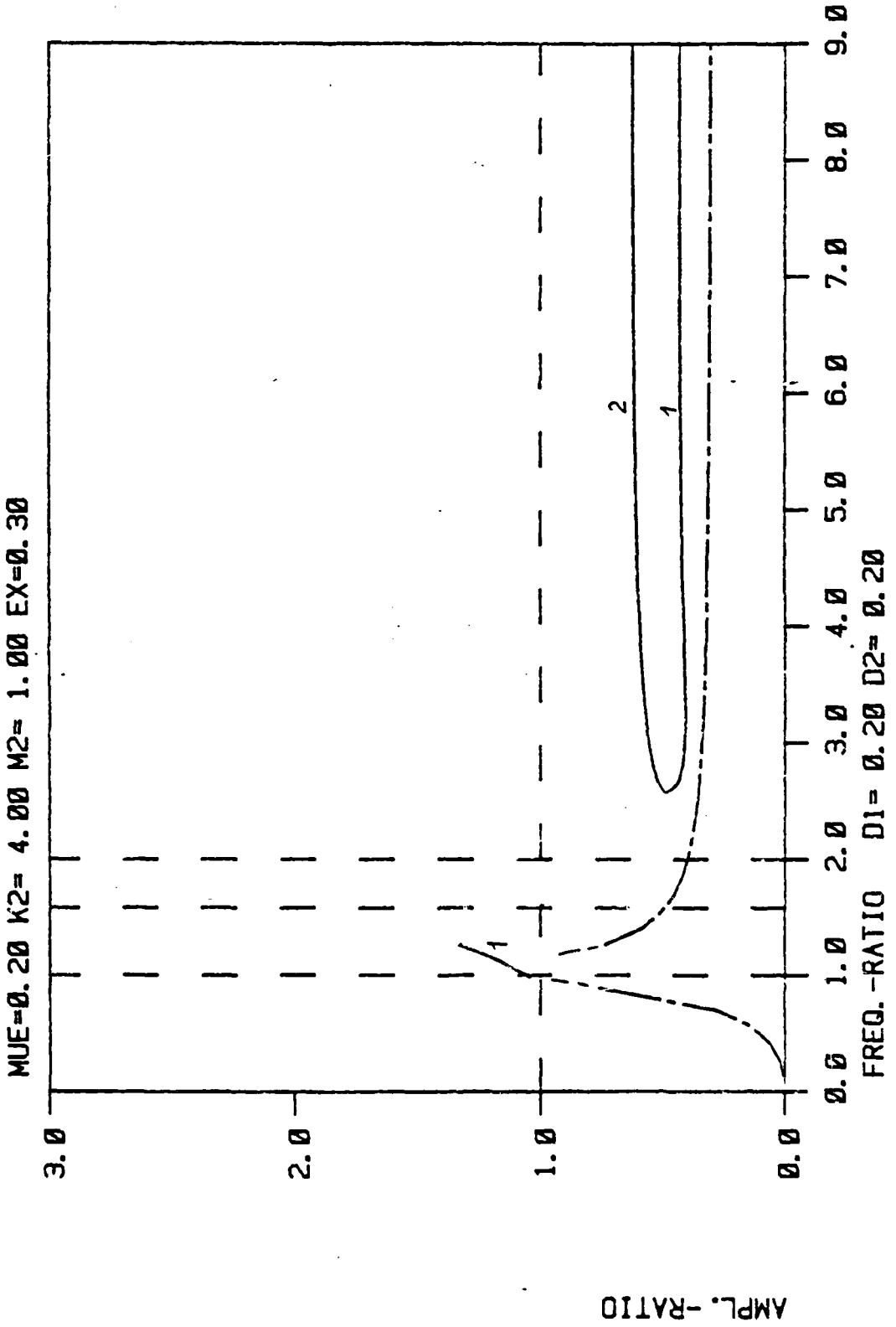
MUE=0.20 K2= 4.00 M2= 1.00 EX=0.30
AMPL.-RATIO
FREQ.-RATIO D1= 0.20 D2= 0.20
0.0
1.0
2.0
3.0
4.0
5.0
6.0
7.0
8.0
9.0
1
2

AD-A173 311 DYNAMICS OF FULL ANNULAR ROTOR RUB(U) MASSACHUSETTS INST OF TECH CAMBRIDGE DEPT OF OCEAN ENGINEERING S J STACKLEY JUN 86 2/2

UNCLASSIFIED F/G 20/11 NL

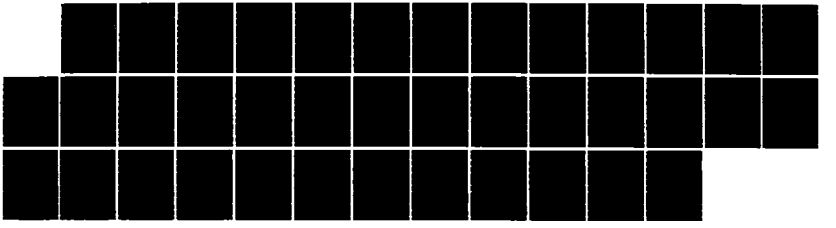

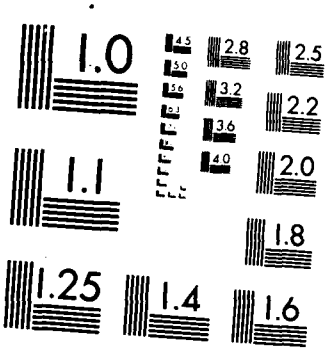

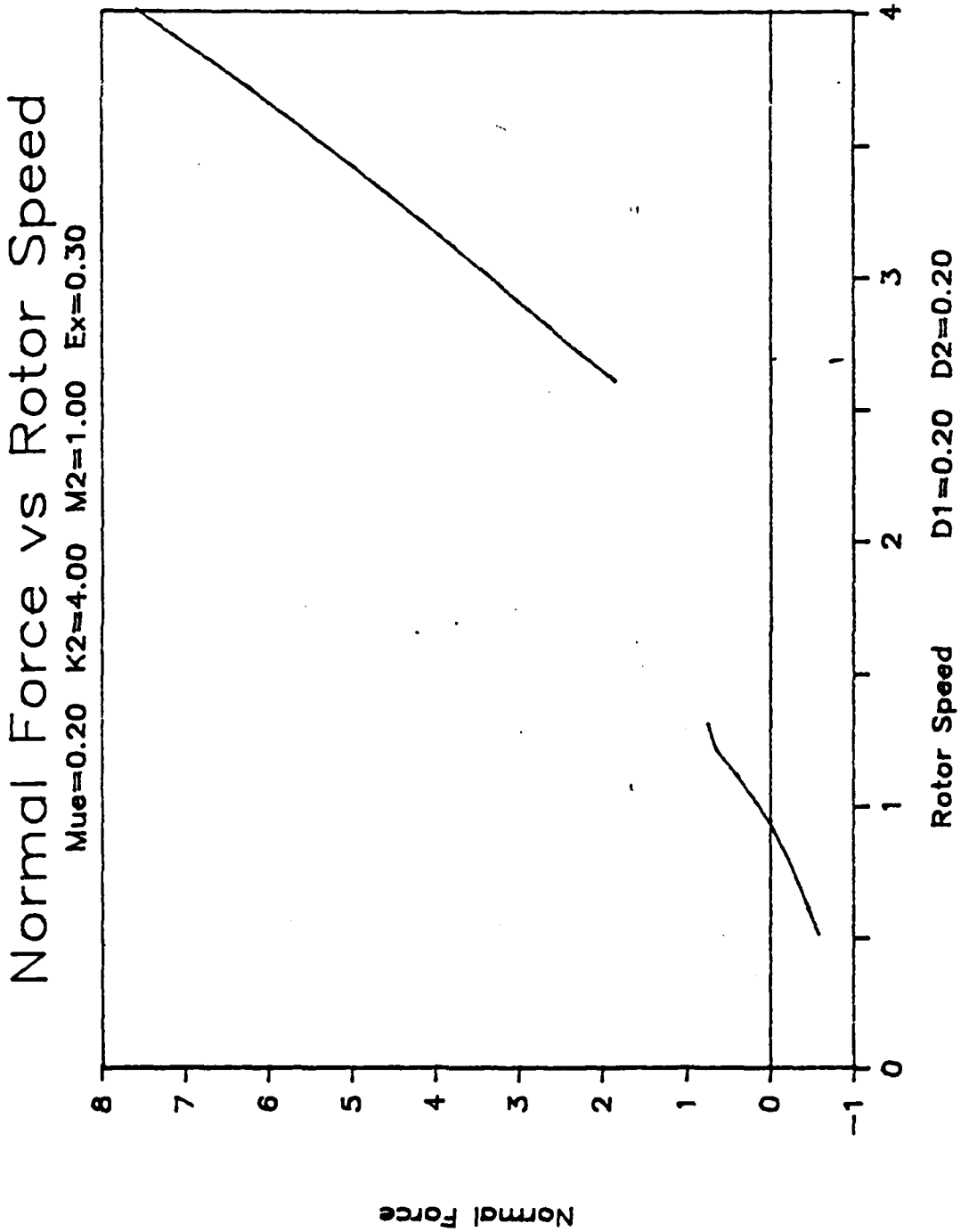
Normal Force vs Rotor Speed
Mue=0.20 K2=4.00 M2=1.00 Ex=0.30
Normal Force
8
7
6
5
4
3
2
1
0
-1
0
1
2
3
4
Rotor Speed
D1=0.20 D2=0.20

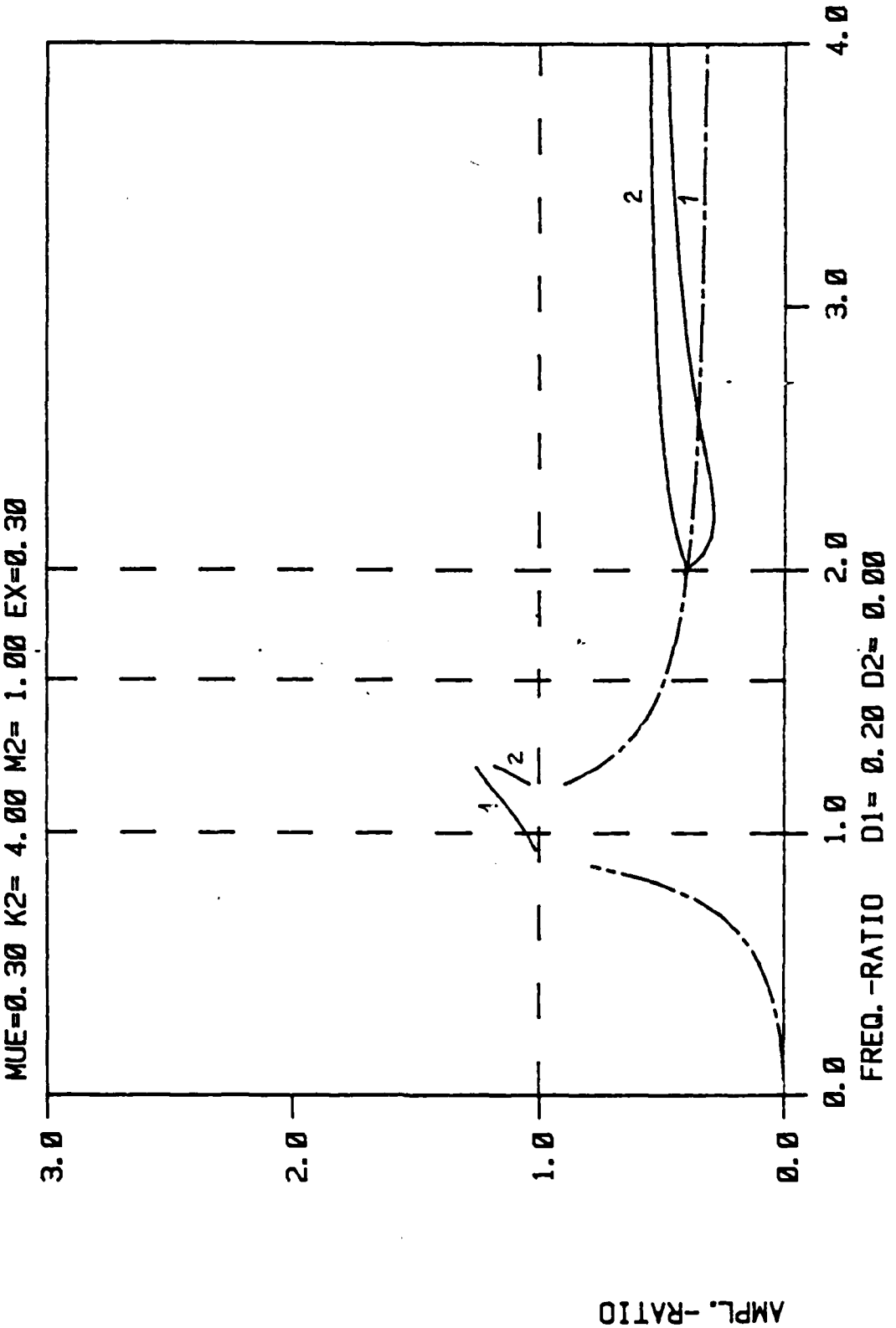
MUE=0.30 K2= 4.00 M2= 1.00 EX=0.30
AMPL.-RATIO
FREQ.-RATIO D1= 0.20 D2= 0.00
0.0
1.0
2.0
3.0
4.0
1
2

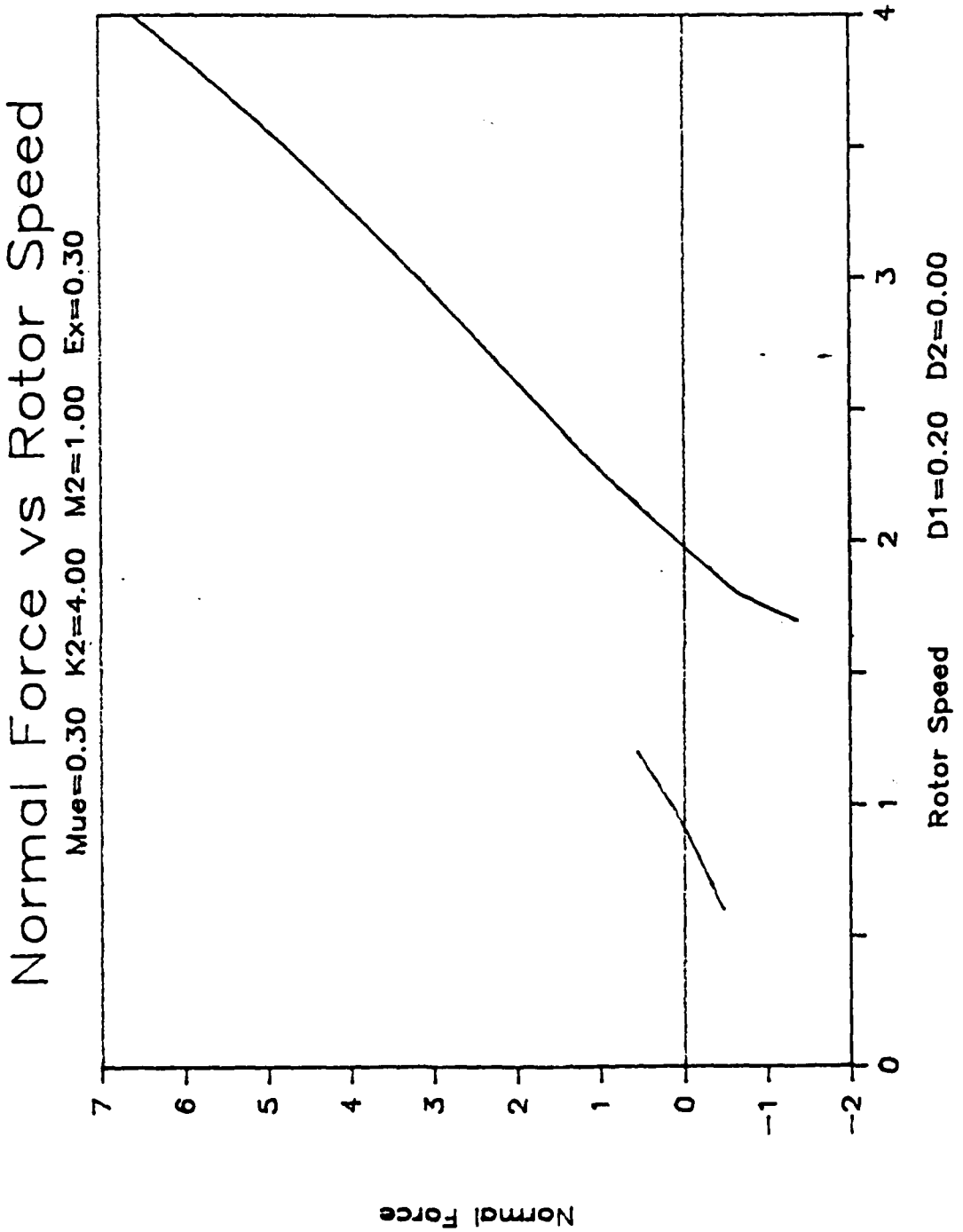
Normal Force vs Rotor Speed
Mue=0.30 K2=4.00 M2=1.00 Ex=0.30
Normal Force
7
6
5
4
3
2
1
0
-1
-2
0
1
2
3
4
Rotor Speed
D1=0.20 D2=0.00

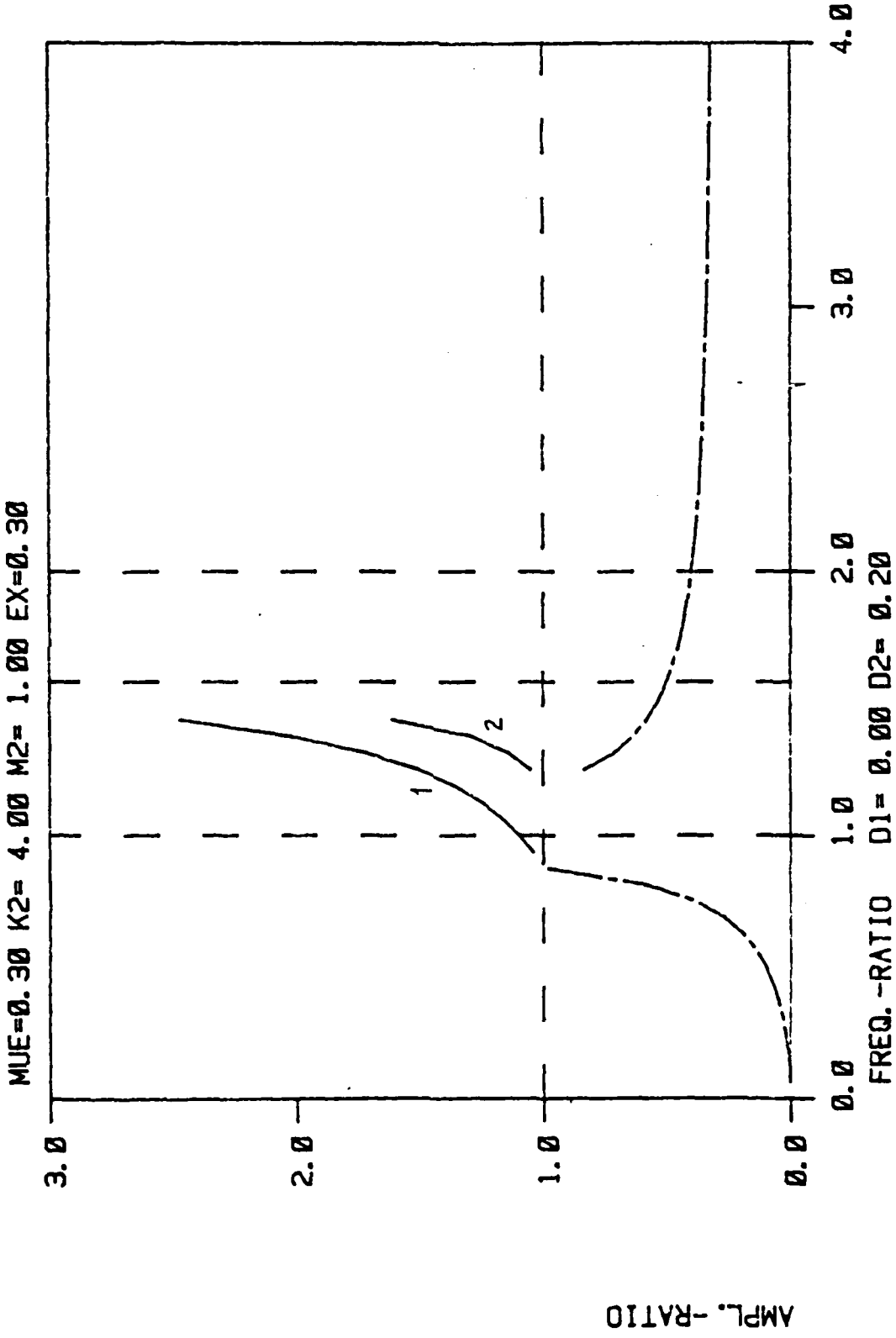
MUE=0.30 K2= 4.00 M2= 1.00 EX=0.30
D1= 0.00 D2= 0.20
AMPL.-RATIO
FREQ.-RATIO
0.0
1.0
2.0
3.0
4.0
1
2

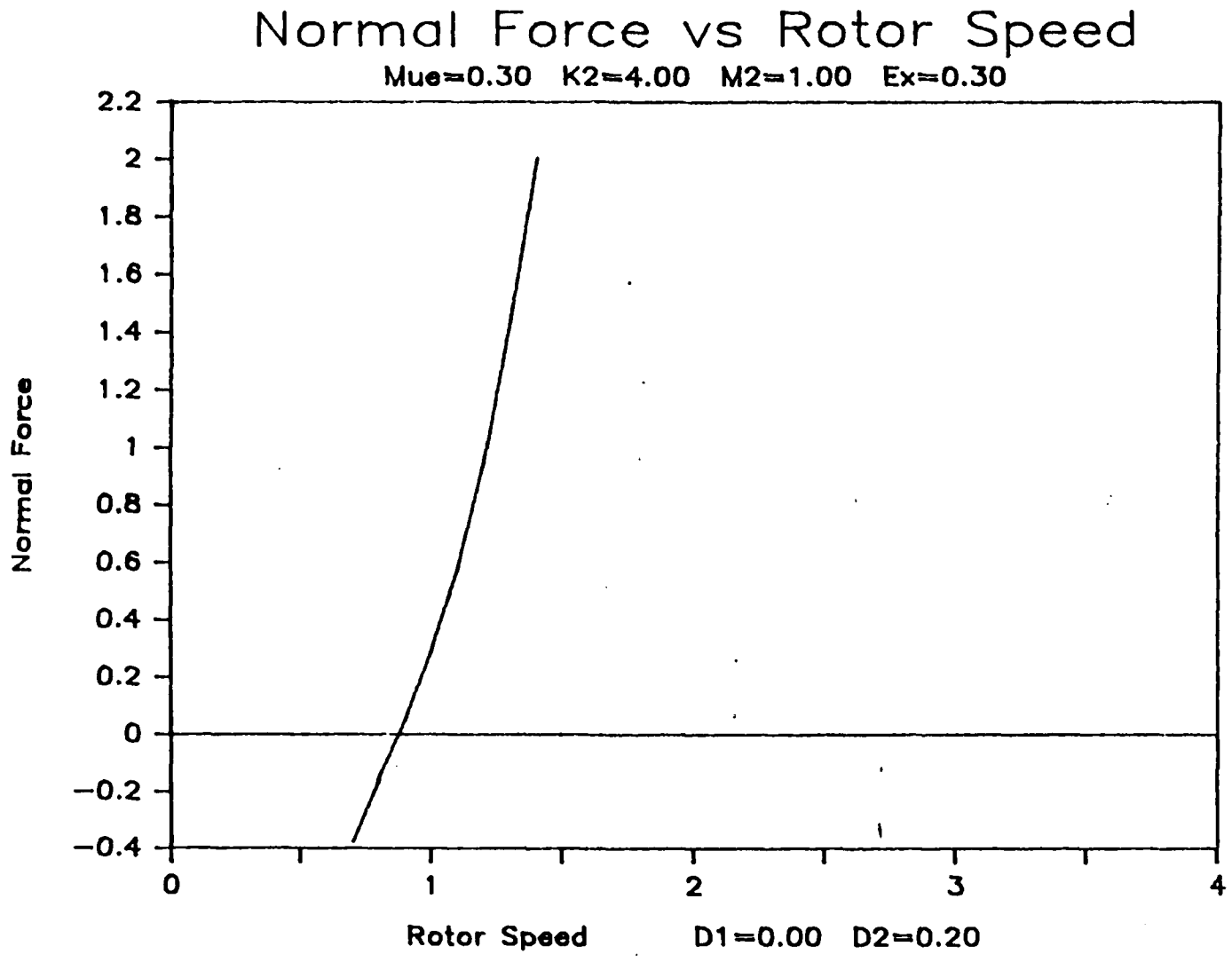
Normal Force vs Rotor Speed
Mue=0.30 K2=4.00 M2=1.00 Ex=0.30
Normal Force
2.2
2
1.8
1.6
1.4
1.2
1
0.8
0.6
0.4
0.2
0
−0.2
−0.4
0
1
2
3
4
Rotor Speed
D1=0.00 D2=0.20

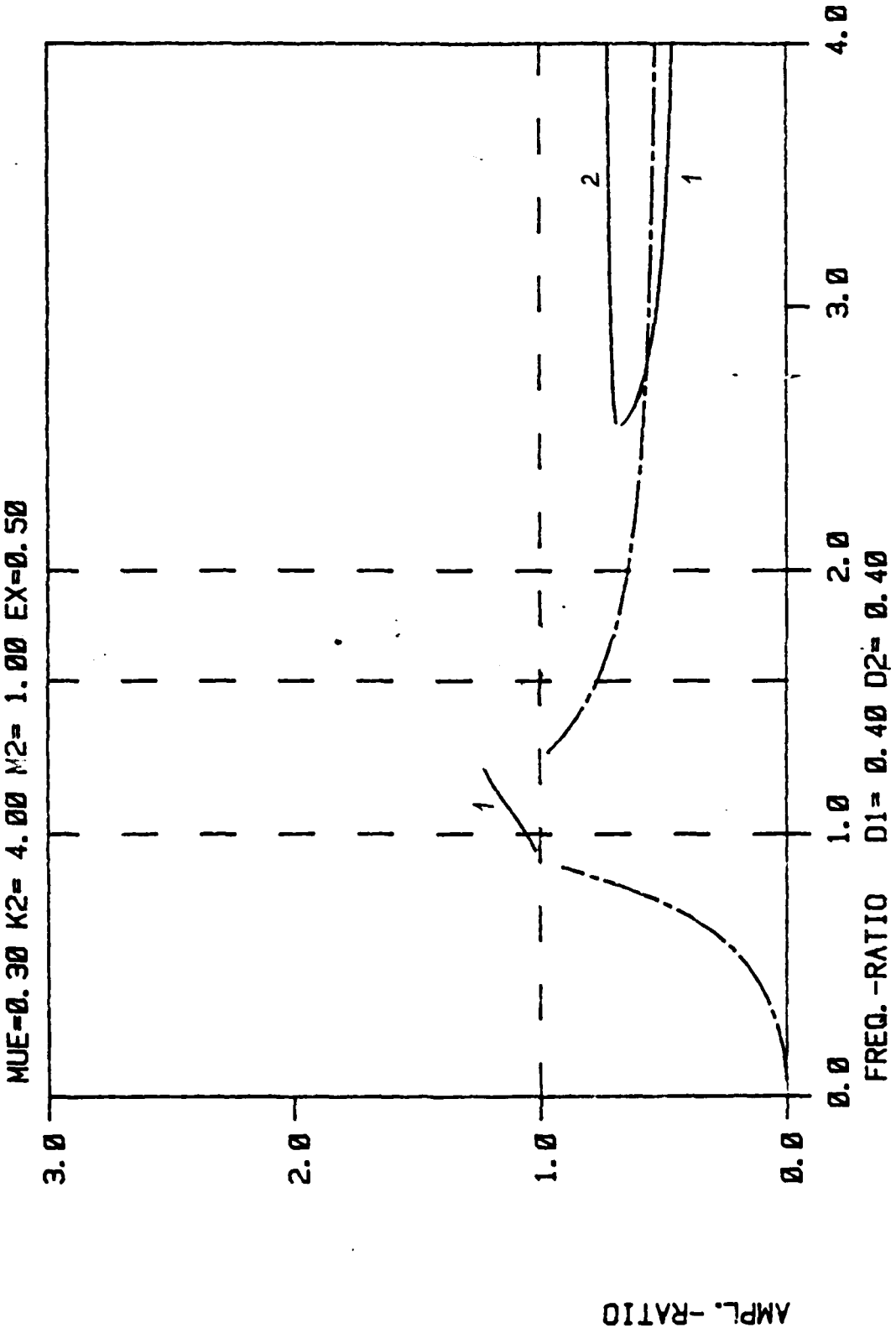
MUE=0.30 K2= 4.00 M2= 1.00 EX=0.50
AMPL.-RATIO
FREQ.-RATIO D1= 0.40 D2= 0.40
0.0
1.0
2.0
3.0
4.0
1
2

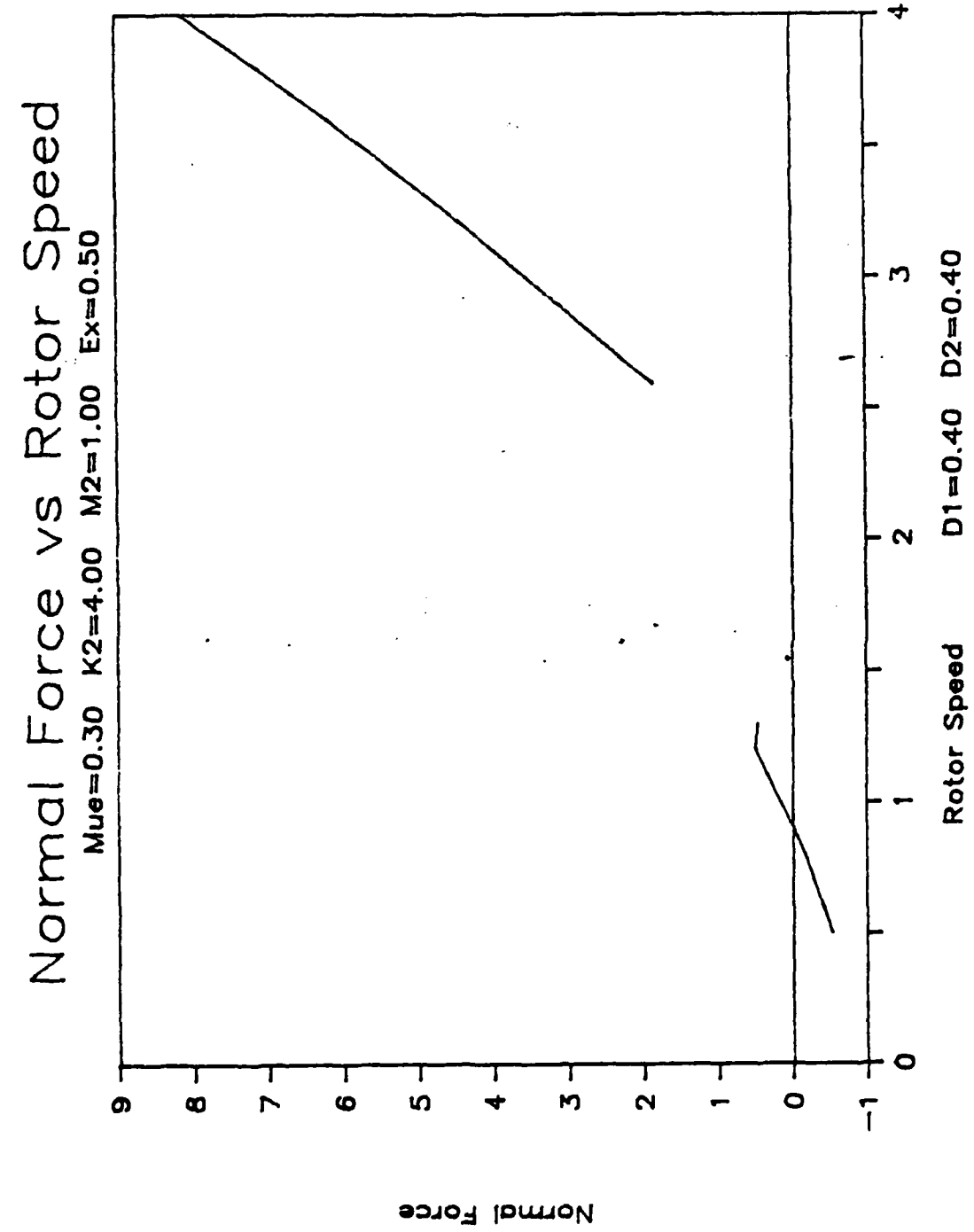
Normal Force vs Rotor Speed
Mue=0.30 K2=4.00 M2=1.00 Ex=0.50
Normal Force
Rotor Speed
D1=0.40 D2=0.40
9
8
7
6
5
4
3
2
1
0
-1
0
1
2
3
4

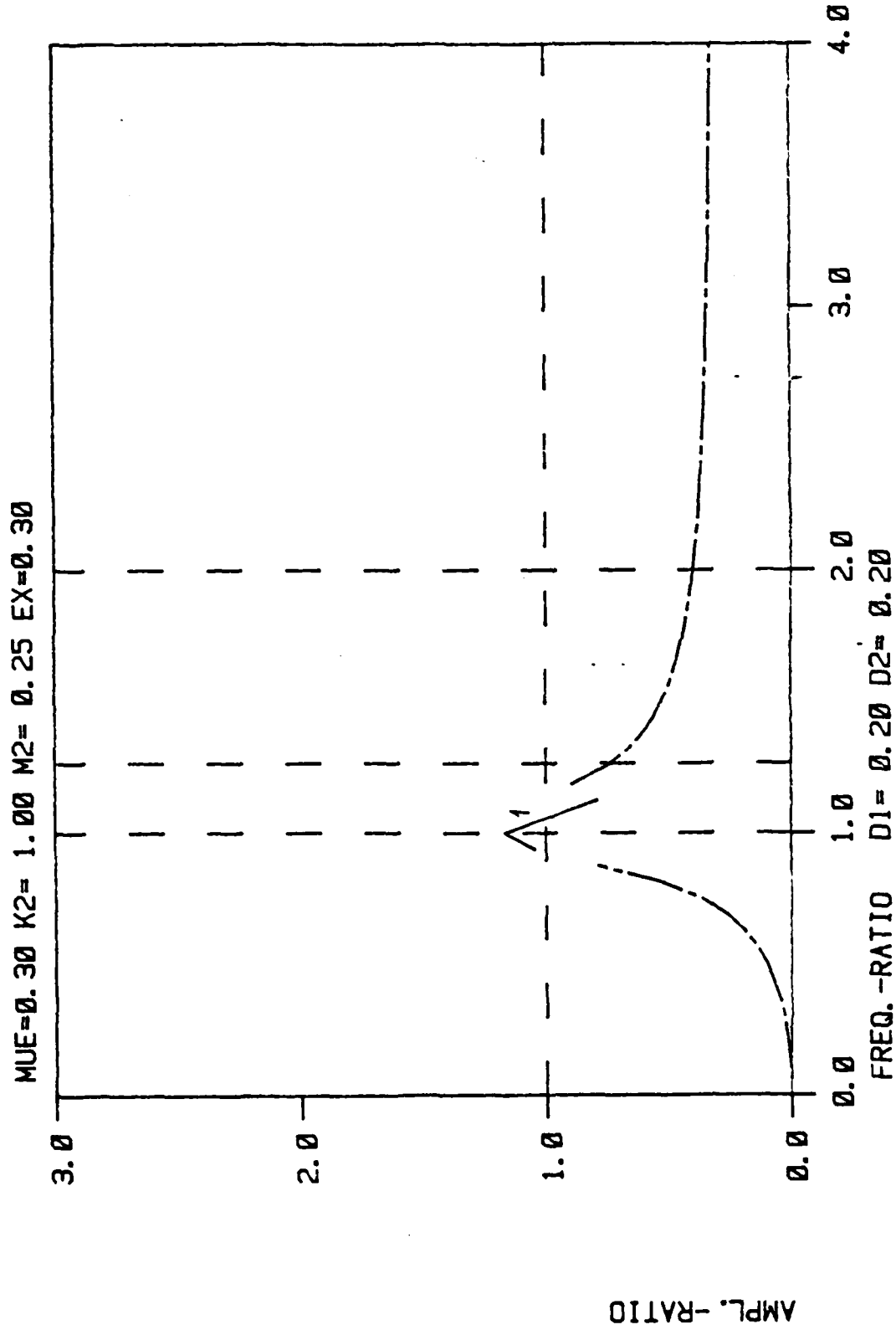
MUE=0.30 K2= 1.00 M2= 0.25 EX=0.30
D1= 0.20 D2= 0.20
FREQ.-RATIO
AMPL.-RATIO
0.0
1.0
2.0
3.0
4.0
0.0
1.0
2.0
3.0

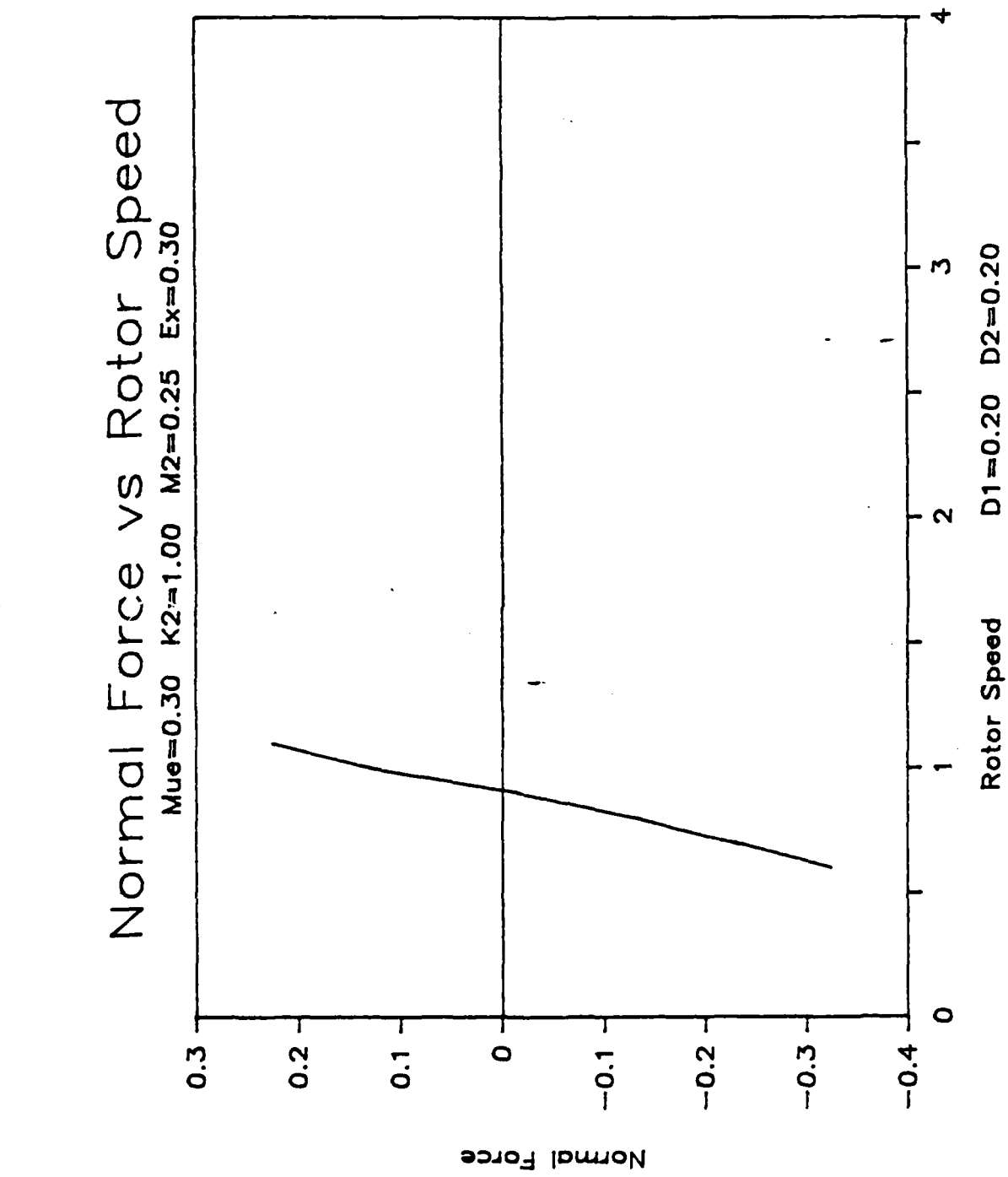
Normal Force vs Rotor Speed
Mue=0.30 K2=1.00 M2=0.25 Ex=0.30
D1=0.20 D2=0.20
Rotor Speed
Normal Force
0.3
0.2
0.1
0
-0.1
-0.2
-0.3
-0.4
0
1
2
3
4

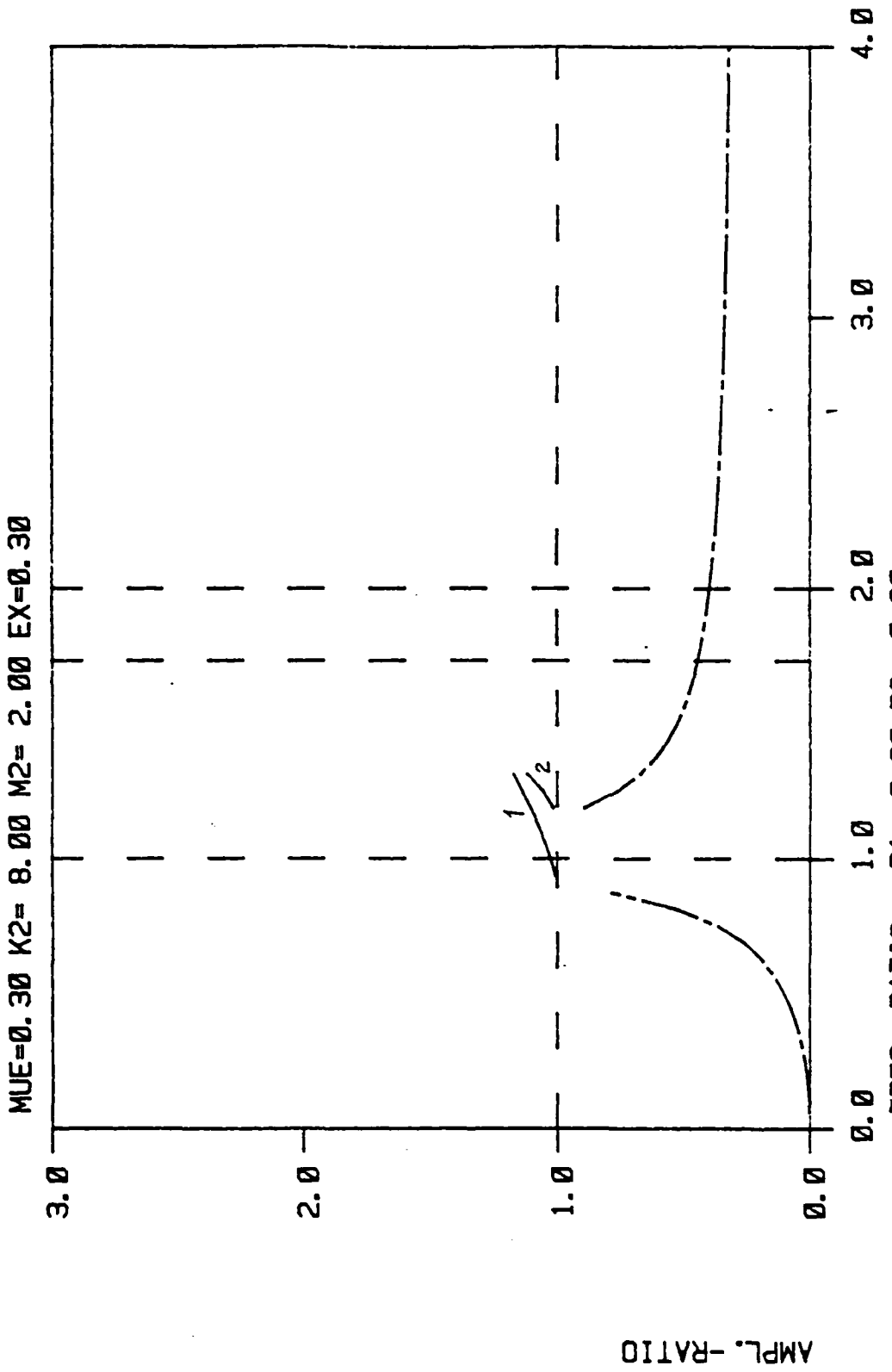
MUE=0.30 K2= 8.00 M2= 2.00 EX=0.30
AMPL.-RATIO
3.0
2.0
1.0
0.0
0.0
1.0
2.0
3.0
4.0
FREQ.-RATIO D1= 0.20 D2= 0.20
1
2

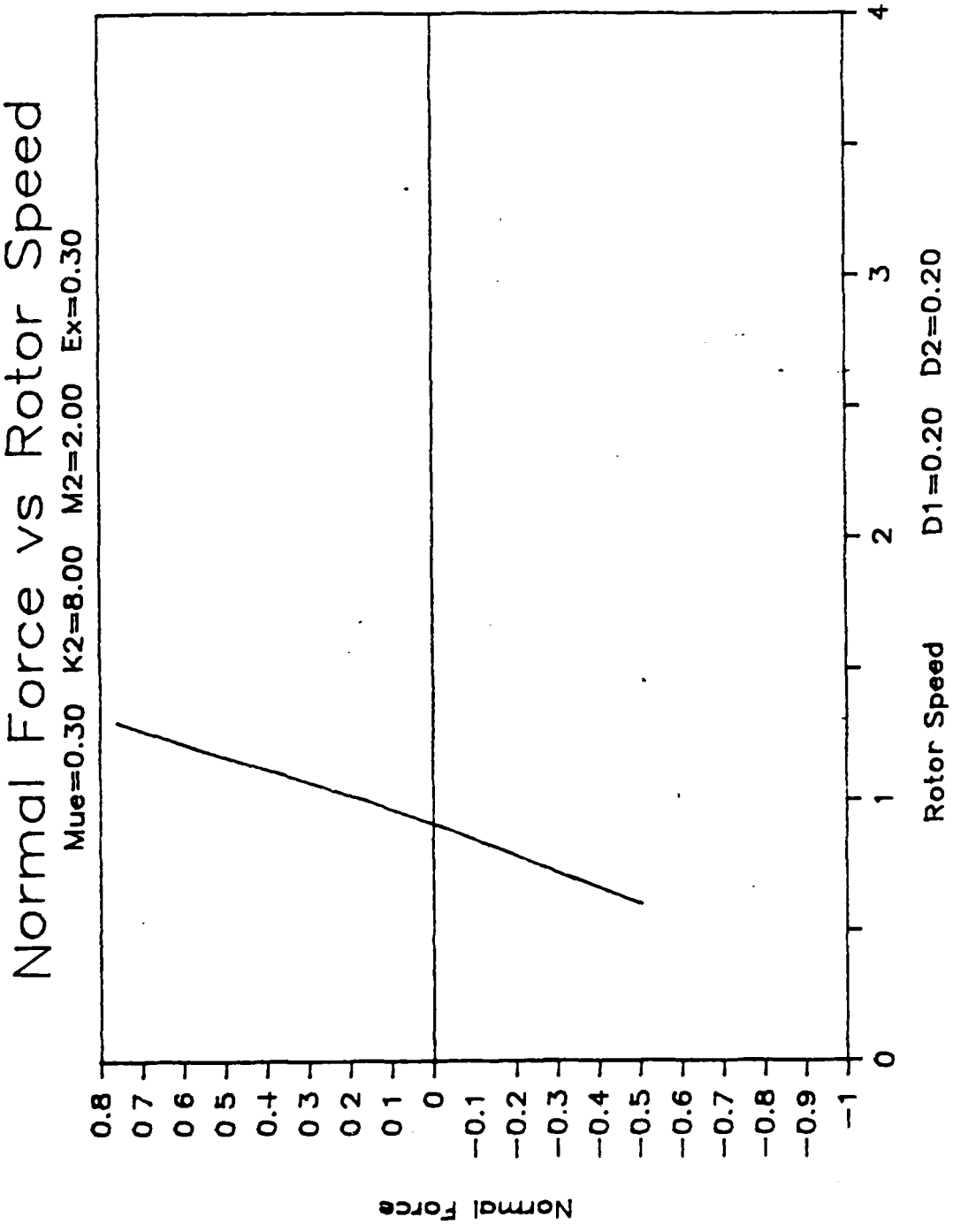
Normal Force vs Rotor Speed
Mue=0.30 K2=8.00 M2=2.00 Ex=0.30
Normal Force
0.8
0.7
0.6
0.5
0.4
0.3
0.2
0.1
0
-0.1
-0.2
-0.3
-0.4
-0.5
-0.6
-0.7
-0.8
-0.9
-1
0
1
2
3
4
Rotor Speed
D1=0.20 D2=0.20

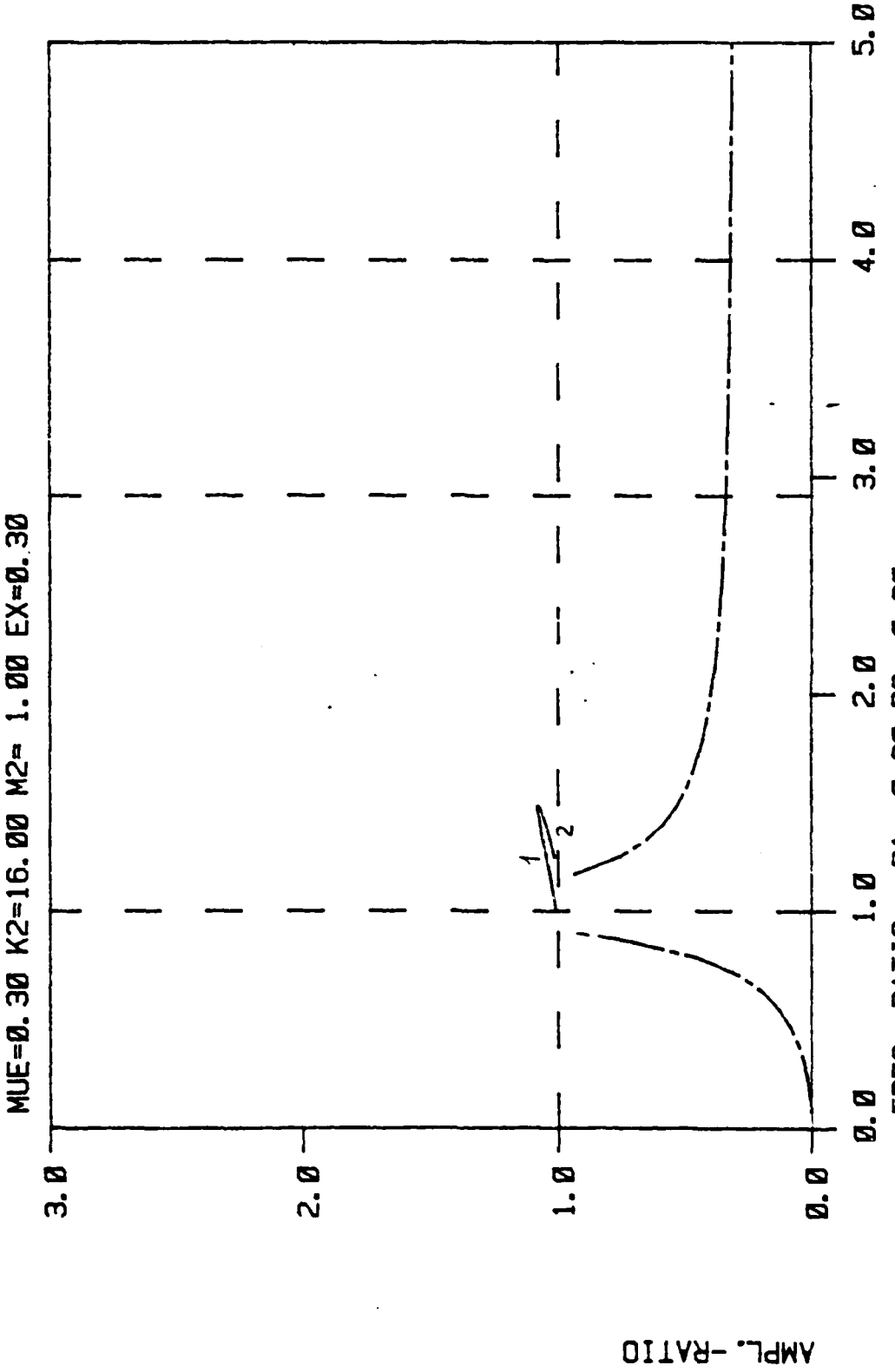
MUE=0.30 K2=16.00 M2= 1.00 EX=0.30
AMPL.-RATIO
FREQ.-RATIO D1= 0.20 D2= 0.20
0.0
1.0
2.0
3.0
4.0
5.0
1
2

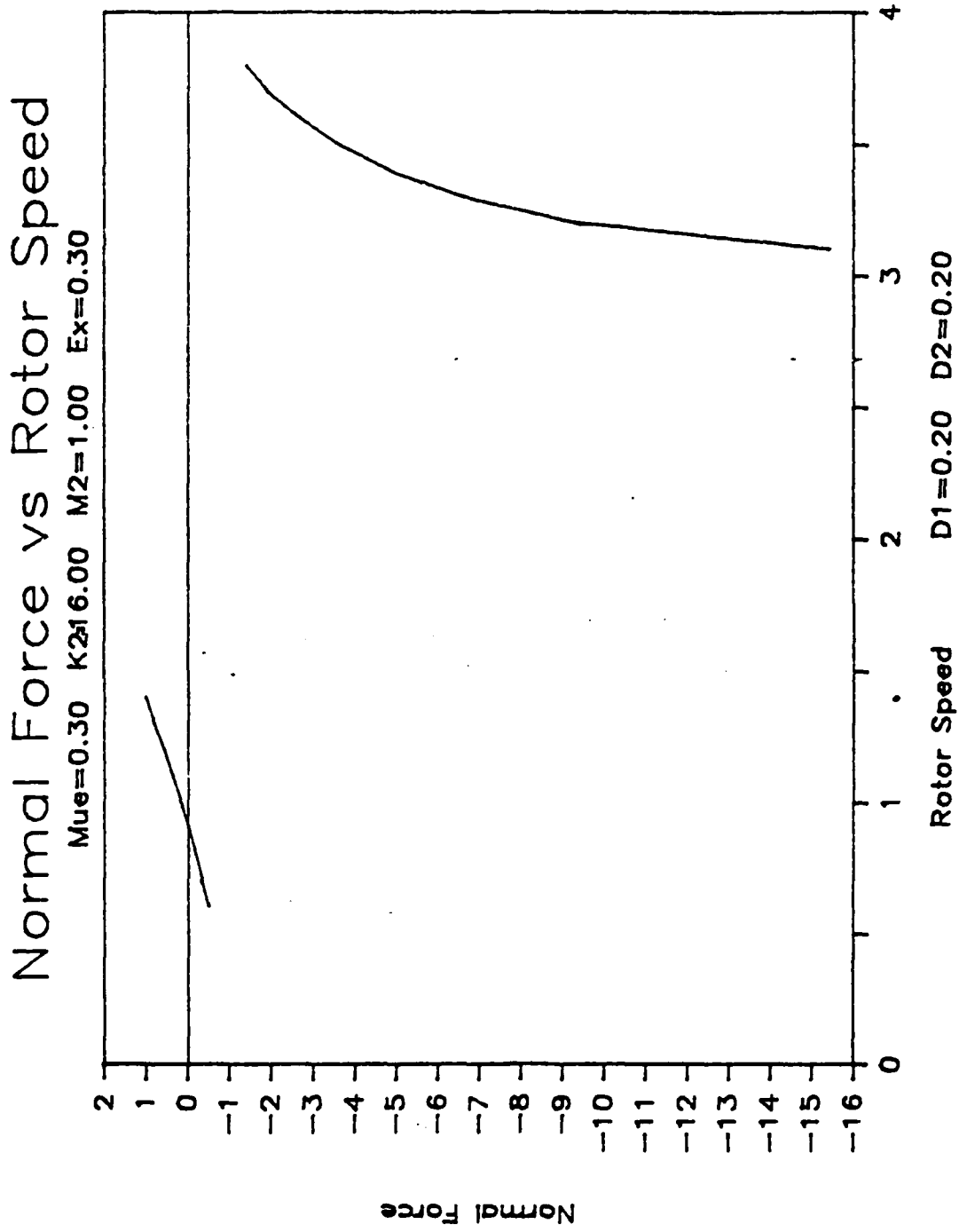
Normal Force vs Rotor Speed
Mue=0.30 K2=16.00 M2=1.00 Ex=0.30
Normal Force
2
1
0
-1
-2
-3
-4
-5
-6
-7
-8
-9
-10
-11
-12
-13
-14
-15
-16
0
1
2
3
4
Rotor Speed
D1=0.20 D2=0.20

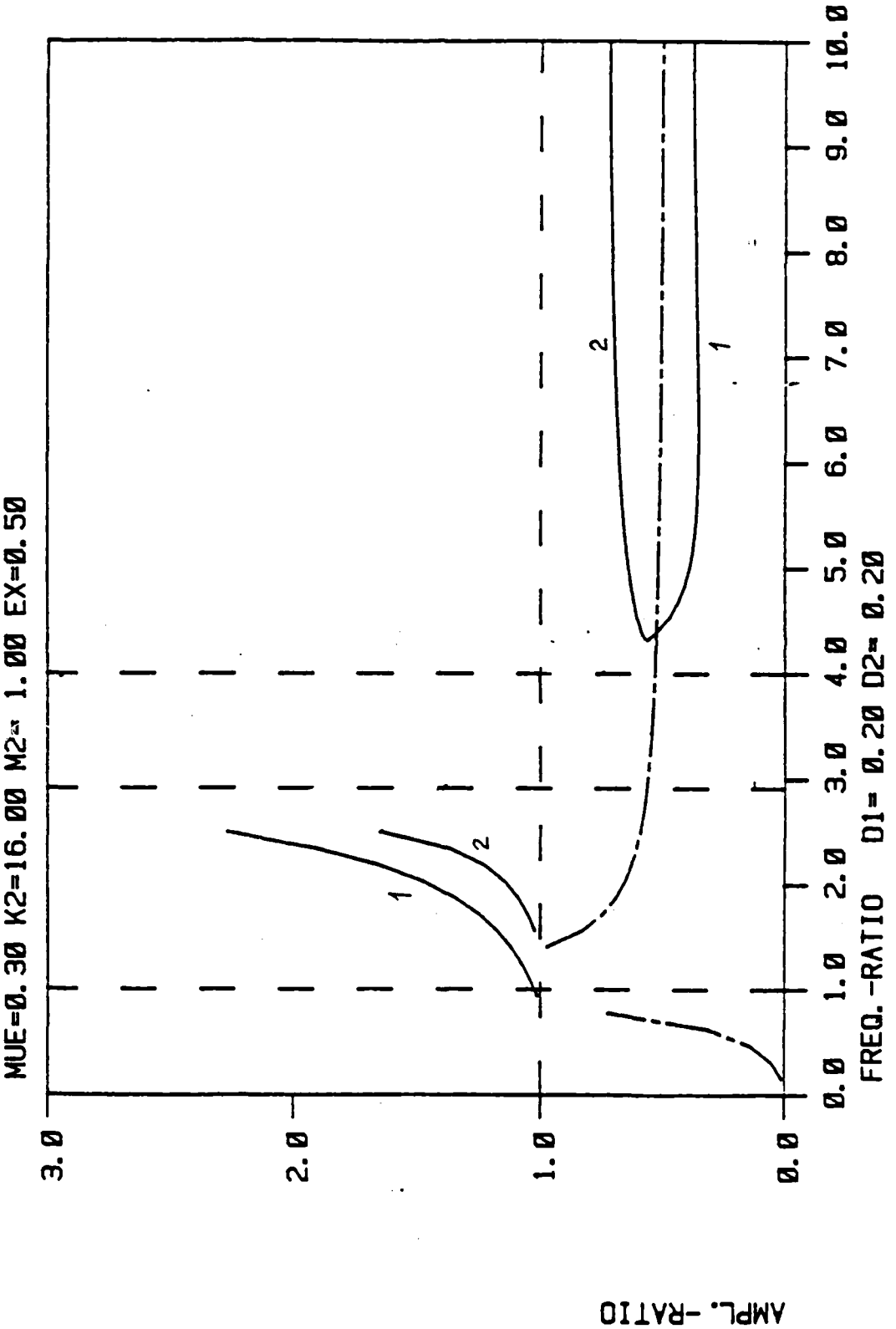
MUE=0.30 K2=16.00 M2= 1.00 EX=0.50
AMPL.-RATIO
FREQ.-RATIO D1= 0.20 D2= 0.20
0.0
1.0
2.0
3.0
4.0
5.0
6.0
7.0
8.0
9.0
10.0
1
2
1
2

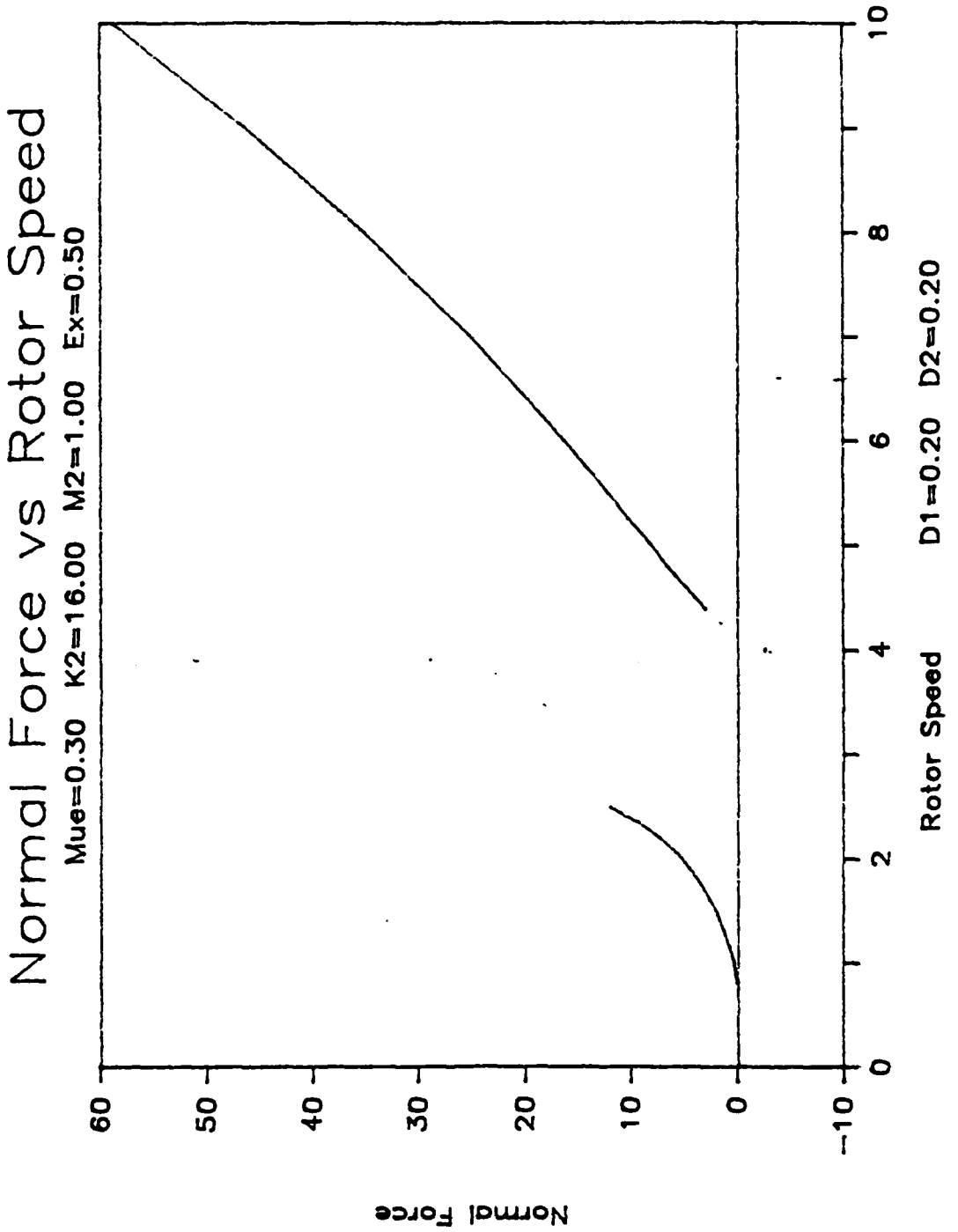
Normal Force vs Rotor Speed
Mue=0.30 K2=16.00 M2=1.00 Ex=0.50
Normal Force
60
50
40
30
20
10
0
-10
0
2
4
6
8
10
Rotor Speed
D1=0.20 D2=0.20

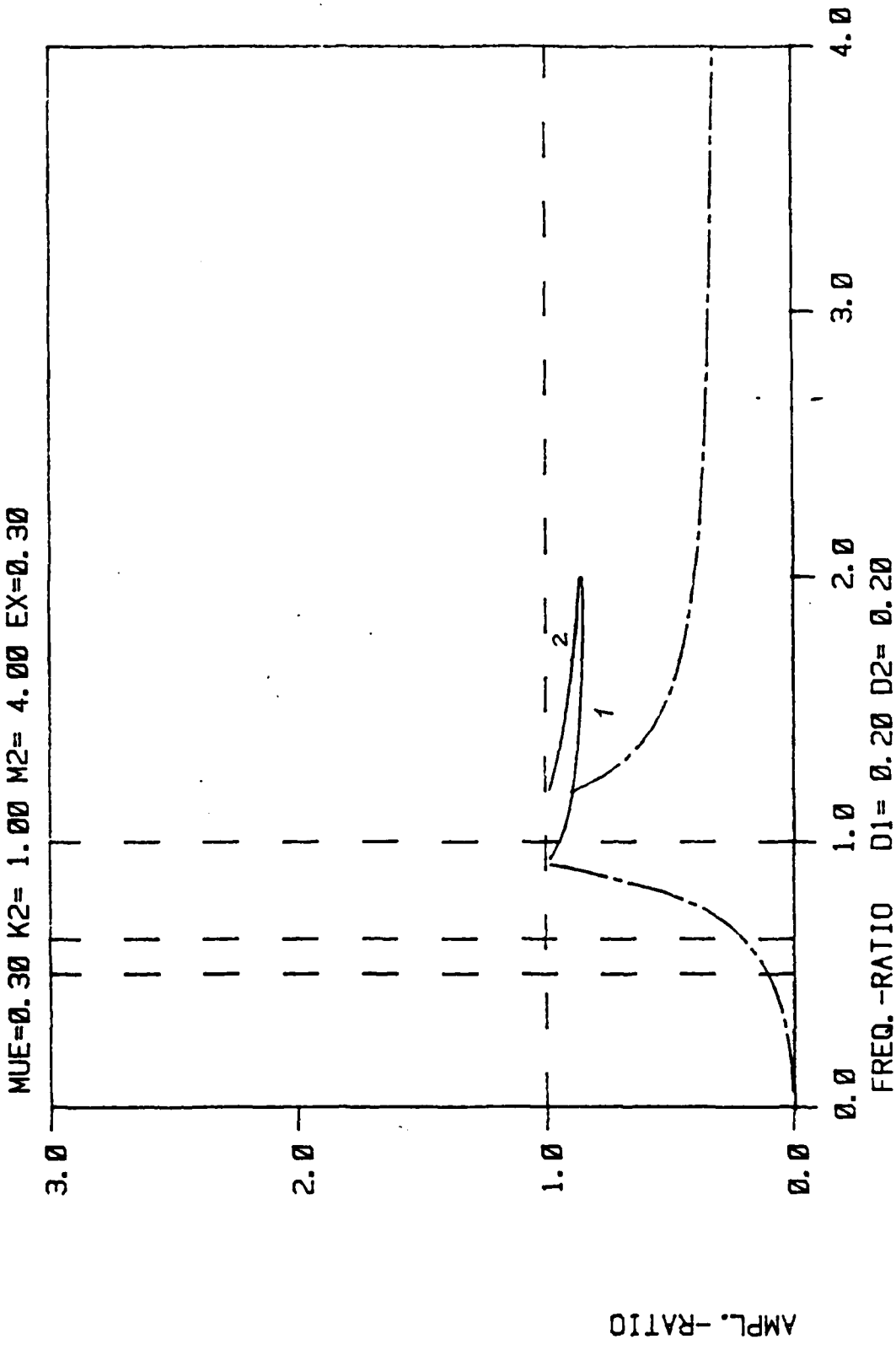
MUE=0.30 K2= 1.00 M2= 4.00 EX=0.30
D1= 0.20 D2= 0.20
AMPL.-RATIO
FREQ.-RATIO
0.0
1.0
2.0
3.0
4.0
1
2

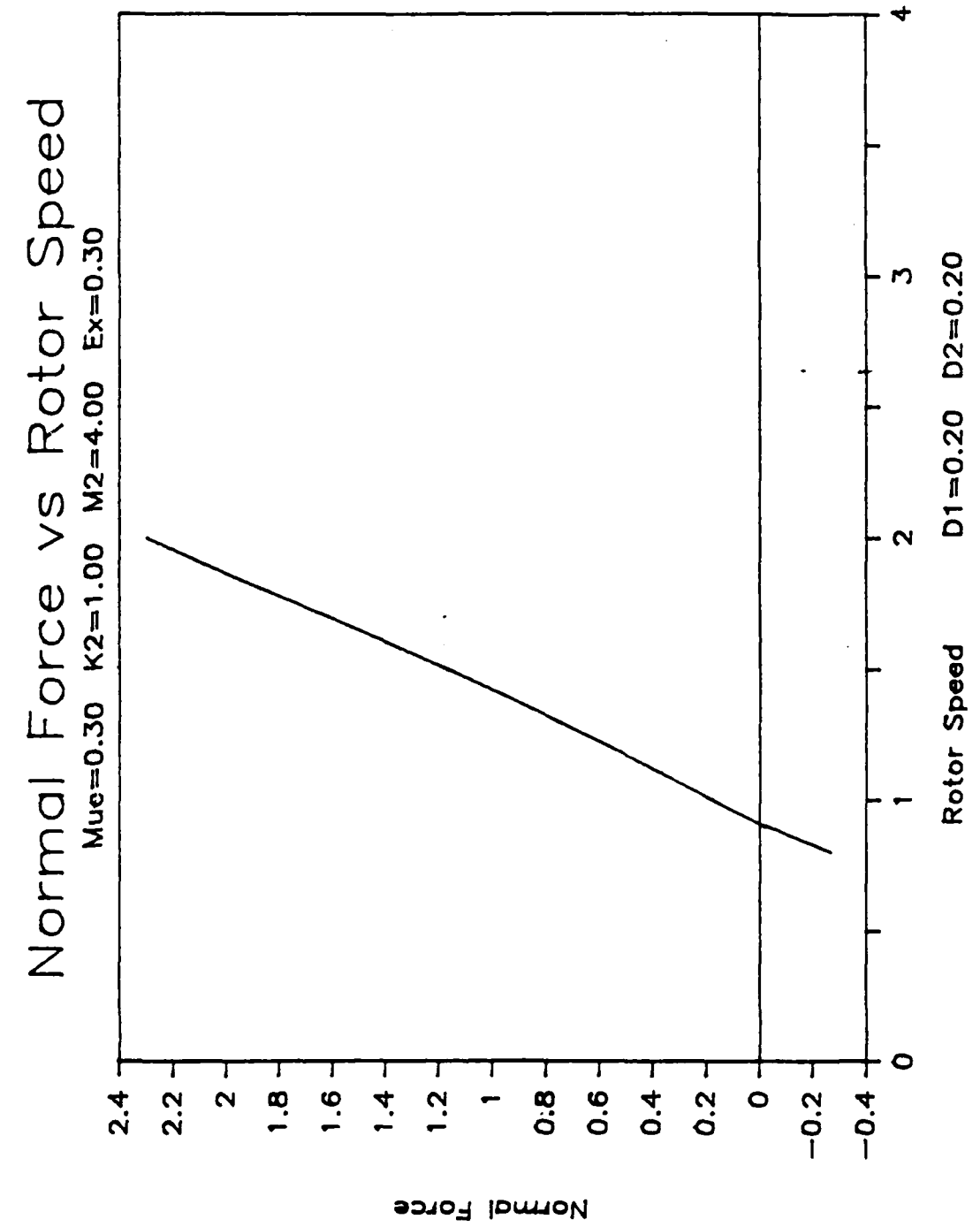
Normal Force vs Rotor Speed
Mue=0.30 K2=1.00 M2=4.00 Ex=0.30
Normal Force
2.4
2.2
2
1.8
1.6
1.4
1.2
1
0.8
0.6
0.4
0.2
0
-0.2
-0.4
0
1
2
3
4
Rotor Speed
D1=0.20 D2=0.20

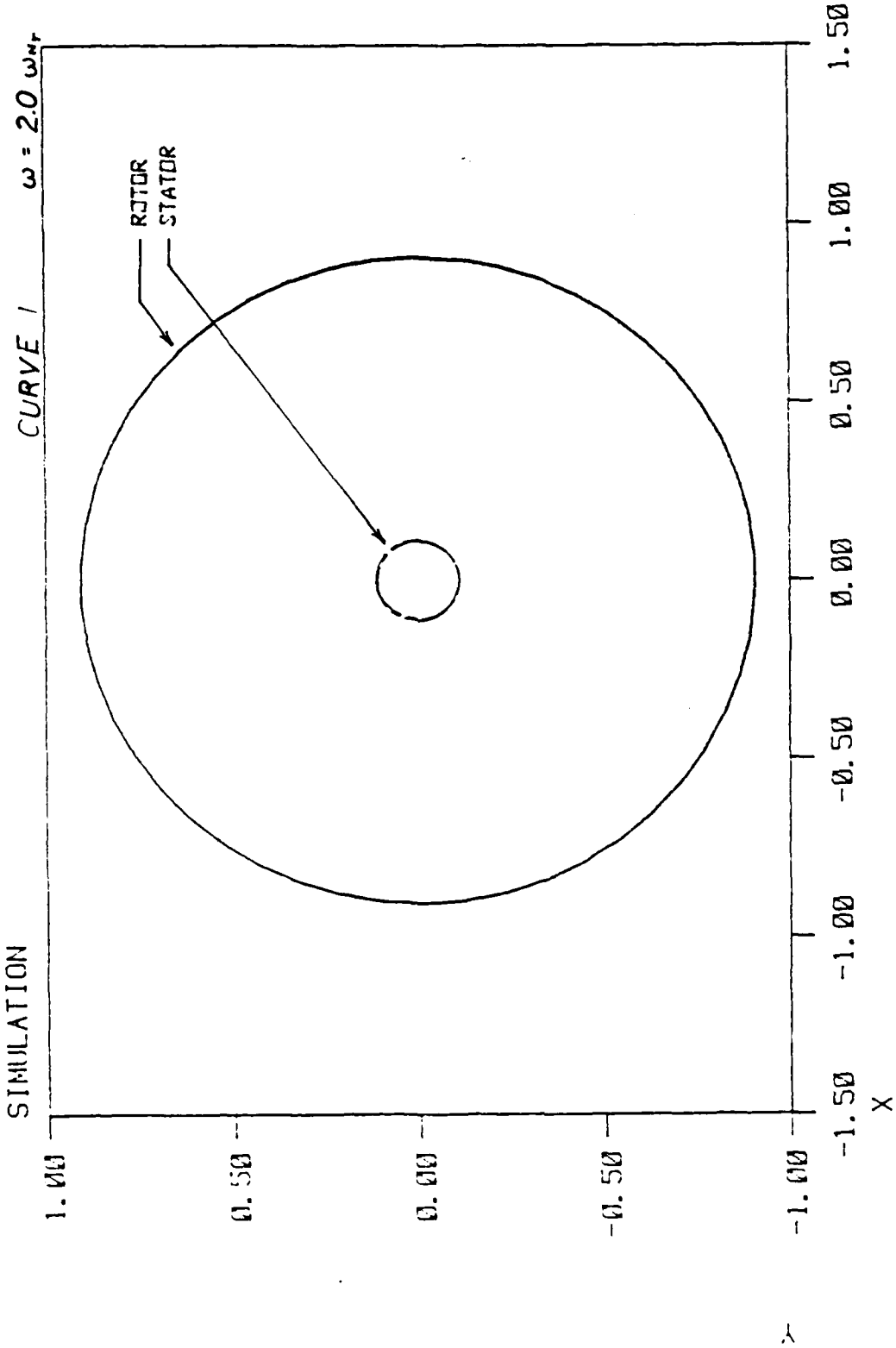
SIMULATION
CURVE 1
ω = 2.0 ωr
ROTOR
STATOR
1.00
0.50
0.00
-0.50
-1.00
-1.50
-1.00
-0.50
0.00
0.50
1.00
1.50
X
Y

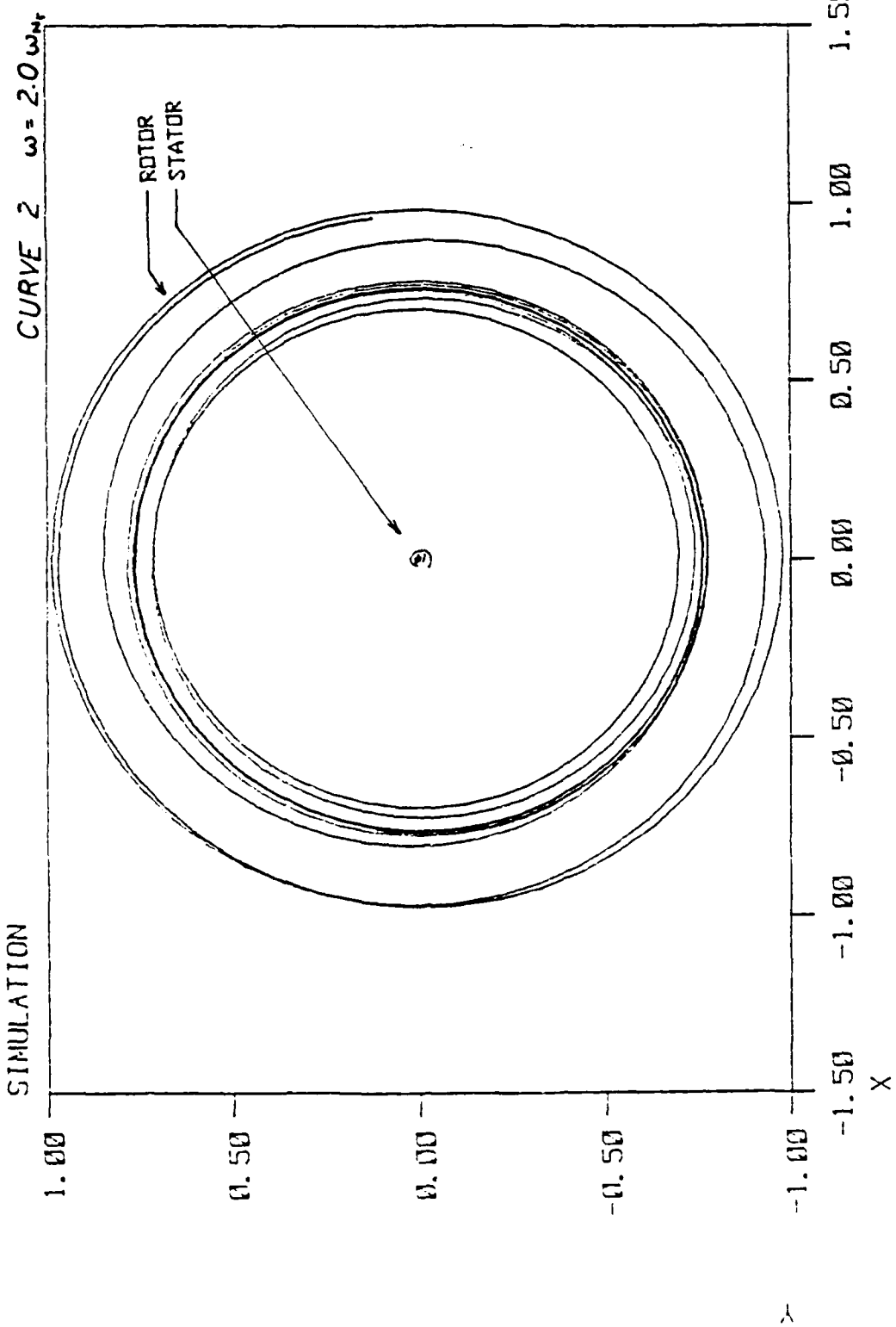
SIMULATION
CURVE 2 ω = 2.0 ω_n
ROTOR
STATOR
1.00
0.50
0.00
-0.50
-1.00
-1.50
-1.00
-0.50
0.00
0.50
1.00
1.50
X

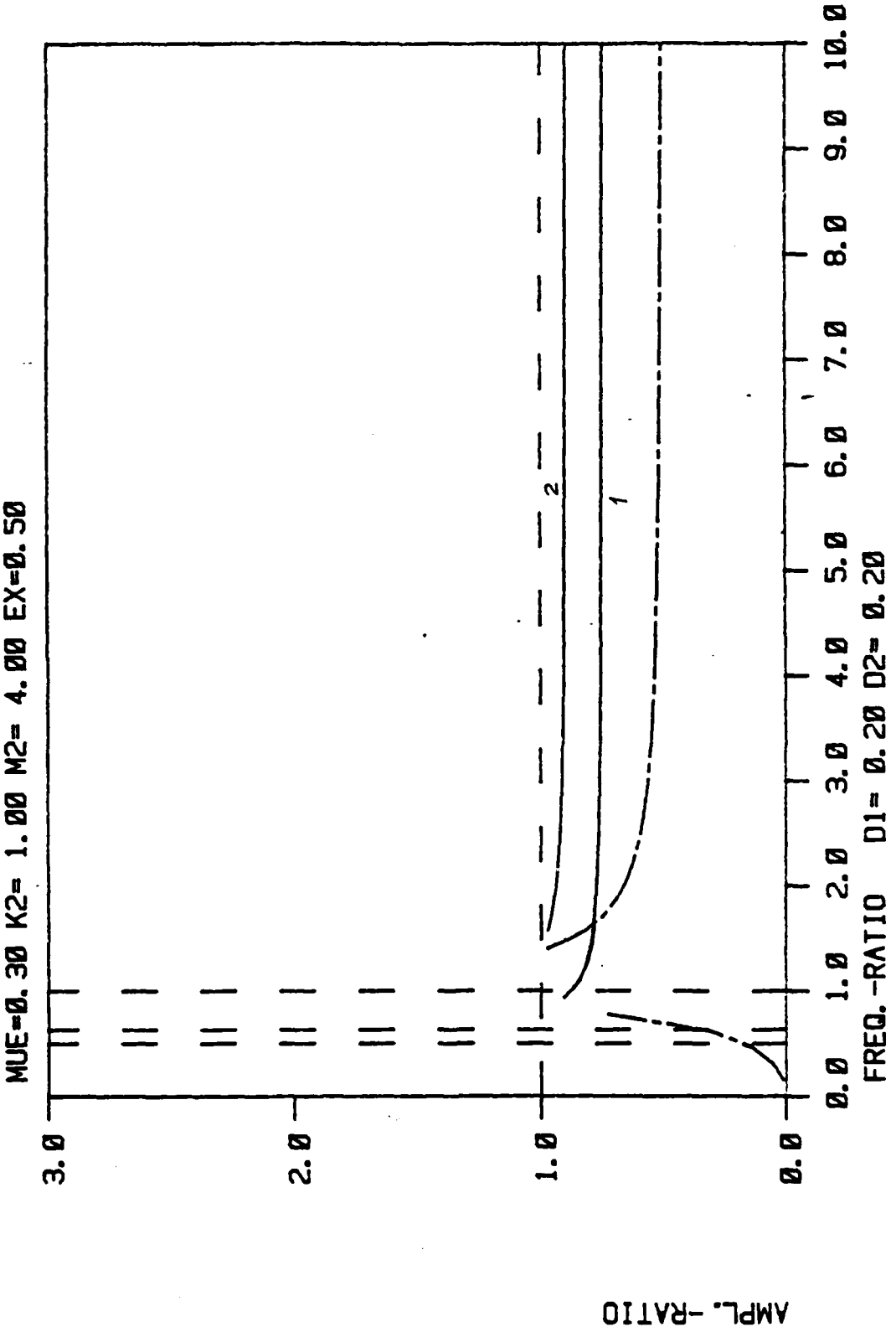
MUE=0.30 K2= 1.00 M2= 4.00 EX=0.50
AMPL.-RATIO
3.0
2.0
1.0
0.0
0.0 1.0 2.0 3.0 4.0 5.0 6.0 7.0 8.0 9.0 10.0
FREQ.-RATIO D1= 0.20 D2= 0.20
1
2

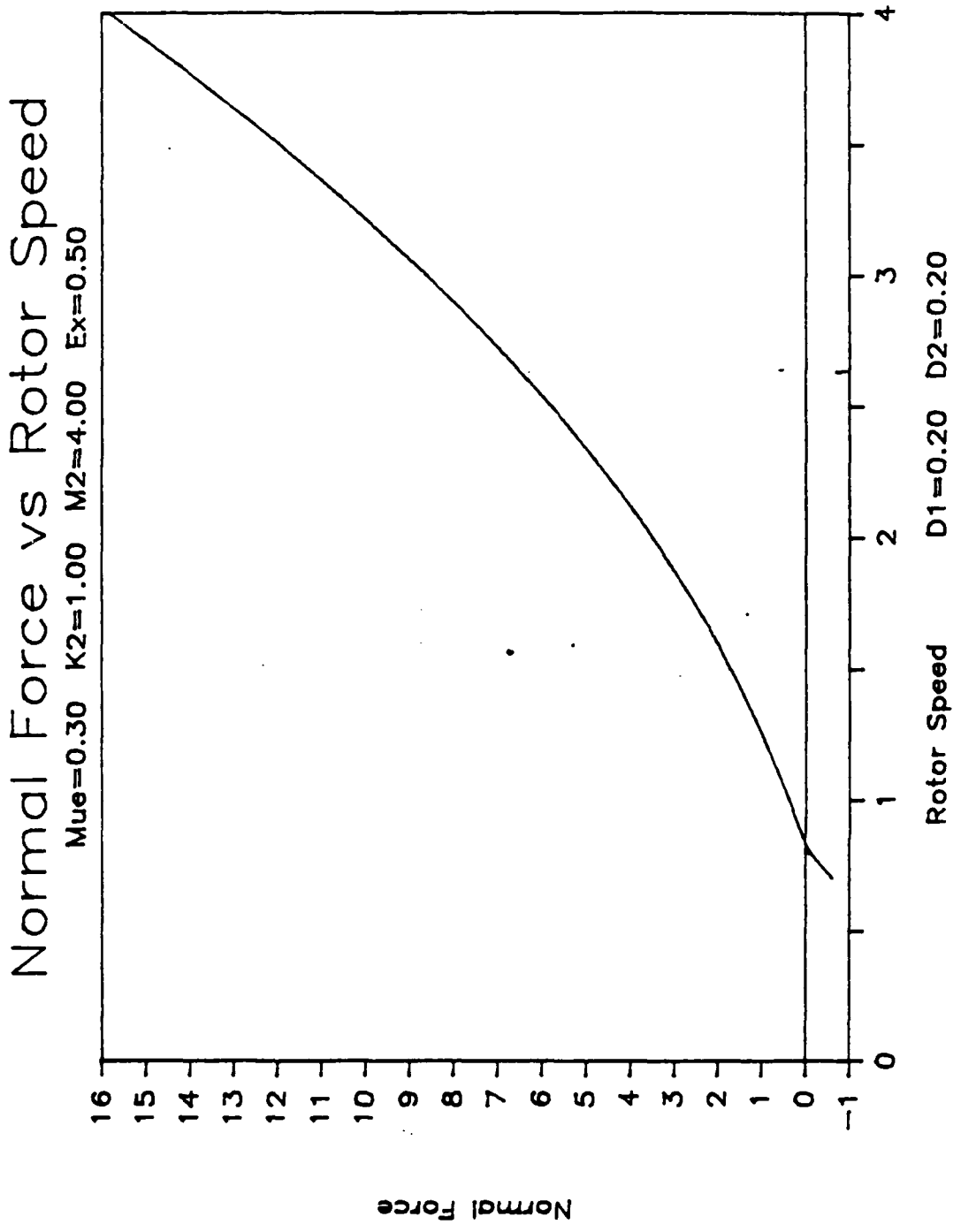
Normal Force vs Rotor Speed
Mue=0.30 K2=1.00 M2=4.00 Ex=0.50
Normal Force
16
15
14
13
12
11
10
9
8
7
6
5
4
3
2
1
0
-1
0
1
2
3
4
Rotor Speed
D1=0.20 D2=0.20

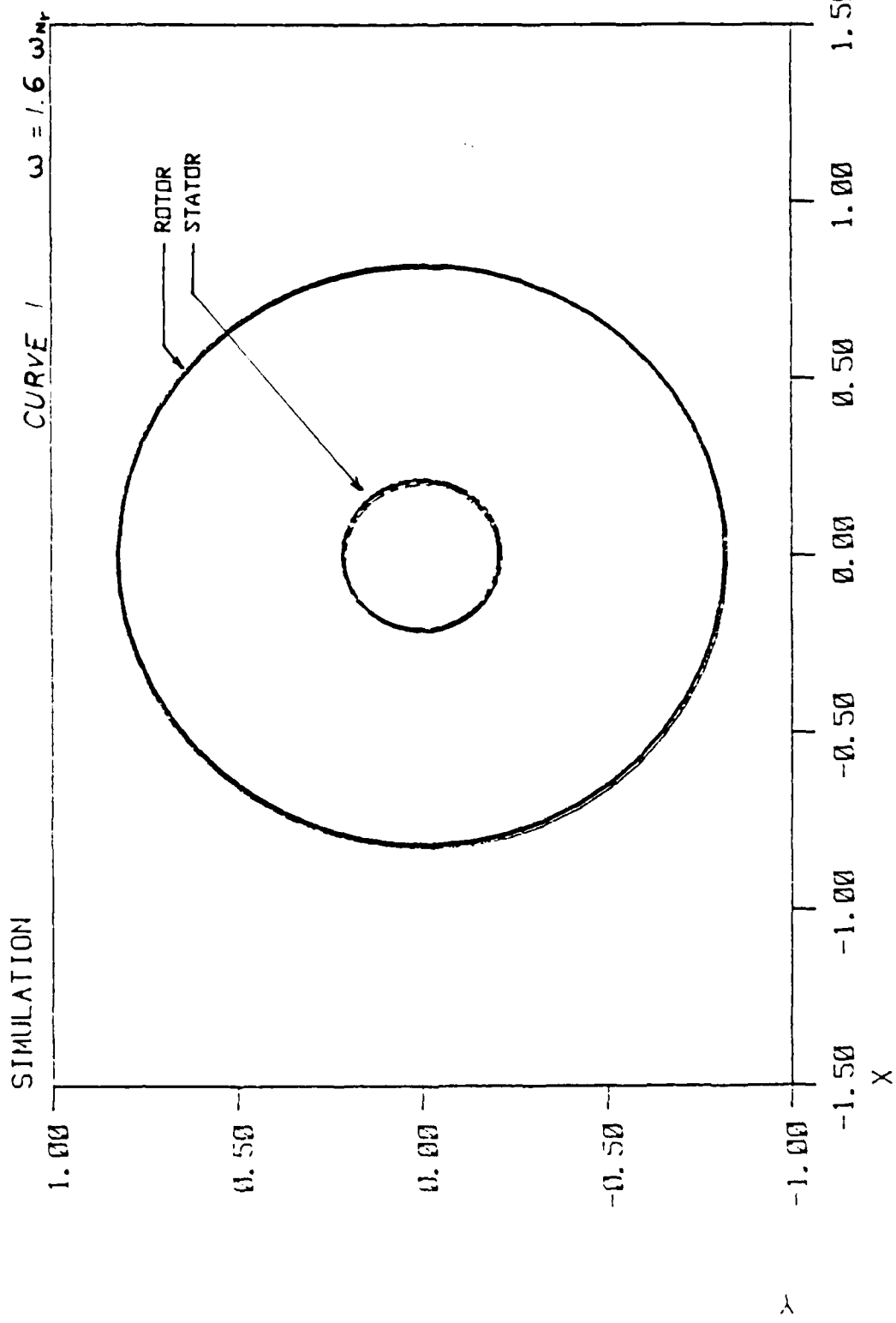
SIMULATION
CURVE 1
ω = 1.6 ω_Nr
ROTOR
STATOR
1.00
0.50
0.00
-0.50
-1.00
-1.50
-1.00
-0.50
0.00
0.50
1.00
1.50
X
Y

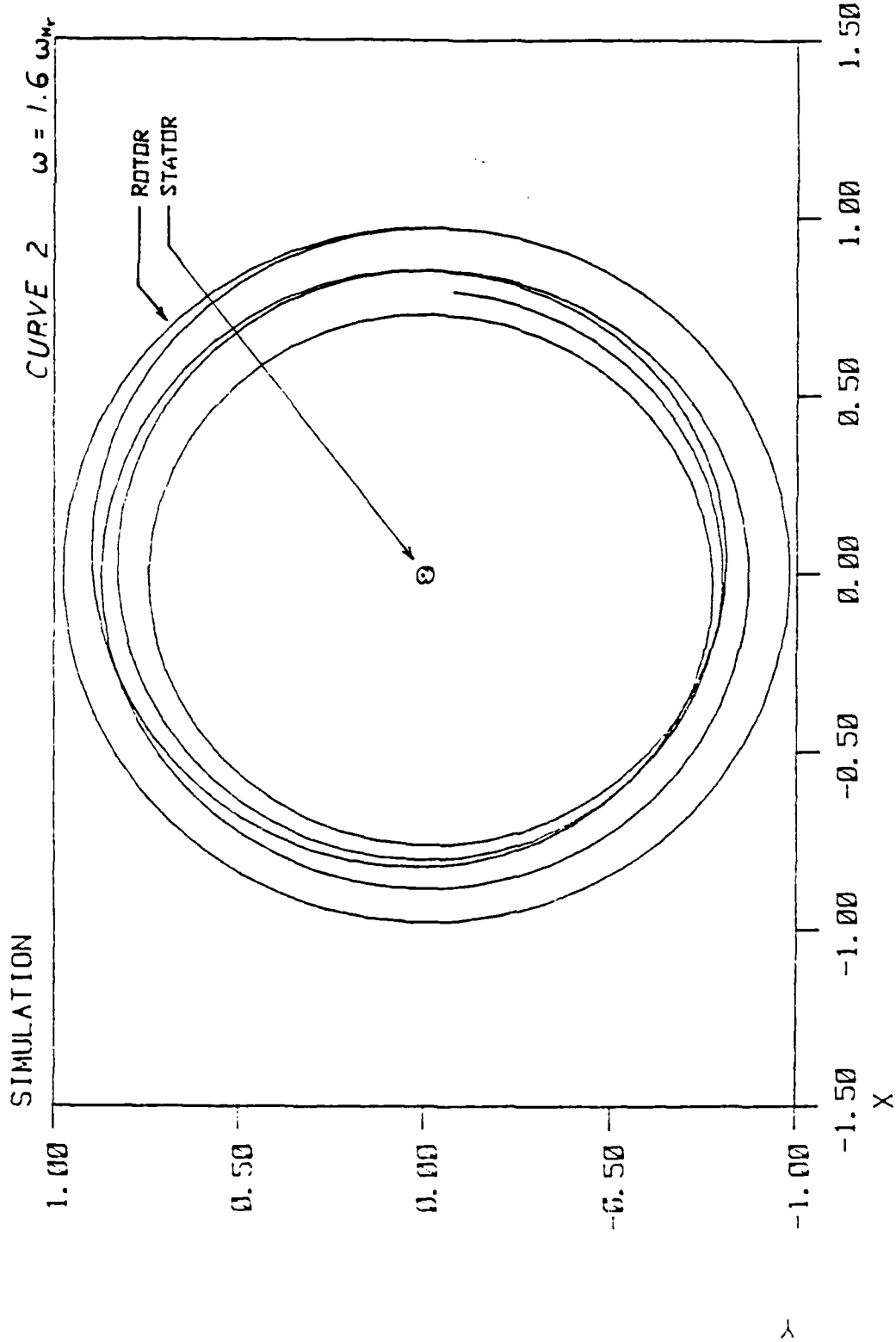
SIMULATION
CURVE 2 ω = 1.6 ω_r
ROTOR
STATOR
θ
1.00
0.50
0.00
-0.50
-1.00
-1.50
-1.00
-0.50
0.00
0.50
1.00
1.50
X
Y

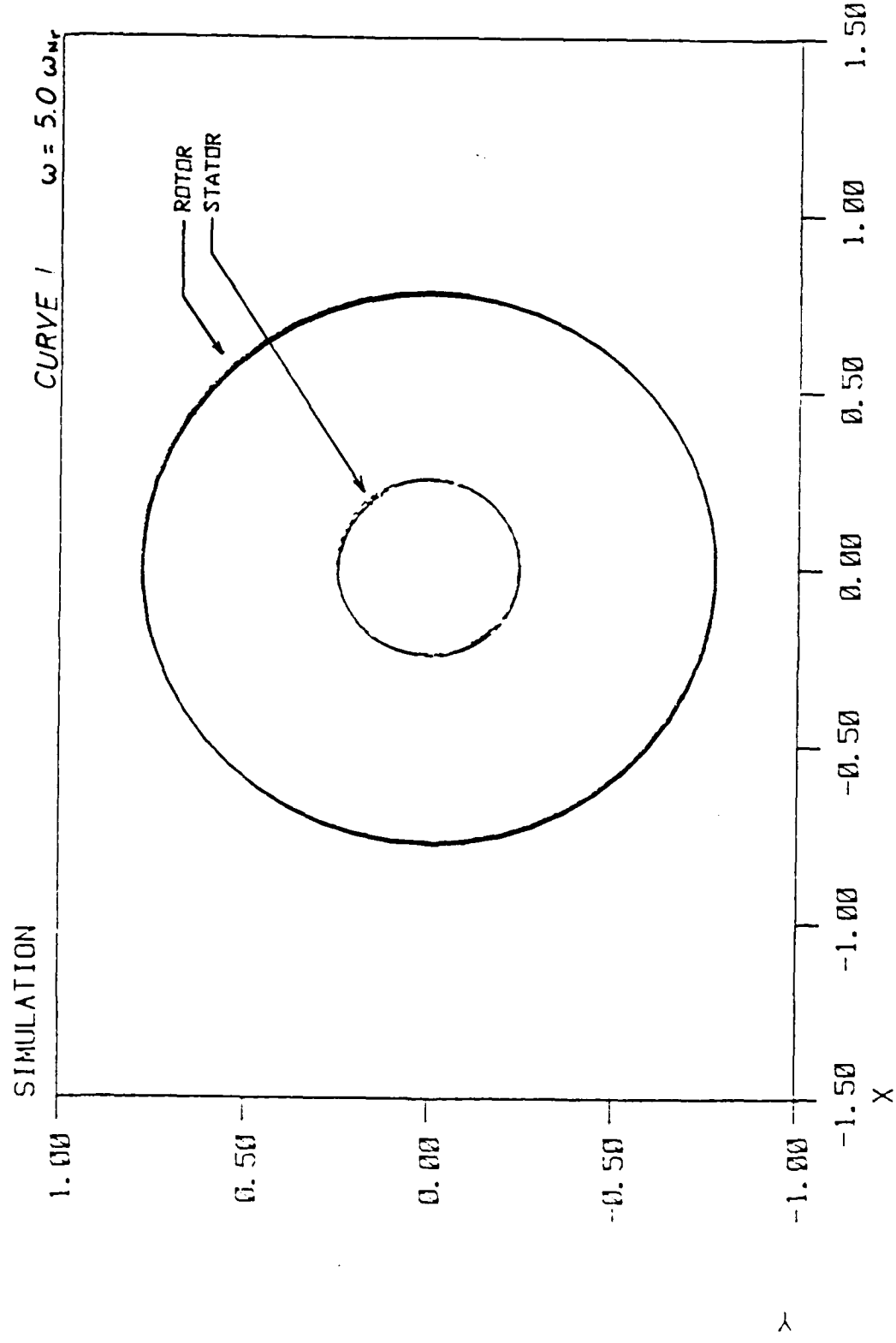
SIMULATION
CURVE 1
ω = 5.0 ωNr
ROTOR
STATOR
1.00
0.50
0.00
-0.50
-1.00
-1.50
-1.00
-0.50
0.00
0.50
1.00
1.50
X
Y

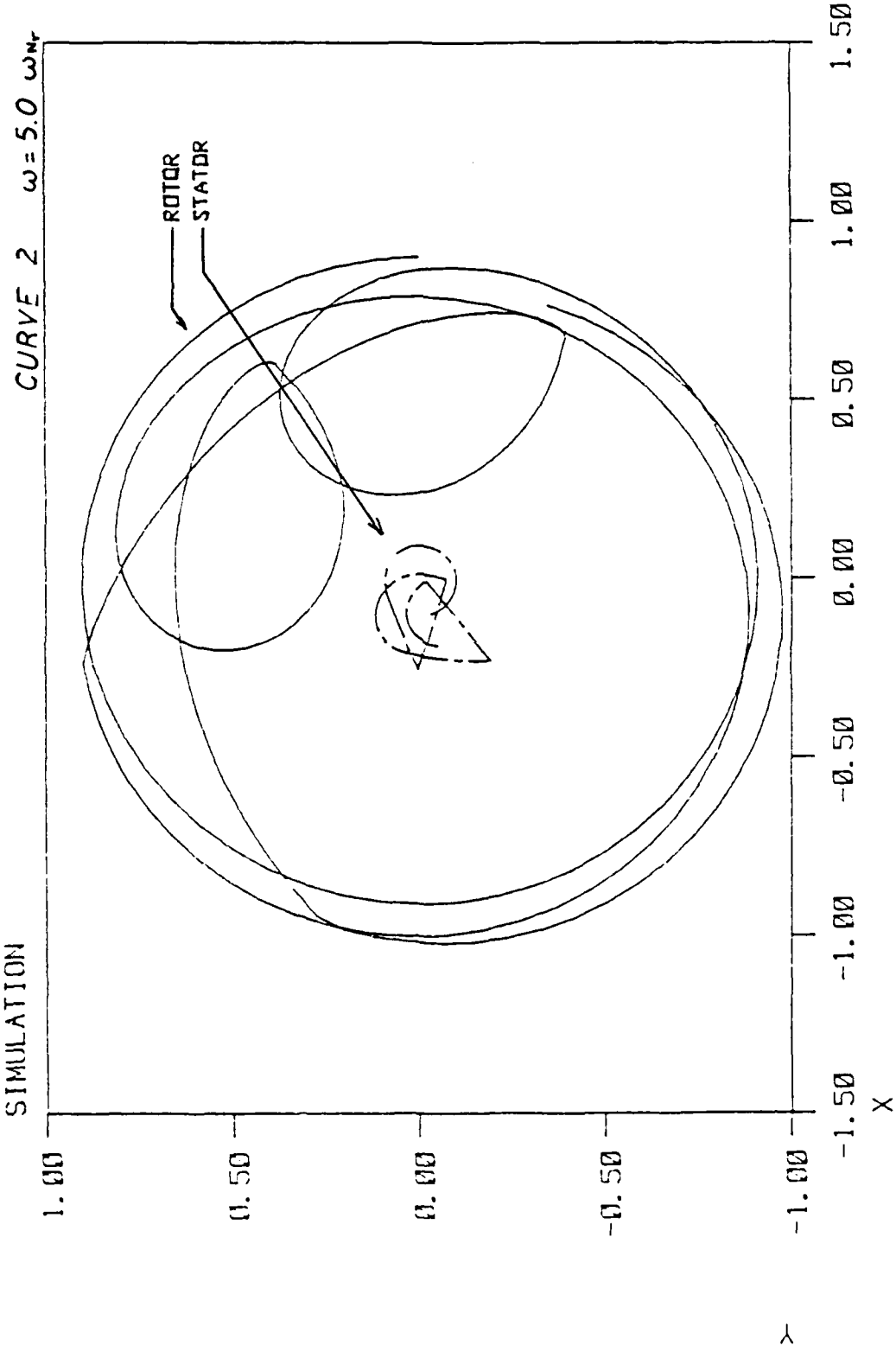
SIMULATION
CURVE 2 ω = 5.0 ωNr
ROTOR
STATOR
1.00
0.50
0.00
-0.50
-1.00
-1.50
-1.00
-0.50
0.00
0.50
1.00
1.50
X
Y

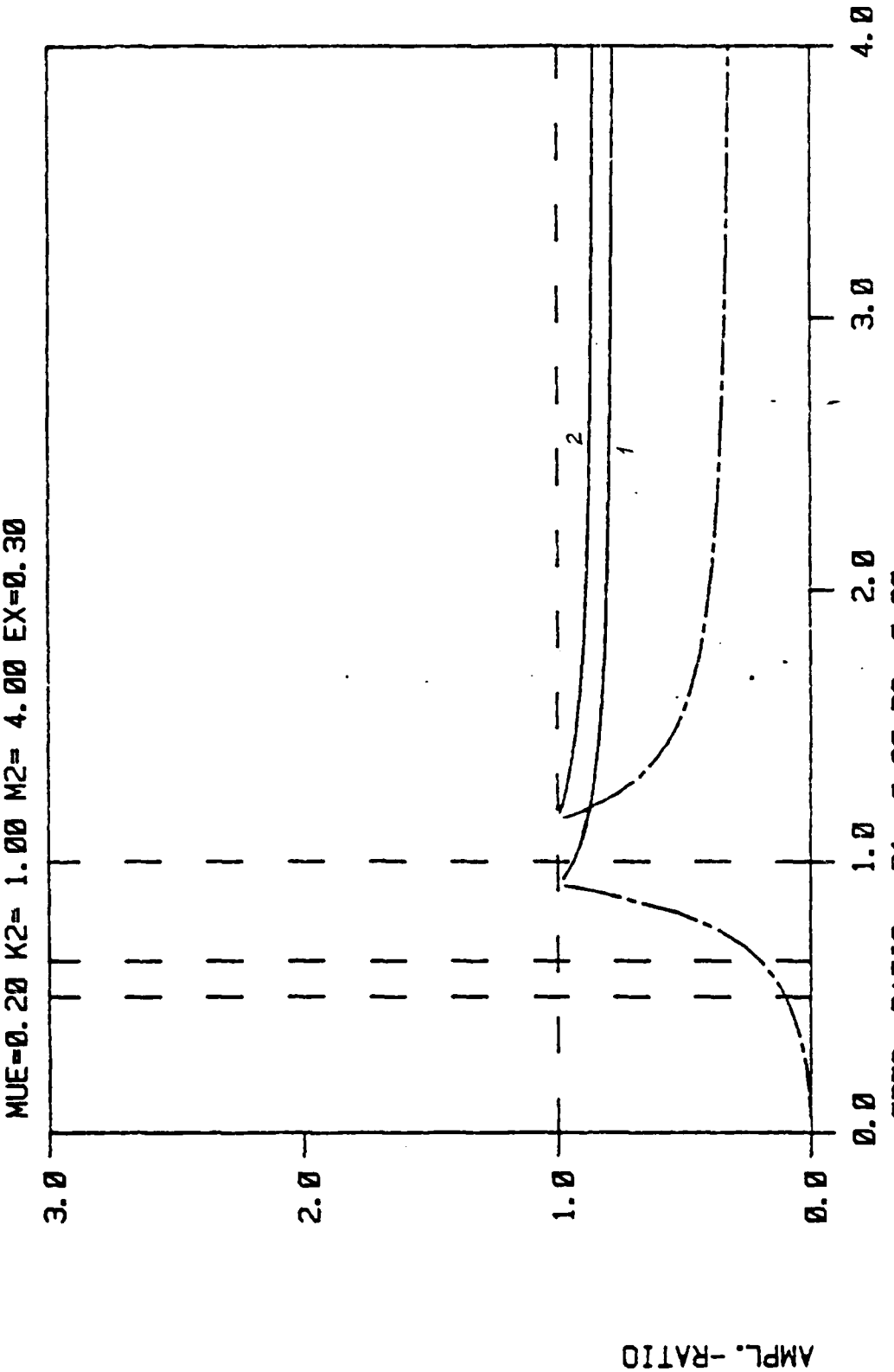
MUE=0.20 K2= 1.00 M2= 4.00 EX=0.30
AMPL.-RATIO
FREQ.-RATIO D1= 0.20 D2= 0.20
0.0
1.0
2.0
3.0
4.0
1
2

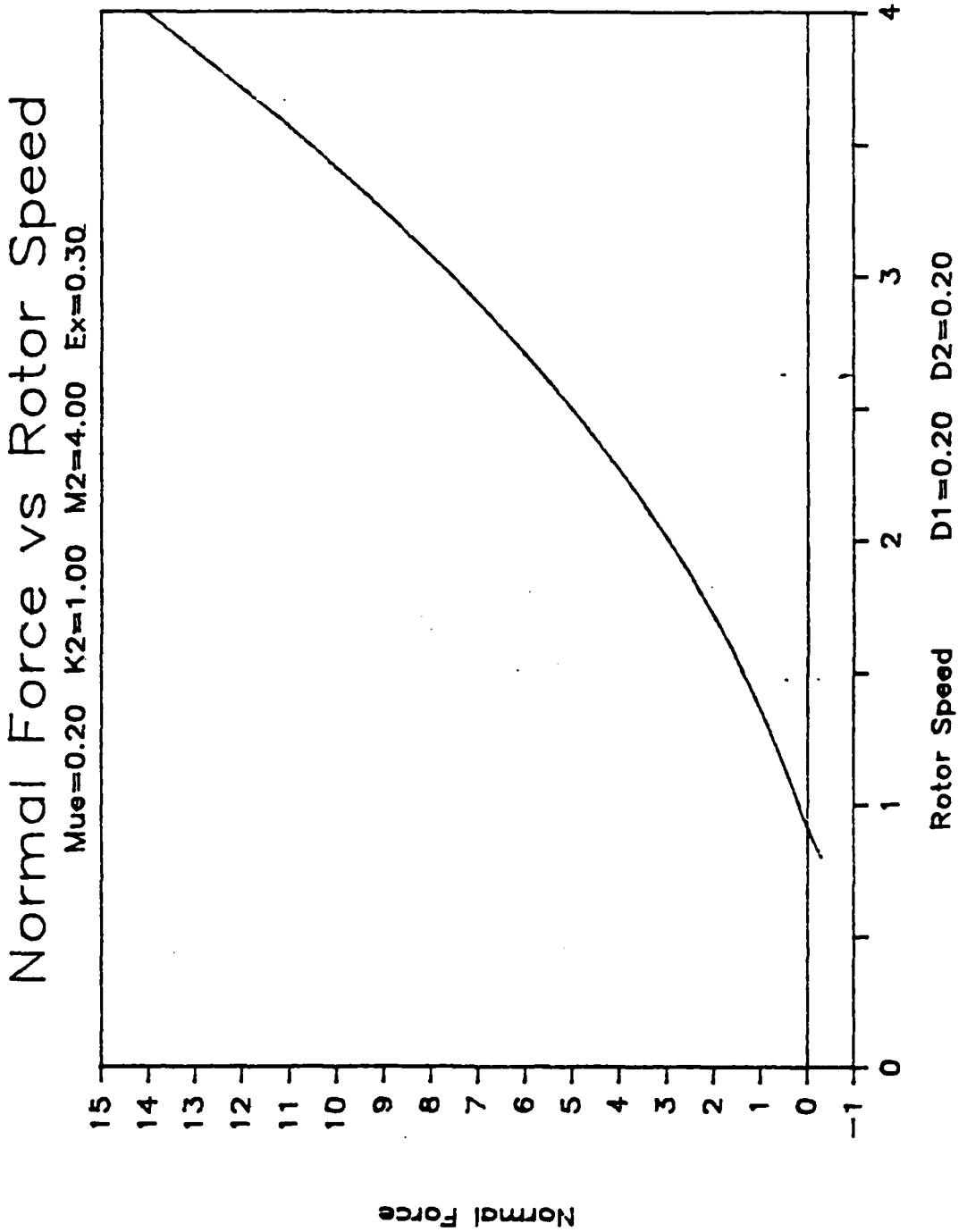
Normal Force vs Rotor Speed
Mue=0.20 K2=1.00 M2=4.00 Ex=0.30
Normal Force
15
14
13
12
11
10
9
8
7
6
5
4
3
2
1
0
-1
0
1
2
3
4
Rotor Speed
D1=0.20 D2=0.20

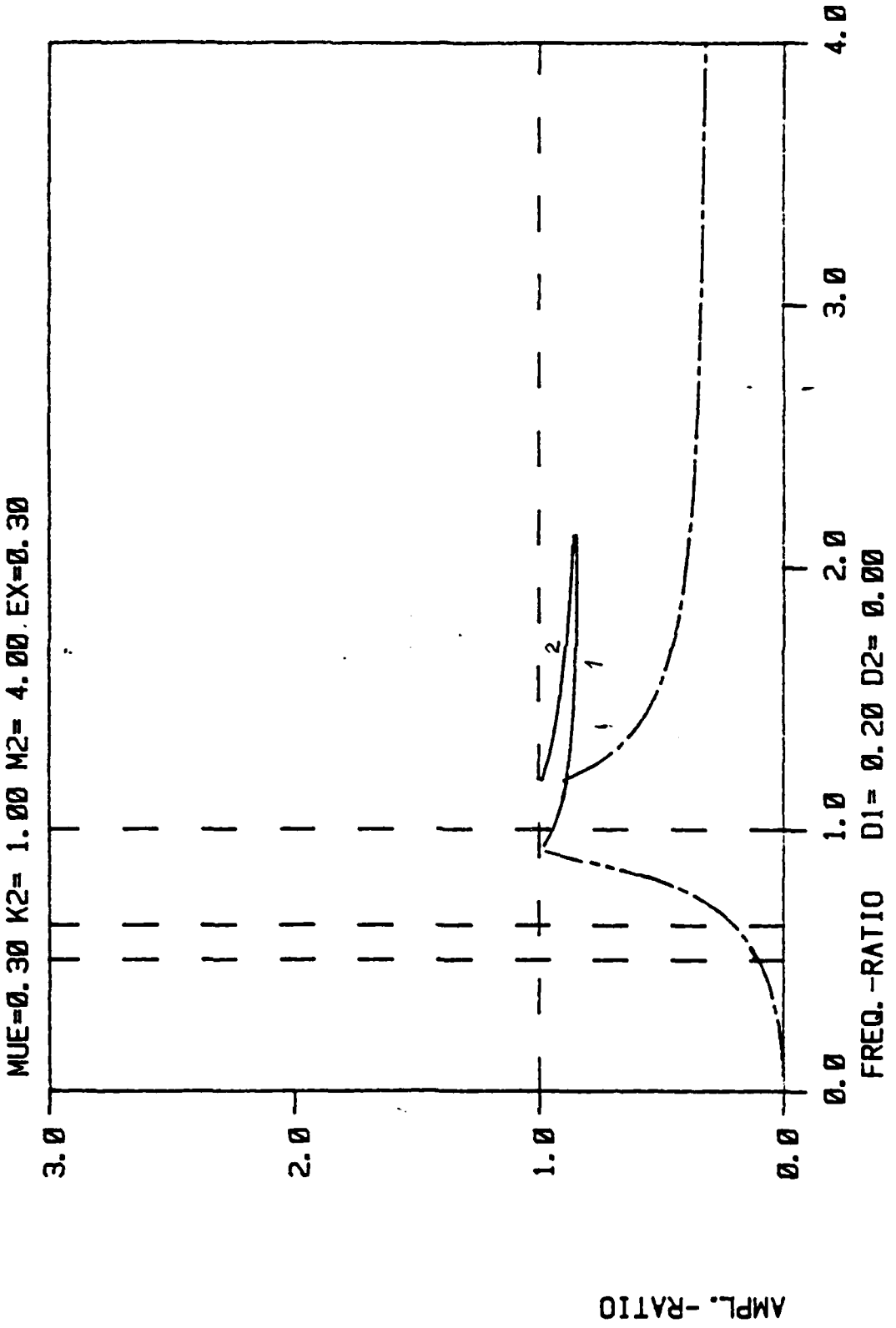
MUE=0.30 K2= 1.00 M2= 4.00 EX=0.30
AMPL.-RATIO
FREQ.-RATIO D1= 0.20 D2= 0.00
0.0
1.0
2.0
3.0
4.0
1
2

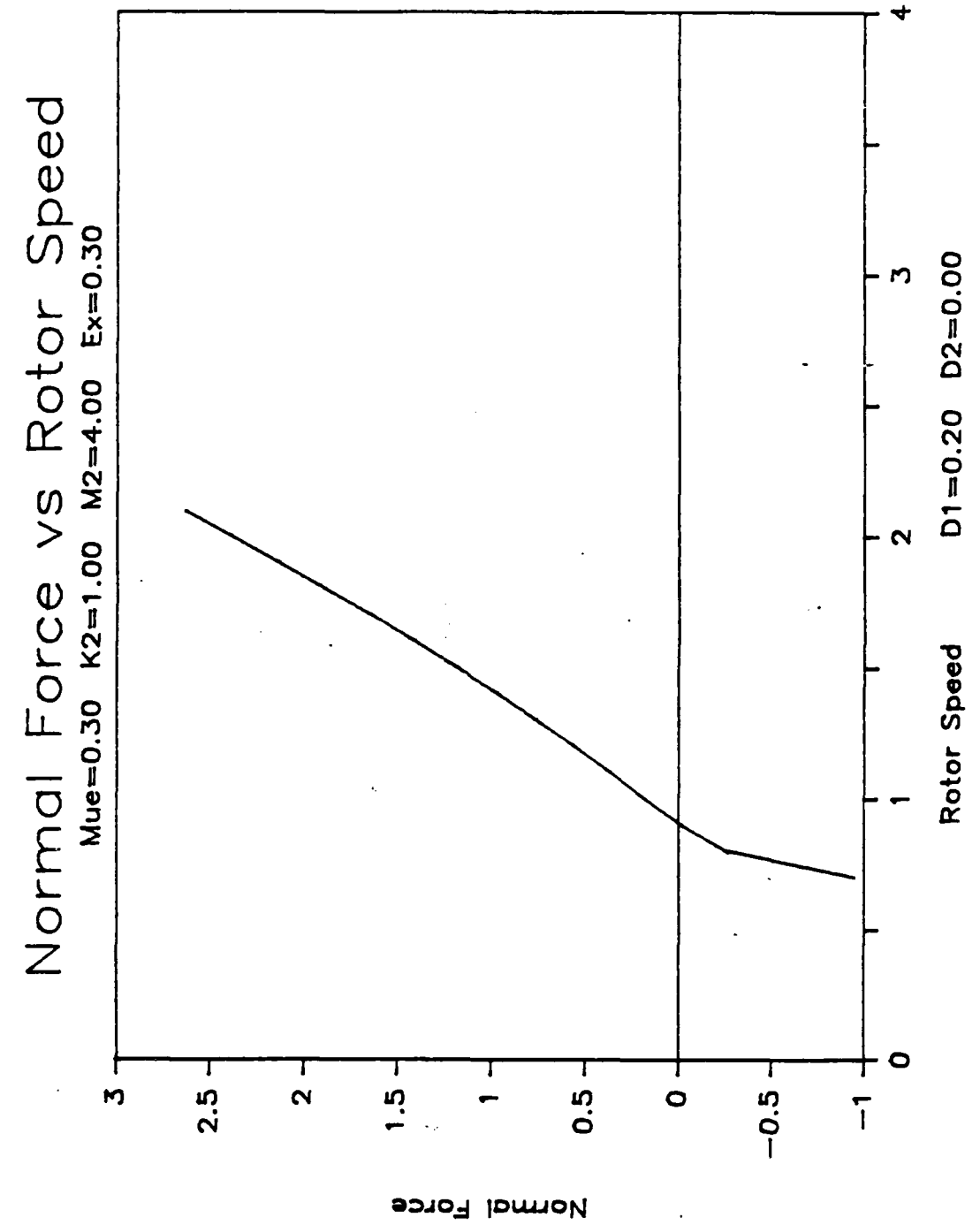
Normal Force vs Rotor Speed
Mue=0.30 K2=1.00 M2=4.00 Ex=0.30
Normal Force
3
2.5
2
1.5
1
0.5
0
-0.5
-1
0
1
2
3
4
Rotor Speed
D1=0.20 D2=0.00

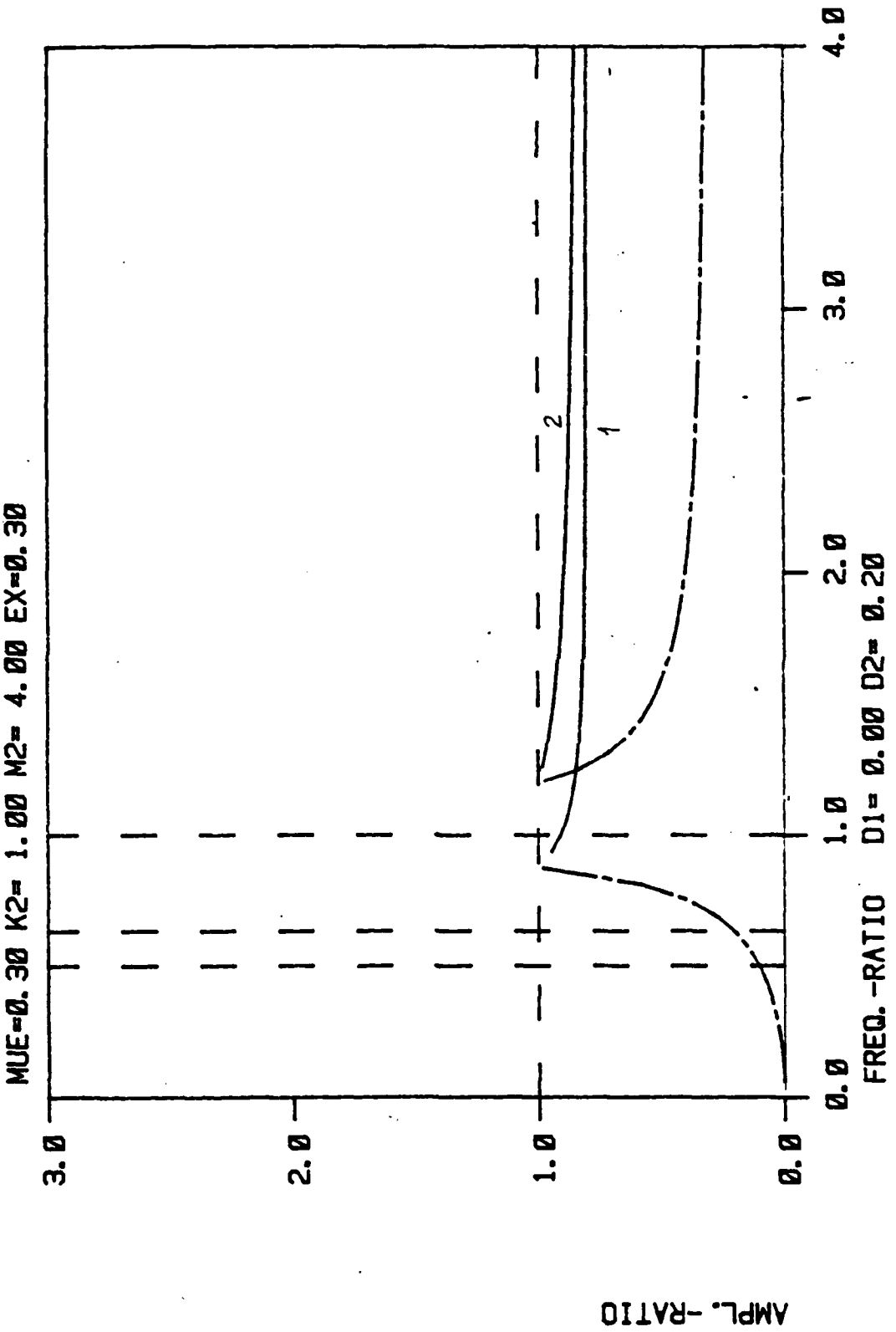
MUE=0.30 K2= 1.00 M2= 4.00 EX=0.30
D1= 0.00 D2= 0.20
FREQ.-RATIO
AMPL.-RATIO
0.0
1.0
2.0
3.0
4.0
1
2

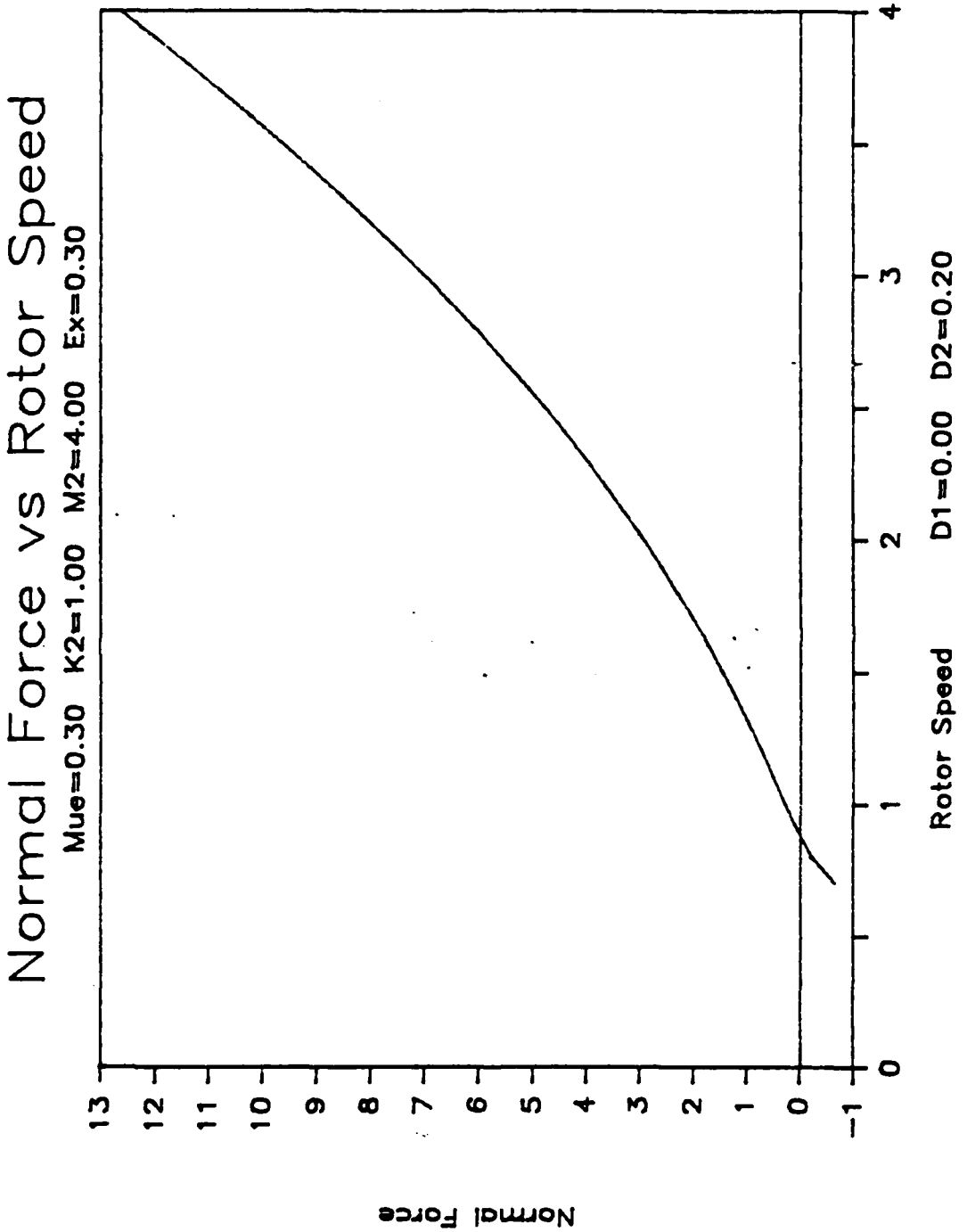
Normal Force vs Rotor Speed
Mue=0.30 K2=1.00 M2=4.00 Ex=0.30
Normal Force
13
12
11
10
9
8
7
6
5
4
3
2
1
0
-1
0
1
2
3
4
Rotor Speed
D1=0.00 D2=0.20

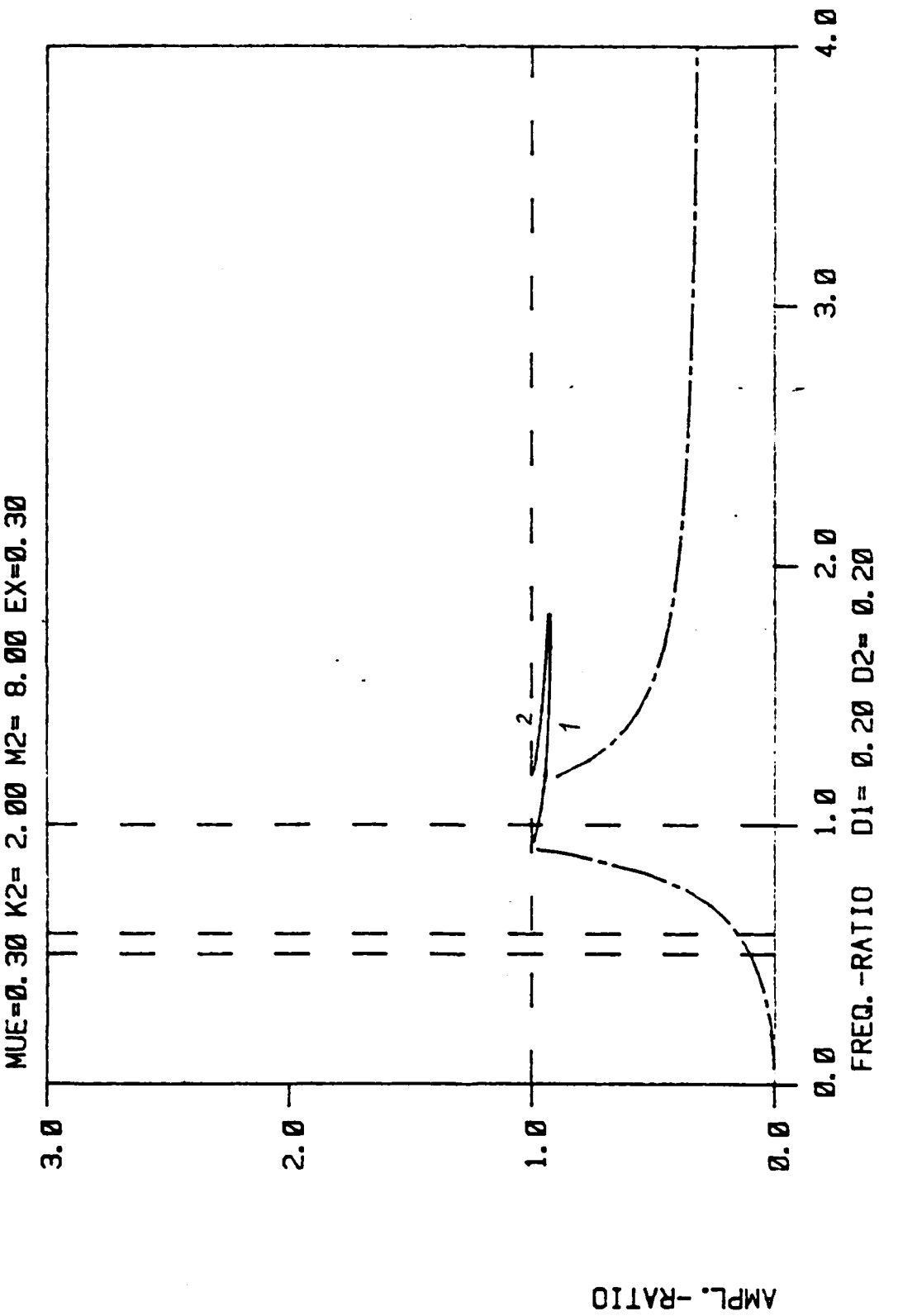
MUE=0.30 K2= 2.00 M2= 8.00 EX=0.30
AMPL.-RATIO
FREQ.-RATIO D1= 0.20 D2= 0.20
0.0
1.0
2.0
3.0
4.0
1
2

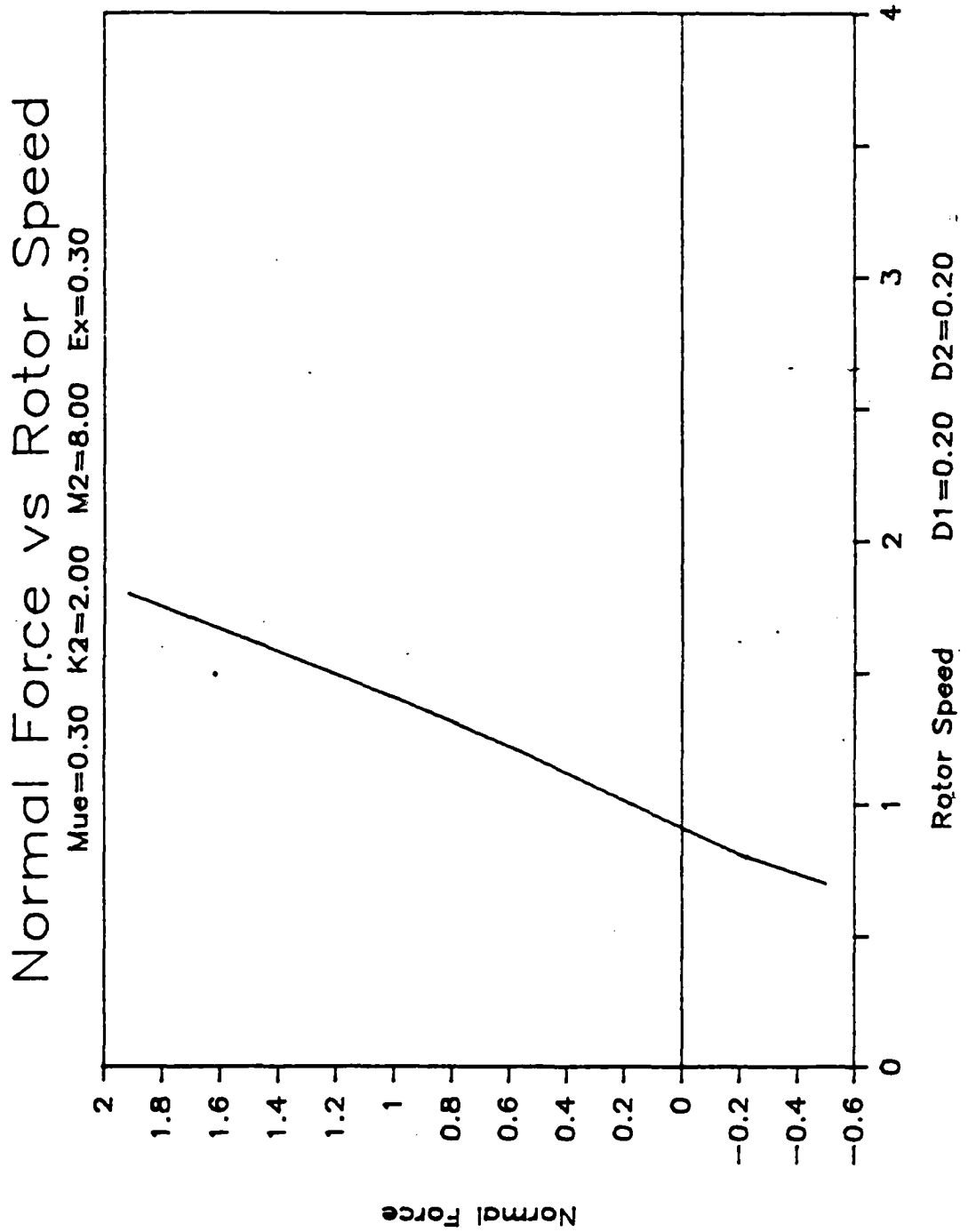
Normal Force vs Rotor Speed
Mue=0.30 K2=2.00 M2=8.00 Ex=0.30
Normal Force
2
1.8
1.6
1.4
1.2
1
0.8
0.6
0.4
0.2
0
-0.2
-0.4
-0.6
0
1
2
3
4
Rotor Speed
D1=0.20 D2=0.20

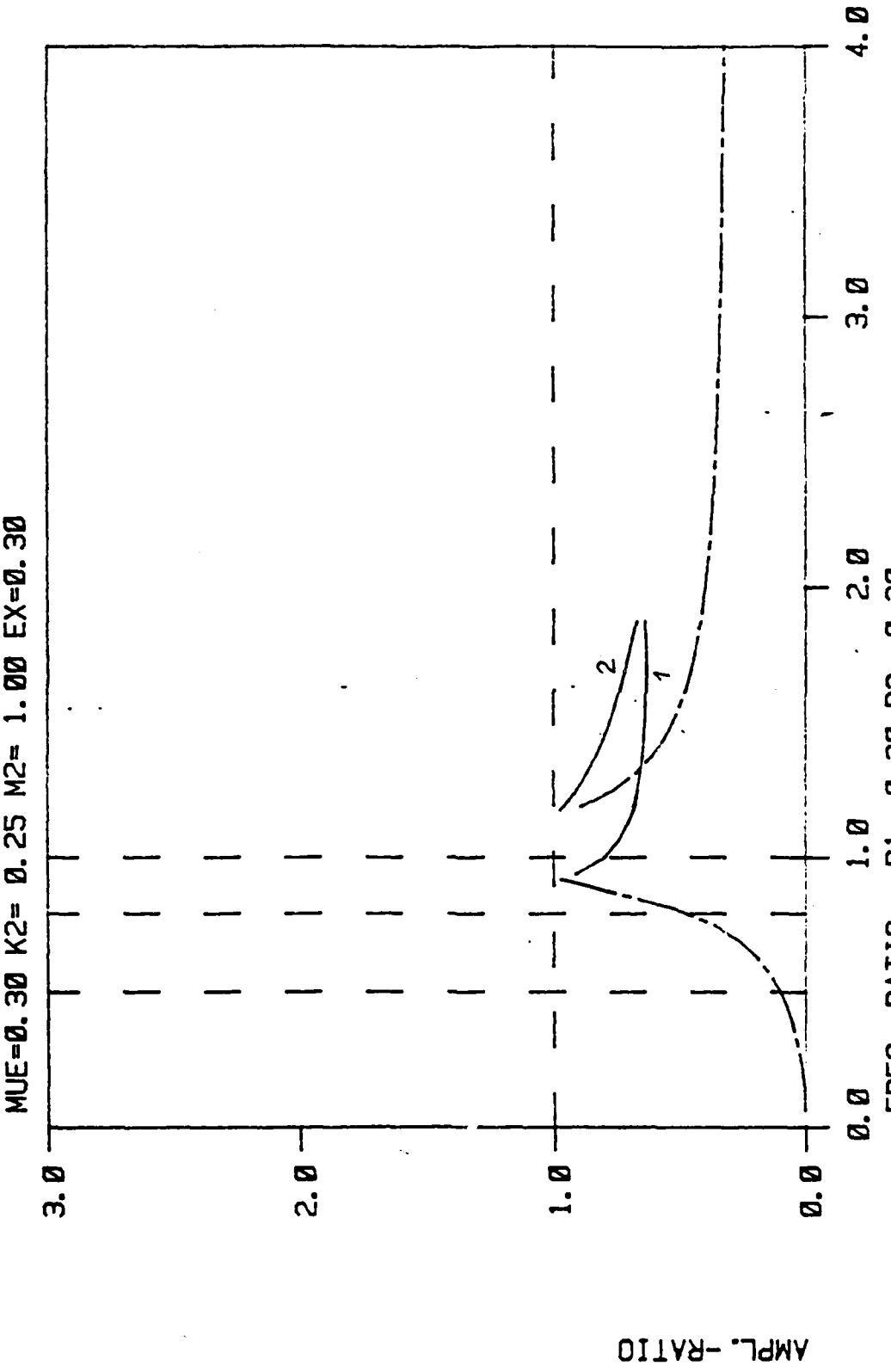
MUE=0.30 K2= 0.25 M2= 1.00 EX=0.30
AMPL.-RATIO
FREQ.-RATIO D1= 0.20 D2= 0.20
0.0
1.0
2.0
3.0
4.0
1
2

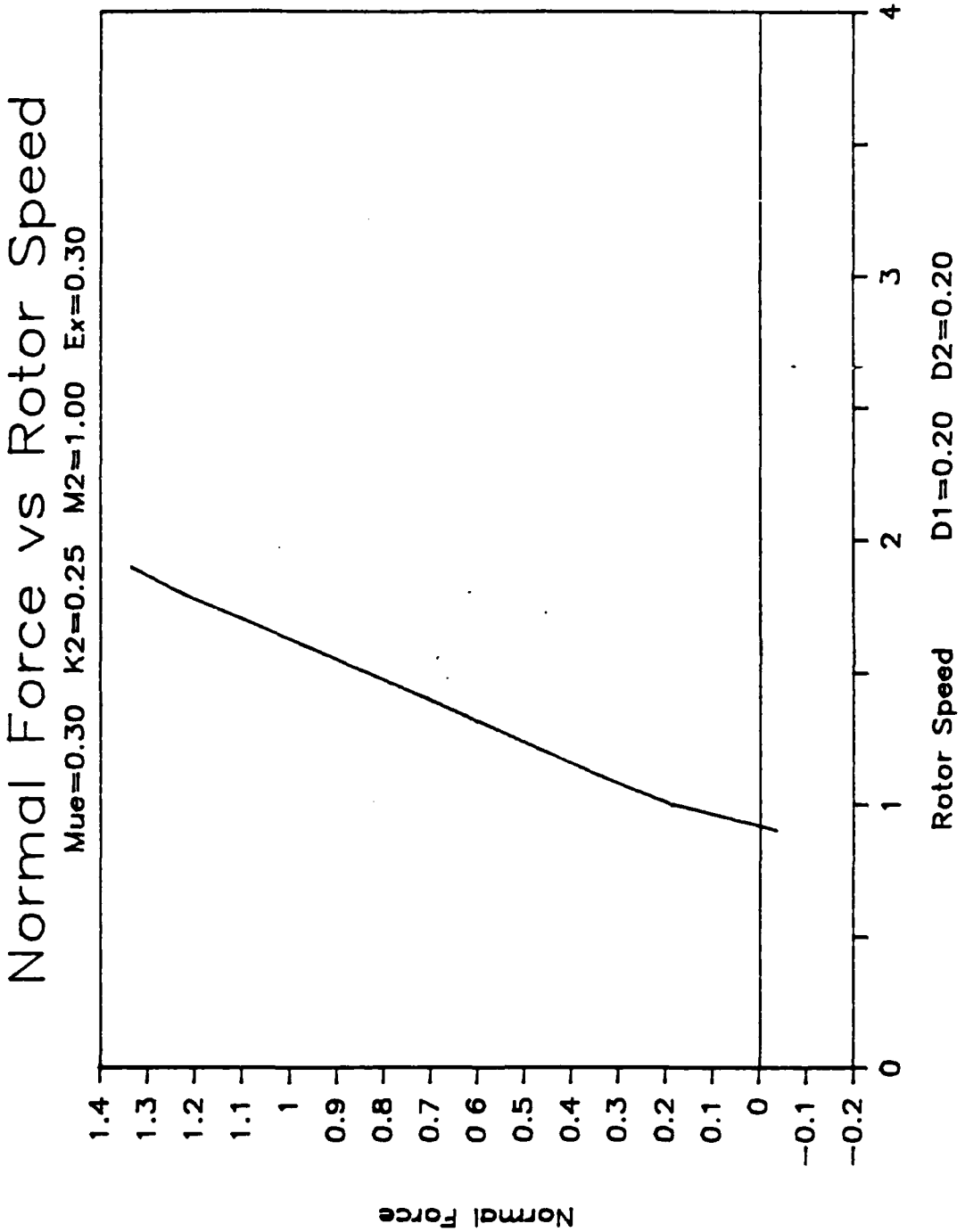
Normal Force vs Rotor Speed
Mue=0.30 K2=0.25 M2=1.00 Ex=0.30
Normal Force
1.4
1.3
1.2
1.1
1
0.9
0.8
0.7
0.6
0.5
0.4
0.3
0.2
0.1
0
-0.1
-0.2
0
1
2
3
4
Rotor Speed
D1=0.20 D2=0.20

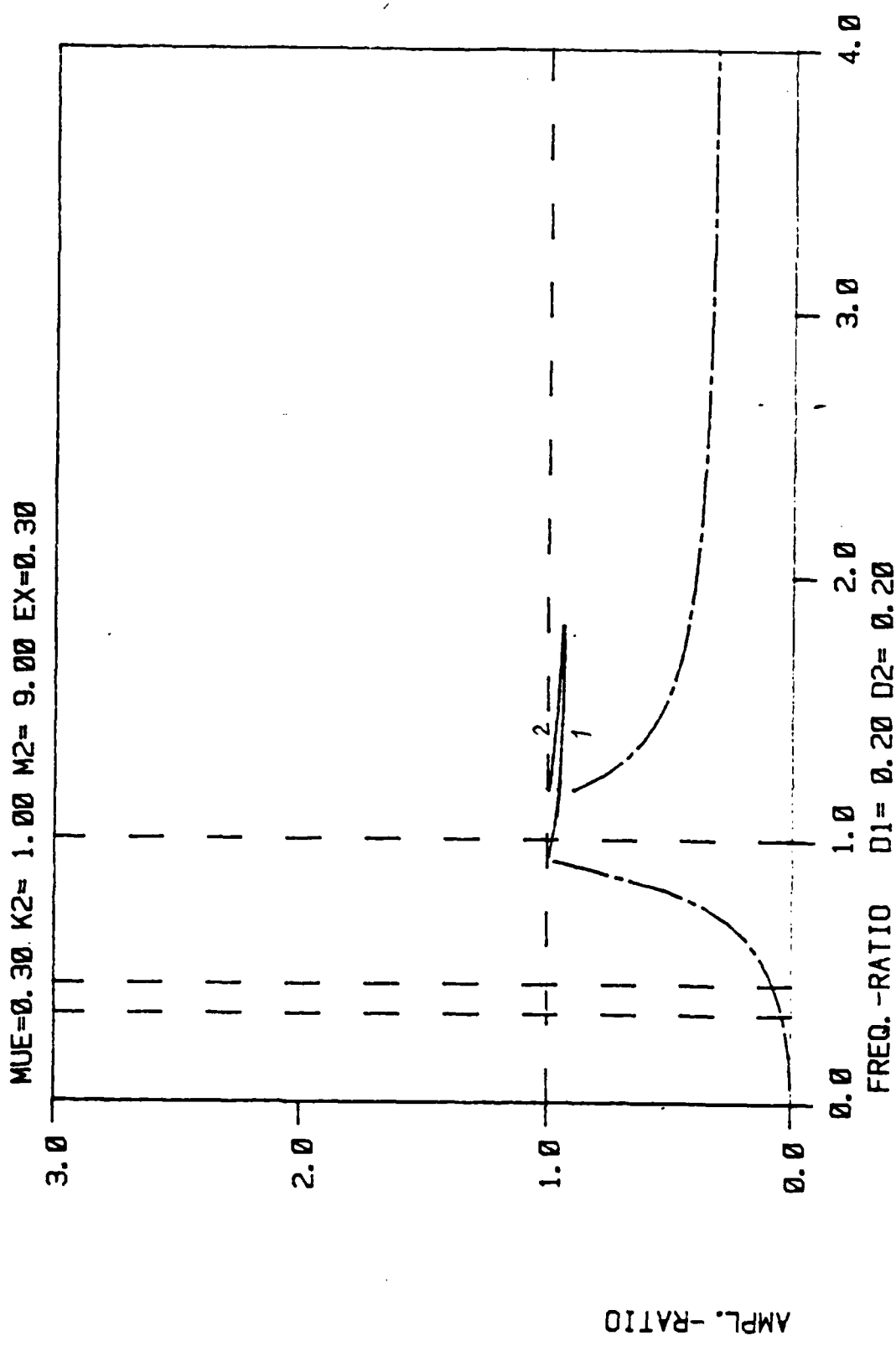
MUE=0.30 K2= 1.00 M2= 9.00 EX=0.30
AMPL.-RATIO
FREQ.-RATIO D1= 0.20 D2= 0.20
0.0
1.0
2.0
3.0
4.0
1
2

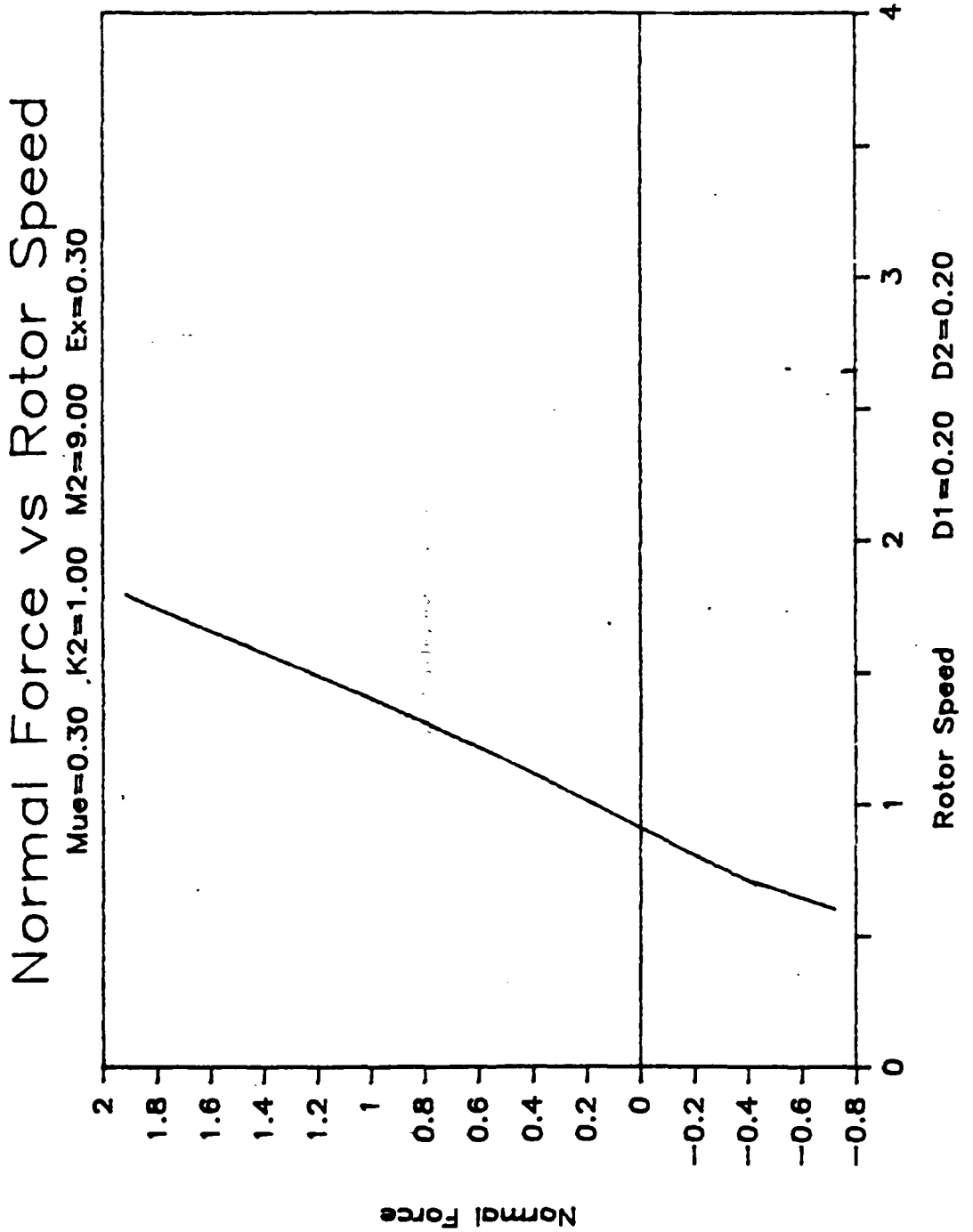
Normal Force vs Rotor Speed
Mue=0.30 K2=1.00 M2=9.00 Ex=0.30
Normal Force
2
1.8
1.6
1.4
1.2
1
0.8
0.6
0.4
0.2
0
-0.2
-0.4
-0.6
-0.8
0
1
2
3
4
Rotor Speed
D1=0.20 D2=0.20

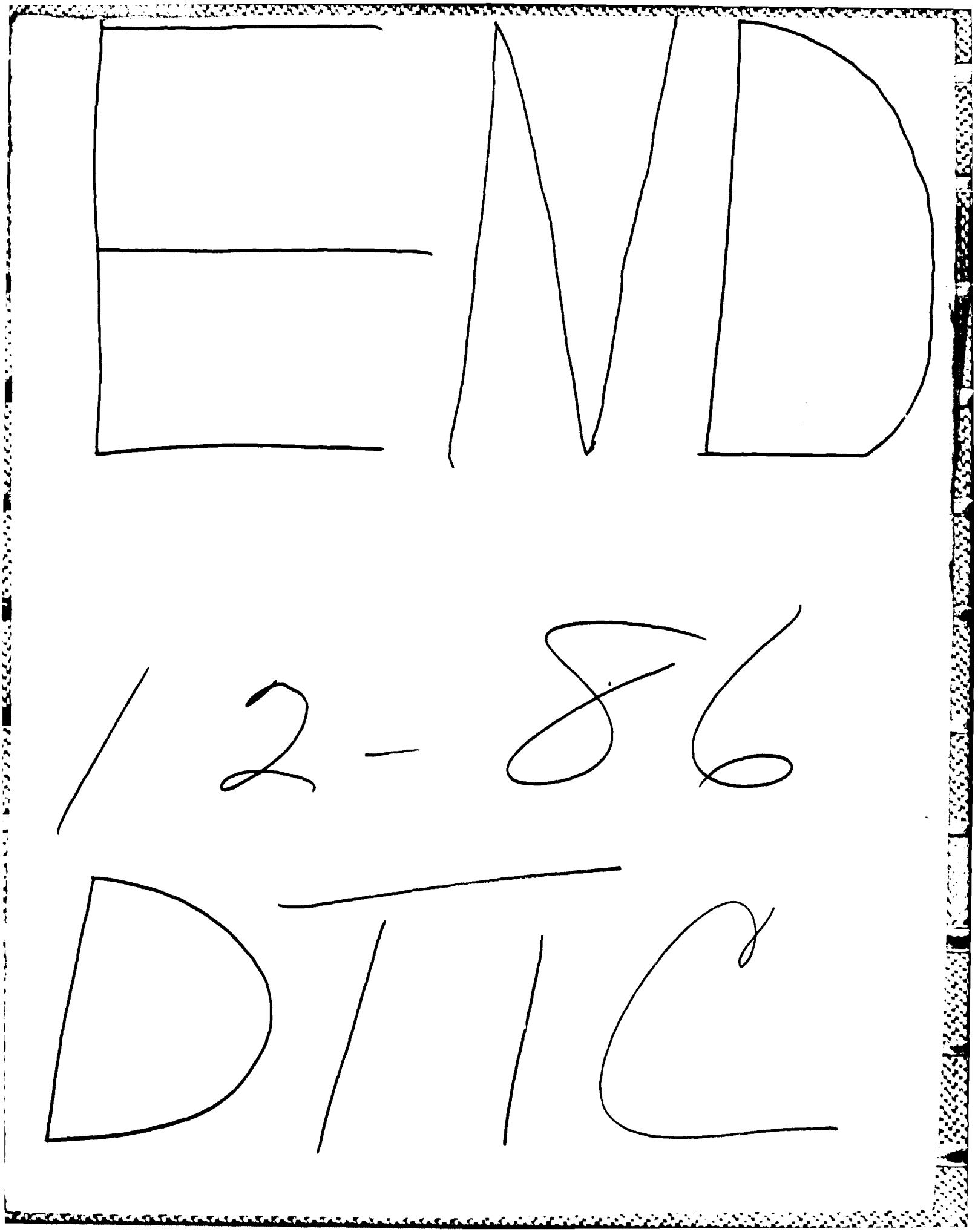
END
12-86
DTIC